OCTOBER 29 | 2021

Appendix CC:
Seabed Morphology Study

Coastal Virginia Offshore Wind Commercial Project

Dominion Energy®

Submitted by:
Dominion Energy Services, Inc.
707 E. Main Street,
Richmond, VA 23219

Prepared by:
Ramboll
One Boston Place, Suite 3520
Boston, MA 02108

Submitted to:
Bureau of Ocean Energy Management
45600 Woodland Road
Sterling, VA 20166

Coastal Virginia OWF Seabed Mobility Study

Final Report 2.0

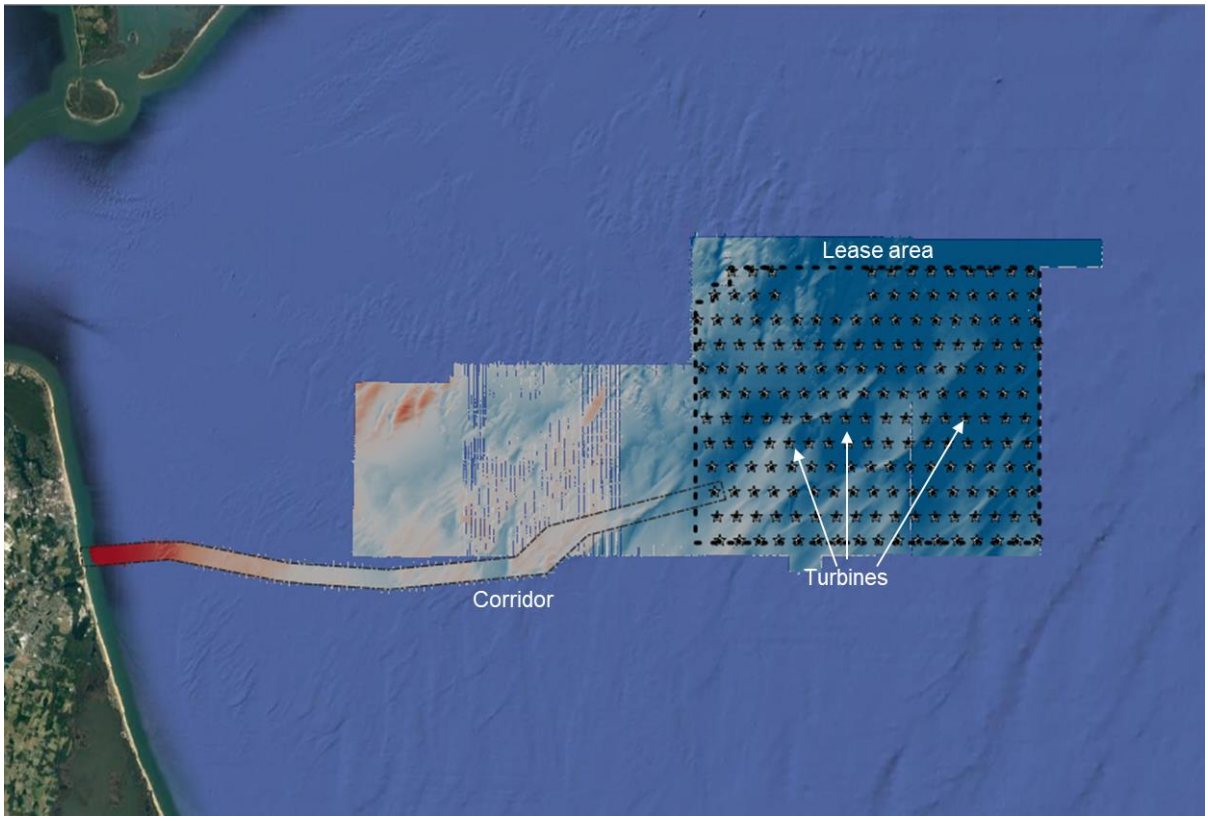

Rambøll

Report

May 2021

The expert in WATER ENVIRONMENTS

This report has been prepared under the DHI Business Management System certified by Bureau Veritas to comply with ISO 9001 (Quality Management)

The expert in WATER ENVIRONMENTS

Coastal Virginia OWF Seabed Mobility Study

Final Report 2.0

Prepared for	Rambøll
Represented by	Mr. Joseph Vitale

Overview of the wind farm area

Author	Arnaud Doré
Quality supervisor	Kasper Kærgaard

Project number	11825661
Approval date	6 May 2021
Revision	Final: 2.0
Classification	**Confidential:** This document is only accessible to the project team members and sharing it outside the project team is subject to the client's prior approval.

DHI A/S • Agern Allé 5 • • DK-2970 Hørsholm • Denmark
Telephone: +45 4516 9200 • Telefax: +45 4516 9292 • dhi@dhigroup.com • www.dhigroup.com
Company Reg. No.: Click or tap here to enter text.

CONTENTS

FIGURES

TABLES

APPENDICES

This page is intentionally left blank.

1 Executive Summary

DHI A/S (hereafter DHI) have conducted a study of the seabed mobility in the Coastal Virginia Wind Farm project area. The present report presents the results from the analysis, including estimations of the migration rates of the main bed features and predictions of future seabed levels in the wind farm area and along the export cable route.

The detailed study is based on the available data from the site including bathymetry data from 2010, 2011, 2012, 2013 and 2020, geotechnical data and met-ocean data from a hindcast study of the met-ocean conditions. The aim of the study is to understand the seabed mobility in the wind farm area as well as in the export cable route corridor.

An overview of the area is shown in shown in Figure 1-1.

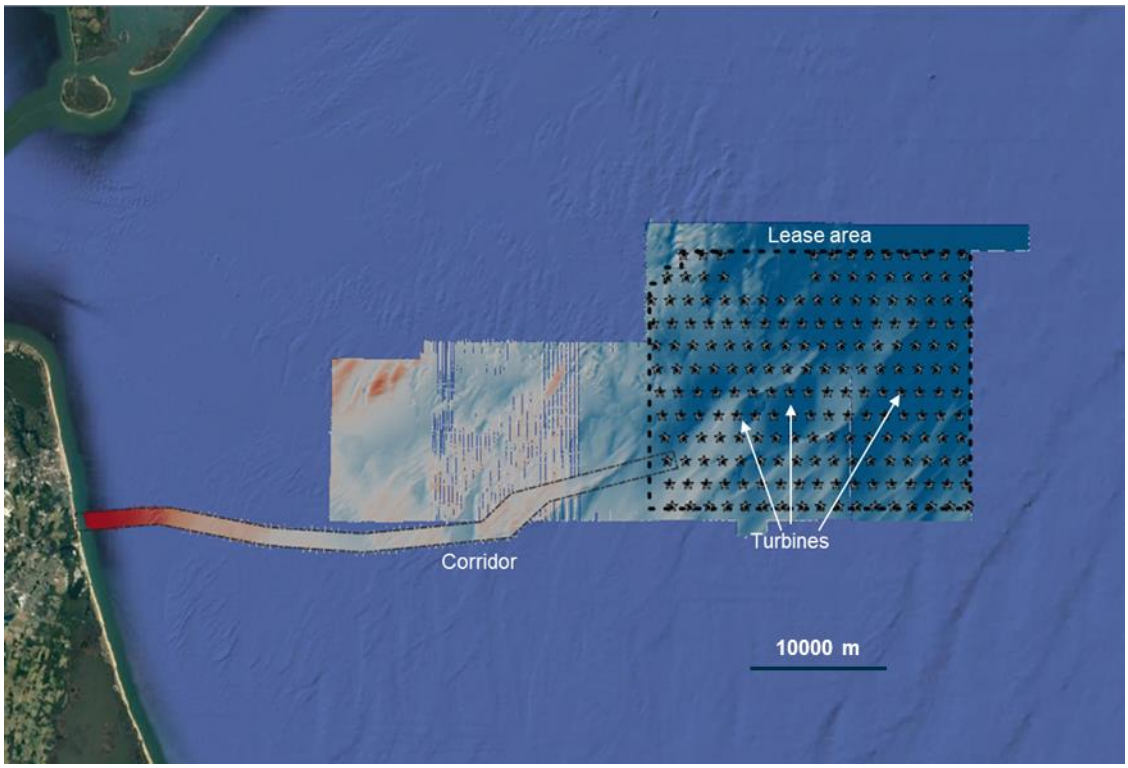

Figure 1-1 Overview of study area including the lease area and the corridor area.

The Lease area covers an area of approximately 460 km^2 and is 44.5 km from the shoreline of Virginia Beach. The export cable route corridor lies between the lease area and the shore and has a length of 44.5 km. The wind turbines are located on a gently sloping continental shelf (~ 20 – 40 m water depth) bordered in the west by a shallow nearshore plateau. For the areas highlighted in Figure 1-1 the following has been found:

- The lease area can be divided into two areas where the seabed is mobile (northwest and south of the lease area) and mostly immobile (northeast quadrant),
- The sand ridges in the lease and export cable route corridor are observed to be migrating towards the southwest by 1 to 2 meters per year,
- The sand waves in the lease area have relatively low migration rates in the order of 1 to 3 meters per year.

- Sand waves in the export cable route corridor have higher migration rates up to 18 meters per year.
- In both lease and export cable route corridor, flat areas are mostly immobile, except for a few erosional spots with erosion rates in the order of 5 cm per year.

2 Introduction

DHI have been commissioned by Rambøll to conduct a seabed mobility study for the wind farm project located offshore of the Chesapeake Bay, the location is shown in Figure 2-1.

Figure 2-1 The location of the study area.

A previous study by Fugro (2014) has shown that there are sand waves and sand ridges in the project area with asymmetric fronts indicating a primary migration direction.

The present seabed mobility study comprises the analysis of available bathymetry surveys that are analysed to assess the properties of the sand waves and other seabed features including their migration rates.

Furthermore, the estimated migration rates and the existing bathymetry is used to make detailed predictions of the future seabed levels at each wind turbine foundation and at selected locations along the cable corridor.

It is noted that a dedicated study of the cable crossing of the shoreline is not included in the present scope.

The study focuses first on the lease area and then on the export cable route corridor.

A previous final 1.0 version of the report incorporated comments and suggestions from Rambøll to a previous draft report.

The present final 2.0 version of the report further clarifies the comments and suggestions. However, there are no significant changes to the conclusions of the study compared with the draft report or the final 1.0 report.

It is noted that the nomenclature for the wind turbine locations in the present report (WTG_XXX) is different than the one normally used in the project (WTG_YY_ZZ). This was discovered at a late stage in the project and to avoid having to redo all figures in the report and rewrite all the text, Table 2-1 provides a conversion between the two. Furthermore, Figure 2-2 shows the location of the wind turbine foundations with both names.

Table 2-1 Nomenclature for wind turbine foundation locations.

DHI Report	Project nomenclature	East, [m UTM]	North, [m UTM]
WTG-001	WTG-1-1	458460	4075324
WTG-002	WTG-1-2	459846	4075324
WTG-003	WTG-1-3	461232	4075324
WTG-004	WTG-1-4	462618	4075324
WTG-005	WTG-1-5	464004	4075324
WTG-006	WTG-1-6	465390	4075324
WTG-007	WTG-1-7	466776	4075324
WTG-008	WTG-1-8	468162	4075324
WTG-009	WTG-1-9	469548	4075324
WTG-010	WTG-1-10	470934	4075324
WTG-011	WTG-1-11	472320	4075324
WTG-012	WTG-1-12	473706	4075324
WTG-013	WTG-1-13	475092	4075324
WTG-014	WTG-1-14	476478	4075324
WTG-015	WTG-1-15	477864	4075324
WTG-016	WTG-1-16	479250	4075324
WTG-017	WTG-1-17	480636	4075324
WTG-018	WTG-2-1	458290	4077036
WTG-019	WTG-2-2	459676	4077036
WTG-020	WTG-2-3	461062	4077036
WTG-021	WTG-2-4	462448	4077036
WTG-022	WTG-2-5	463834	4077036
WTG-023	WTG-2-6	465220	4077036
WTG-024	WTG-2-7	466606	4077036
WTG-025	WTG-2-8	467992	4077036
WTG-026	WTG-2-9	469378	4077036
WTG-027	WTG-2-10	470764	4077036
WTG-028	WTG-2-11	472150	4077036

DHI Report	Project nomenclature	East, [m UTM]	North, [m UTM]
WTG-029	WTG-2-12	473536	4077036
WTG-030	WTG-2-13	474922	4077036
WTG-031	WTG-2-14	476308	4077036
WTG-032	WTG-2-15	477694	4077036
WTG-033	WTG-2-16	479080	4077036
WTG-034	WTG-2-17	480466	4077036
WTG-035	WTG-3-1	458121	4078748
WTG-036	WTG-3-2	459507	4078748
WTG-037	WTG-3-3	460893	4078748
WTG-038	WTG-3-4	462279	4078748
WTG-039	WTG-3-5	463665	4078748
WTG-040	WTG-3-6	465051	4078748
WTG-041	WTG-3-7	466437	4078748
WTG-042	WTG-3-8	467823	4078748
WTG-043	WTG-3-9	469209	4078748
WTG-044	WTG-3-10	470595	4078748
WTG-045	WTG-3-11	471981	4078748
WTG-046	WTG-3-12	473367	4078748
WTG-047	WTG-3-13	474753	4078748
WTG-048	WTG-3-14	476139	4078748
WTG-049	WTG-3-15	477525	4078748
WTG-050	WTG-3-16	478911	4078748
WTG-051	WTG-3-17	480297	4078748
WTG-052	WTG-4-1	457951	4080459
WTG-053	WTG-4-2	459337	4080459
WTG-054	WTG-4-3	460723	4080459
WTG-055	WTG-4-4	462109	4080459
WTG-056	WTG-4-5	463495	4080459
WTG-057	WTG-4-6	464881	4080459

DHI Report	Project nomenclature	East, [m UTM]	North, [m UTM]
WTG-058	WTG-4-7	466267	4080459
WTG-059	WTG-4-8	467653	4080459
WTG-060	WTG-4-9	469039	4080459
WTG-061	WTG-4-10	470425	4080459
WTG-062	WTG-4-11	471811	4080459
WTG-063	WTG-4-12	473197	4080459
WTG-064	WTG-4-13	474583	4080459
WTG-065	WTG-4-14	475969	4080459
WTG-066	WTG-4-15	477355	4080459
WTG-067	WTG-4-16	478741	4080459
WTG-068	WTG-4-17	480127	4080459
WTG-069	WTG-5-1	457782	4082171
WTG-070	WTG-5-2	459168	4082171
WTG-071	WTG-5-3	460554	4082171
WTG-072	WTG-5-4	461940	4082171
WTG-073	WTG-5-5	463326	4082171
WTG-074	WTG-5-6	464712	4082171
WTG-075	WTG-5-7	466098	4082171
WTG-076	WTG-5-8	467484	4082171
WTG-077	WTG-5-9	468870	4082171
WTG-078	WTG-5-10	470256	4082171
WTG-079	WTG-5-11	471642	4082171
WTG-080	WTG-5-12	473028	4082171
WTG-081	WTG-5-13	474414	4082171
WTG-082	WTG-5-14	475800	4082171
WTG-083	WTG-5-15	477186	4082171
WTG-084	WTG-5-16	478572	4082171
WTG-085	WTG-5-17	479958	4082171
WTG-086	WTG-6-1	457612	4083883

DHI Report	Project nomenclature	East, [m UTM]	North, [m UTM]
WTG-087	WTG-6-2	458998	4083883
WTG-088	WTG-6-3	460384	4083883
WTG-089	WTG-6-4	461770	4083883
WTG-090	WTG-6-5	463156	4083883
WTG-091	WTG-6-6	464542	4083883
WTG-092	WTG-6-7	465928	4083883
WTG-093	WTG-6-8	467314	4083883
WTG-094	WTG-6-9	468700	4083883
WTG-095	WTG-6-10	470086	4083883
WTG-096	WTG-6-11	471472	4083883
WTG-097	WTG-6-12	472858	4083883
WTG-098	WTG-6-13	474244	4083883
WTG-099	WTG-6-14	475630	4083883
WTG-100	WTG-6-15	477016	4083883
WTG-101	WTG-6-16	478402	4083883
WTG-102	WTG-6-17	479788	4083883
WTG-103	WTG-7-1	457443	4085595
WTG-104	WTG-7-2	458829	4085595
WTG-105	WTG-7-3	460215	4085595
WTG-106	WTG-7-4	461601	4085595
WTG-107	WTG-7-5	462987	4085595
WTG-108	WTG-7-6	464373	4085595
WTG-109	WTG-7-7	465759	4085595
WTG-110	WTG-7-8	467145	4085595
WTG-111	WTG-7-9	468531	4085595
WTG-112	WTG-7-10	469917	4085595
WTG-113	WTG-7-11	471303	4085595
WTG-114	WTG-7-12	472689	4085595
WTG-115	WTG-7-13	474075	4085595

DHI Report	Project nomenclature	East, [m UTM]	North, [m UTM]
WTG-116	WTG-7-14	475461	4085595
WTG-117	WTG-7-15	476847	4085595
WTG-118	WTG-7-16	478233	4085595
WTG-119	WTG-7-17	479619	4085595
WTG-120	WTG-8-1	457273	4087306
WTG-121	WTG-8-2	458659	4087306
WTG-122	WTG-8-3	460045	4087306
WTG-123	WTG-8-4	461431	4087306
WTG-124	WTG-8-5	462817	4087306
WTG-125	WTG-8-6	464203	4087306
WTG-126	WTG-8-7	465589	4087306
WTG-127	WTG-8-8	466975	4087306
WTG-128	WTG-8-9	468361	4087306
WTG-129	WTG-8-10	469747	4087306
WTG-130	WTG-8-11	471133	4087306
WTG-131	WTG-8-12	472519	4087306
WTG-132	WTG-8-13	473905	4087306
WTG-133	WTG-8-14	475291	4087306
WTG-134	WTG-8-15	476677	4087306
WTG-135	WTG-8-16	478063	4087306
WTG-136	WTG-8-17	479449	4087306
WTG-137	WTG-9-1	457104	4089018
WTG-138	WTG-9-2	458490	4089018
WTG-139	WTG-9-3	459876	4089018
WTG-140	WTG-9-4	461262	4089018
WTG-141	WTG-9-5	462648	4089018
WTG-142	WTG-9-6	464034	4089018
WTG-143	WTG-9-7	465420	4089018
WTG-144	WTG-9-8	466806	4089018

DHI Report	Project nomenclature	East, [m UTM]	North, [m UTM]
WTG-145	WTG-9-9	468192	4089018
WTG-146	WTG-9-10	469578	4089018
WTG-147	WTG-9-11	470964	4089018
WTG-148	WTG-9-12	472350	4089018
WTG-149	WTG-9-13	473736	4089018
WTG-150	WTG-9-14	475122	4089018
WTG-151	WTG-9-15	476508	4089018
WTG-152	WTG-9-16	477894	4089018
WTG-153	WTG-9-17	479280	4089018
WTG-154	Spare WTG-9-18	480666	4089018
WTG-155	Spare WTG-10-1	456934	4090730
WTG-156	WTG-10-2	458320	4090730
WTG-157	WTG-10-3	459706	4090730
WTG-158	WTG-10-4	461092	4090730
WTG-159	WTG-10-5	462478	4090730
WTG-160	WTG-10-6	463864	4090730
WTG-161	WTG-10-7	465250	4090730
WTG-162	WTG-10-8	466636	4090730
WTG-163	WTG-10-9	468022	4090730
WTG-164	WTG-10-10	469408	4090730
WTG-165	WTG-10-11	470794	4090730
WTG-166	WTG-10-12	472180	4090730
WTG-167	WTG-10-13	473566	4090730
WTG-168	WTG-10-14	474952	4090730
WTG-169	WTG-10-15	476338	4090730
WTG-170	WTG-10-16	477724	4090730
WTG-171	WTG-10-17	479110	4090730
WTG-172	Spare WTG-10-18	480496	4090730
WTG-173	Spare WTG-11-1	458151	4092442

DHI Report	Project nomenclature	East, [m UTM]	North, [m UTM]
WTG-174	WTG-11-2	459537	4092442
WTG-175	WTG-11-3	460923	4092442
WTG-176	WTG-11-4	469239	4092442
WTG-177	WTG-11-5	470625	4092442
WTG-178	WTG-11-6	472011	4092442
WTG-179	WTG-11-7	473397	4092442
WTG-180	WTG-11-8	474783	4092442
WTG-181	WTG-11-9	476169	4092442
WTG-182	WTG-11-10	477555	4092442
WTG-183	Spare WTG-11-11	478941	4092442
WTG-184	Spare WTG-11-12	480327	4092442
WTG-185	Spare WTG-12-1	459367	4094153
WTG-186	WTG-12-2	460753	4094153
WTG-187	WTG-12-3	462139	4094153
WTG-188	WTG-12-4	469069	4094153
WTG-189	WTG-12-5	470455	4094153
WTG-190	WTG-12-6	471841	4094153
WTG-191	WTG-12-7	473227	4094153
WTG-192	WTG-12-8	474613	4094153
WTG-193	WTG-12-9	475999	4094153
WTG-194	WTG-12-10	477385	4094153
WTG-195	Spare WTG-12-11	478771	4094153
WTG-196	Spare WTG-12-12	480157	4094153
	WTG-11-3A	462309	4092442

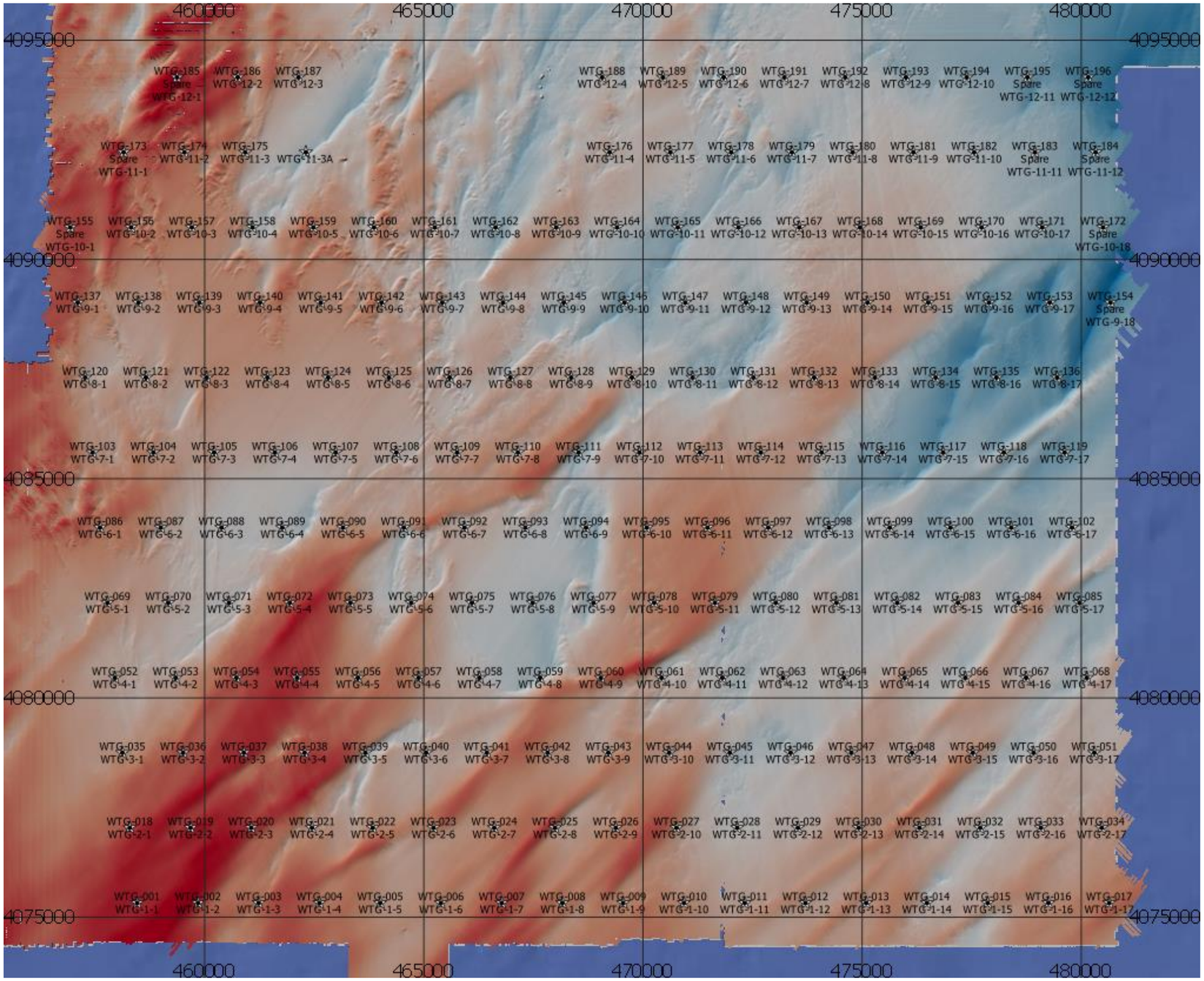

Figure 2-2 Overview of wind turbine foundations with both names.

This page is intentionally left blank.

3 Data

The data for completion of the seabed mobility study was delivered by Rambøll. The data sources utilized for this study are listed below.

High resolution bathymetry over area (see Figure 3-1):

1. Multibeam surveys from NOAA years 2006-2010-2011-2012 (Ref [7]).
2. Bathymetrical data in geodatabase format with 1m spacing in MLLW vertical datum and NAD83 projection with 1mx1m resolution by Fugro in 2013 (Ref [4]).
3. Ensemble of 'tif' files from Terrasond from year 2020: lease area MBES bathymetry with a resolution of 50cmx50cm (Data was provided by Rambøll February 1st, 2020. Preliminary datasets under quality assurance by Rambøll) (Ref [11])
4. Tif file received from Rambøll 'ECR_Alpine_2020_Avg_50cm.tif' with Alpine ECRC 2020 export cable route corridor MBES bathymetry with a resolution of 50cmx50cm (Data was provided by Rambøll February 1st, 2020. Preliminary datasets under quality assurance by Rambøll) (Ref [12])

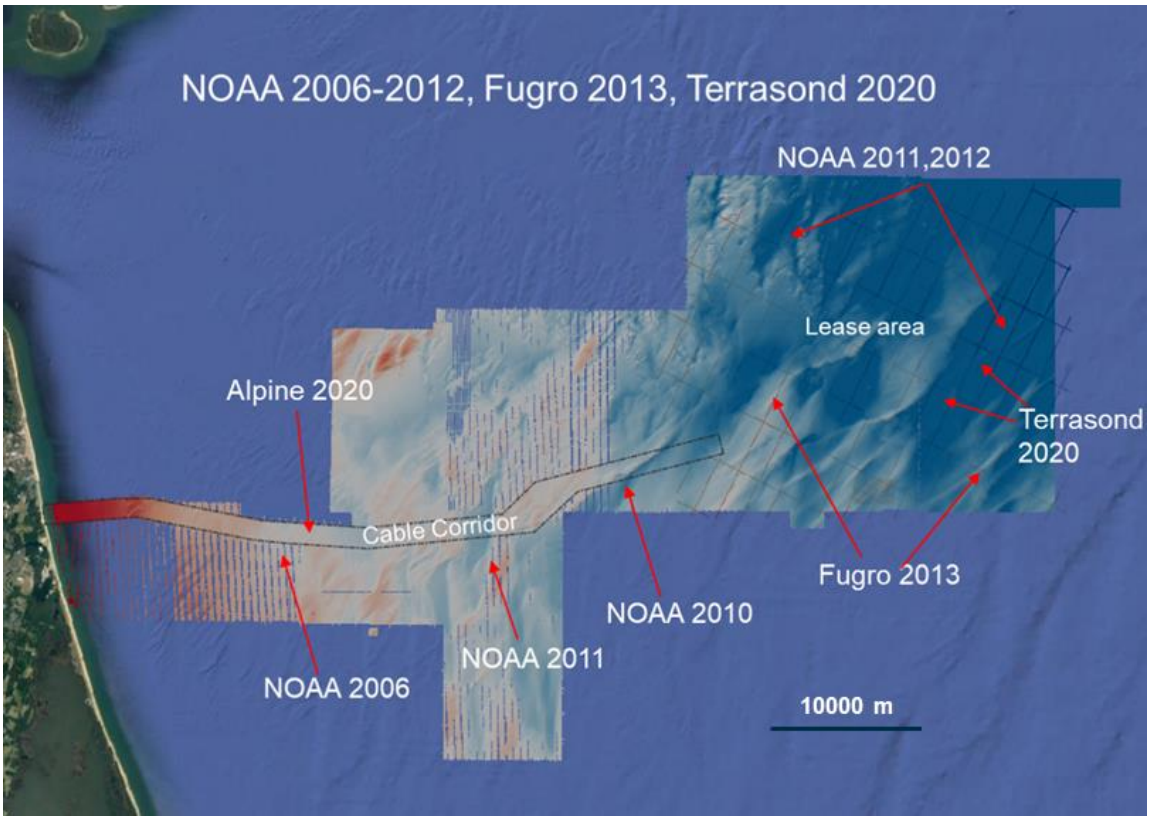

Figure 3-1 Overview of the bathymetric data.

Geotechical data:

1. Geophysical and shallow geotechnical site characterization surveys supporting development of the Virginia Offshore Wind Technology Advancement Project (VOWTAP or Project) performed by Tetra Tech, Inc. (Tetra Tech) in June of 2013 (Ref [10])
2. Geophysical data acquired by Fugro in the lease area (Ref [4])

3. Geophysical marine survey conducted by Fugro in the export cable corridor performed in 2014 (Ref. [6])

4. Report on Dominion Energy (Dominion) Geophysical and Geohazard Interpretation for the Dominion Commercial Virginia Offshore Wind Energy Area (WEA) Lease Number OCS-A 0483 (Lease Area) by TerraSond Limited (Ref [11])

5. Report presenting results sampling and laboratory analysis of surficial sediments within the CVOW from Schnabel Engineering 2020 (seabed) (Ref [9])

6. Letter presenting results of the laboratory tests performed on the samples delivered to the TerraSense laboratory on 11/23/20 in the export cable route corridor and associated shape file sent by Rambøll ('GrabLocations.shp').

Meteocean studies:

1. Meteocean assessment by Rambøll 2021 (Ref [8])

2. Meteocean study by Fugro 2013 (Ref [5])

3. AWS meteocean design assessment (Ref[2])

The existing data collected for this study allowed us to complete the following:

1. Description of the seabed and bedform characteristics in the lease area based on the NOAA data, Fugro 2013, Terrasond 2020 and Alpine ECRC 2020

2. Assessment of sand ridge migration in the lease area.

3. Assessment of sand wave migration in in the lease area (sand waves are mostly found in the North West of the lease area)

4. Assessment of sand wave and ridge migration in the export cable route corridor

5. Detailed predictions of the future seabed levels at each wind turbine foundation and in selected locations along the cable export route.

4 Seabed Mobility Processes

To assess the seabed mobility at the offshore windfarm area and along the export cable route corridor, it is important to understand which sediment transport processes can potentially cause significant seabed mobility.

The key processes are:

- Persistent erosion or accretion of sediment on the seabed
- Migration of large-scale seabed features such as sand waves or sand ridges which cause alternating periods of erosion and accretion of the seabed.

4.1 Persistent Erosion or Accretion of Sediment from the Seabed

Persistent erosion or accretion of sediment from the seabed can occur if there are gradients in the sediment transport in the area: If more sediment is transported away from - than to - the area, then the area will undergo erosion. Likewise, if more sediment is transported to - than away from - the area, then the area will experience accretion.

Over time, the changes in the morphology will cause the gradients in the sediment transport to decrease thereby also decreasing the rate of erosion or accretion: An undisturbed system therefore often attains a state of equilibrium (or cyclic equilibrium); i.e. the morphology is in equilibrium with the hydrodynamic forcing.

Areas with persistent erosion or accretion are usually found in disturbed or very dynamic systems, i.e., close to river mouths or man-made structures such as navigation channels, offshore sand mining pits or land reclamation areas.

In case the seabed mainly consists of compacted fines, persistent erosion can be occurring. However, if there is a significant portion of sand in the seabed material, the coarser less mobile sand fractions will armour the seabed and possibly limit the erosion process.

In the case of persistent deposition, the deposition is expected to occur mainly as sand or finer material because larger gravel fractions require large current speeds to be transported and such current speeds are normally only found in the surf-zone where waves break or in fast flowing rivers.

4.2 Migration of Large-scale Seabed Features

Transport of sand along the seabed causes the formation of seabed features. In the marine environments, bedforms with many different length scales can be found depending on the current speed and the available sediment. The different bed forms are shown in Figure 4-1, which is reproduced after Belderson (1982) (Ref [3]).

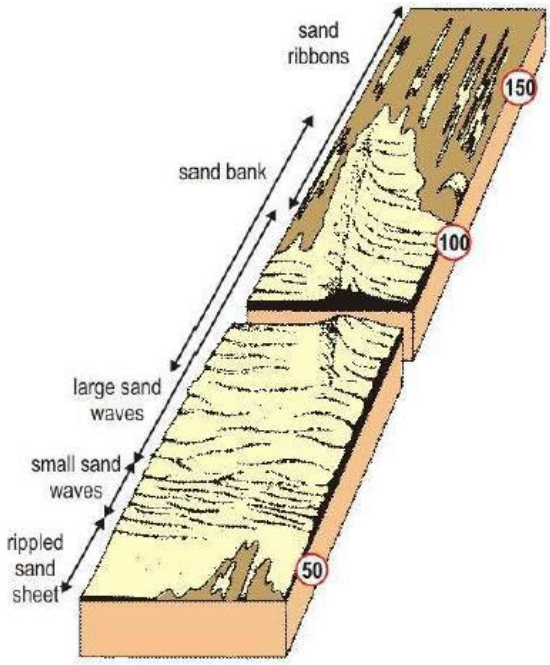

Figure 4-1 The simplified sand wave, ripple and sand ridge classification reproduced from Belderson (1982) (Ref. [3]). Labels correspond to the average current speed in cm/s.

Tidal sand ridges can be many kilometres long and only migrate quite slowly, therefore their movement is potentially not an issue on time scales relevant for an offshore windfarm. Their crest orientation is usually between 10° to 30° to the main flow direction.

The sand waves are smaller than sand ridges, they are often separated into mega ripples and sand waves as proposed by Ashley (1990) (Ref. [1]), the distinction given in Table 4-1 is used in the present study.

Table 4-1 Commonly used terms for shallow marine large scale bedforms, after Ashley (1990).

Commonly used term	Height (H) metres	Spacing (L) meters	H/L ratio
Mega ripple	0.5-1.5	10-20	1:10-1:25
Sand wave	Average: 2.0-5.0 Maximum: 12-18	Average 100-400 Maximum >1,000	1:30-1:100 (or greater)
Sand ridges	Average ~5-30 m	Some Kilometres	> 1:100

The migration of sand waves and mega ripples can cause significant changes to the bed level in an area over relatively short time scales. The potential changes are of a magnitude equal to the height of the sand waves in the area, and the time scale of the change in bed level is related to the migration speed of the sand waves.

It is noted that migrating sand waves will tend to have an asymmetric shape where the distance between the peak and trough of the sand wave is different on the stoss side and the lee side of the sand wave. In case of a slowly migrating or stationary sand waves, the shape is expected to be more symmetric with the same distance between the peak and trough on the stoss and lee side of the sand wave.

The orientation of sand wave crests is generally perpendicular to the main flow direction, but it may deviate somewhat in the case of gradients in the depth or transport rate along the direction of the crests.

Sand waves migrate, when sand is transported over the stoss side of the sand wave and deposits on the lee side. Generally, sand is transported due to the combined effect of currents and waves. The waves stir up or loosen the sand grains such that the current can easier transport the sand, which means that the magnitude of sand transport increases with increasing wave height and with increasing current speed.

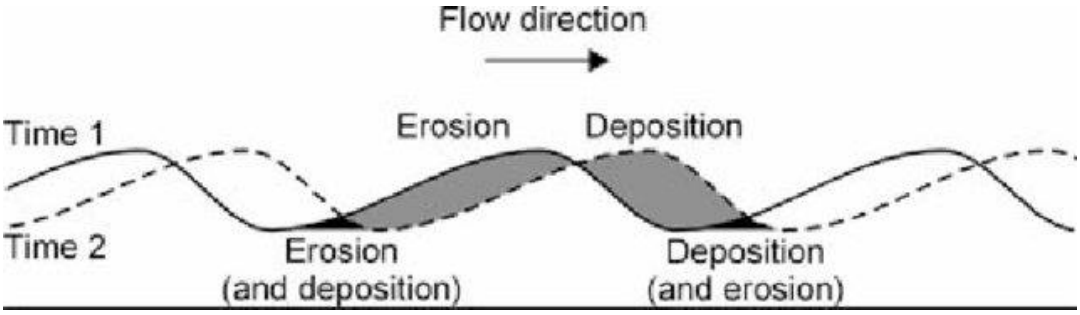

Figure 4-2 Schematic illustration of dune migration in the direction of flow by stoss-side erosion and lee-side deposition used for the determination of bedload transport (Ernstsen et al., 2007).

This page is intentionally left blank.

5 Lease Area Seabed Dynamics

5.1 Description

In Figure 5-1 the overall characterization of the area is presented. This characterization was completed based on the morphological features, which can be observed on the seabed in the different areas, coupled with the available data on the sediment properties.

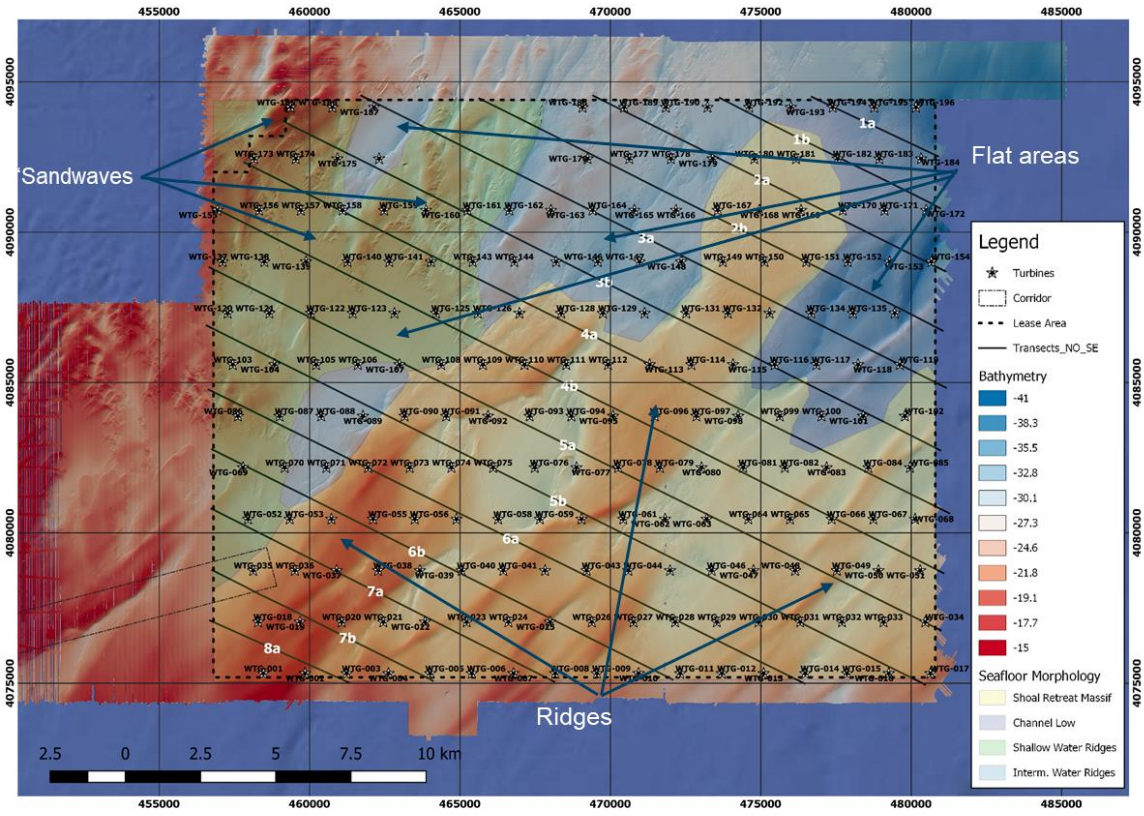

Figure 5-1 Subdivision of the lease area in function of the main geological characteristics. The black lines represent the extracted transects of the seabed mobility analysis.

The site resides on the continental shelf, bordered by a shallow nearshore plateau to the west and sand ridges deeper to the east. The wind turbines are distributed in the 'lease area' across a variety of geological features. The lease area can be divided into four regions as described by Fugro (2014), based on water depth and seafloor features that include: a shallower water depth (typically less than 28 meters) area in the north-western and western section, with a highly irregular seafloor consisting of sand ridges and superimposed bedforms; an intermediate water depth (typically 28 to 34 meters) area in the northern section, which consists of lower relief seafloor features; a deeper water depth (greater than 34 meters) area in the eastern section; and a shallower water depth (typically less than 28 meters) area associated with the shoal retreat massif (and multiple ridge complexes) in the central and southern sections. These areas consist of seafloor features (e.g., bedforms) at various scales which are related to the larger-scale geologic features, surficial sediments, and hydrodynamic environment.

The spaces between the sand ridges consist of deeper flat areas that are mostly immobile with rare signs of bed erosion at some locations where the bathymetry is slightly channelized. No large sand wave fields are detected in the lease area – the sand waves in the north west quadrant have fairly low heights and are not very dynamic compared to sand waves in tidal channels in other submarine areas. They seem to develop at the edges of the sand ridges.

The ridges in shallower water depths (18 to 30 meters) are shorter in length and width when compared to ridges on the shoal retreat massif. They occur at a higher frequency and display a lower bathymetric relief.

Figure 5-1 shows an overview of profiles extracted across the lease areas. The profiles are extracted according to a north-west to south-east direction to align with the Fugro 2013 surveys. Fortunately, this axis is also aligned with the direction of propagation of the bed features (defined by their steep face) which roughly corresponds to the mean flow direction in the area.

The profiles are shown in Figure 5-3 through Figure 5-6 with bathymetries from 2011/2012 (NOAA 2×2m resolution), 2013 (FUGRO 1×1m resolution) and 2020 (TERRASOND 50×50 cm resolution) as well as the locations of the closest wind turbines along each profile. Profiles labelled with a 'b' compare the three sets of bathymetric data. Profiles labelled 'a' compare the NOAA and the TERRASOND data and are extracted to offer a better representation of the bed features in the area. Note that large offsets in the NOAA data (0.2 to 0.4 m) and the low slope of the bed features induce uncertainty in the derivation of migration rates.

For the sake of clarity, the sand ridge massif is further subdivided into three large ridges as shown on Figure 5-2. Extracted profiles clearly show the elevations of the different ridges across the lease area. The height of the ridges lies between 3 and 10 meters, for the highest ridge, at depths between 20 to 40 meters. Sand waves appear as small perturbations on the slopes of the sand ridges in the north west quadrant (areas highlighted with an arrow on the left of transect plots). The observed sand waves have low amplitudes in the range 0.5 – 1.5 meters and wavelengths up to 300 meters. According to the classification shown in Table 4-1, these sand waves are actually in the mega ripple regime in terms of height, but we will continue to use the term sand wave in the present work to characterize these features.

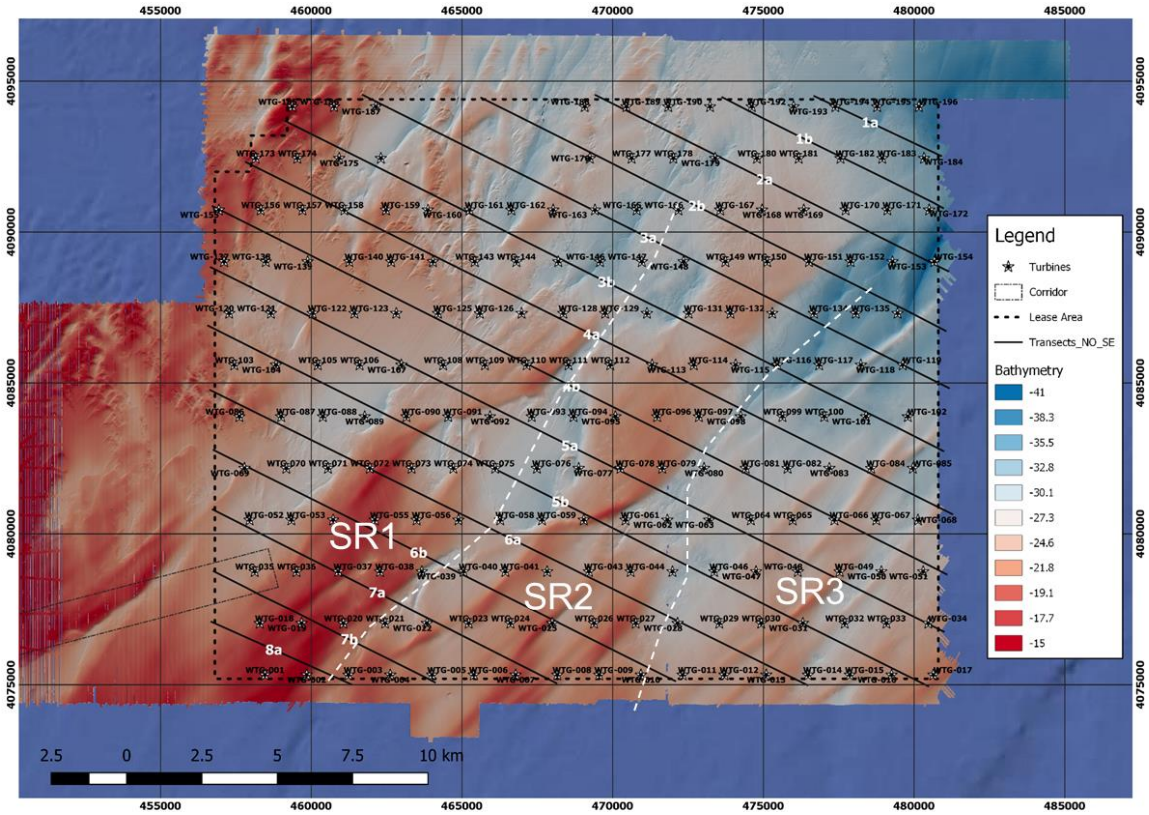

Figure 5-2 Subdivision of the retreat massif into three sand ridges named SR1, SR2 and SR3. All Profiles (see also below) are extracted according to a north west-south east direction.

A careful examination of the profiles was performed, and it was found that the sea bottom is in general very stable in the deeper flat areas. The main bedforms (sand ridges and sand waves),

made of poorly sorted coarse sands, exhibit a slow dynamic that is explained in more detailed in the following.

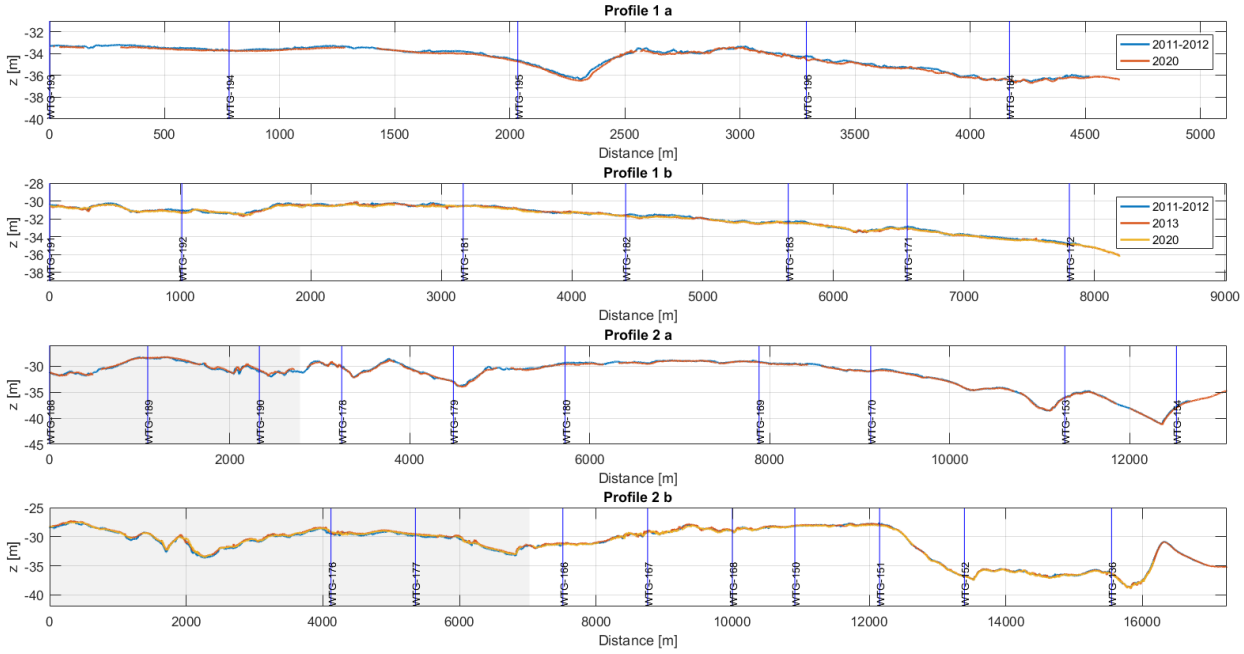

Figure 5-3 North west-south east profiles 1a to 2b across the lease area. Vertical lines show positions of closest wind turbines along the profile. Shaded areas correspond to the NOAA 2011 data.

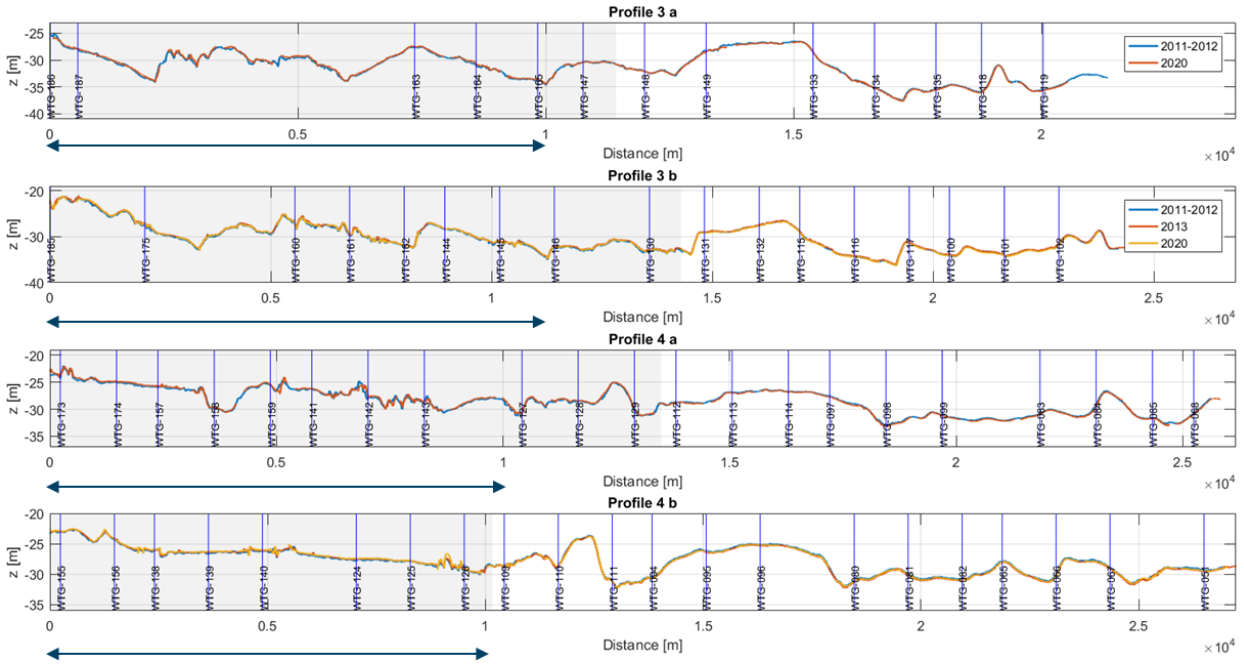

Figure 5-4 North west-south east profiles 3a to 4b across the lease area. Horizontal arrowed lines highlight the region in the north west where sand waves are present.

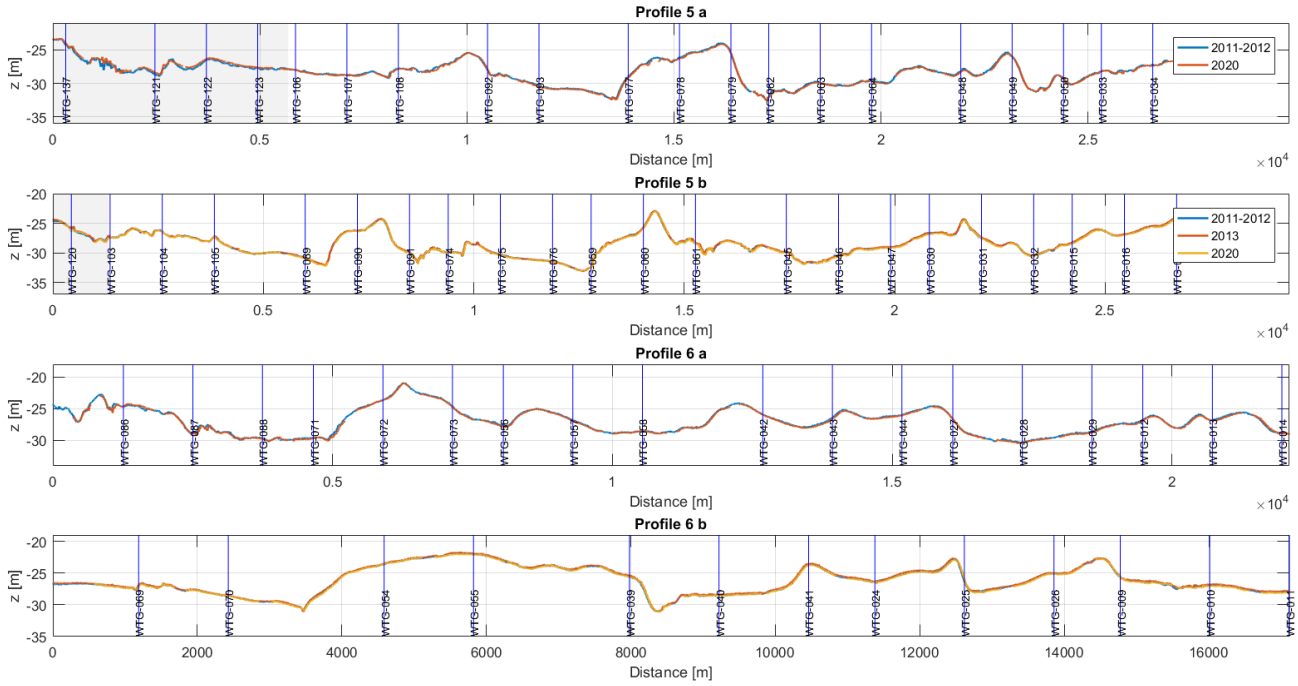

Figure 5-5 North west-south east profiles 5a to 6b across the lease area.

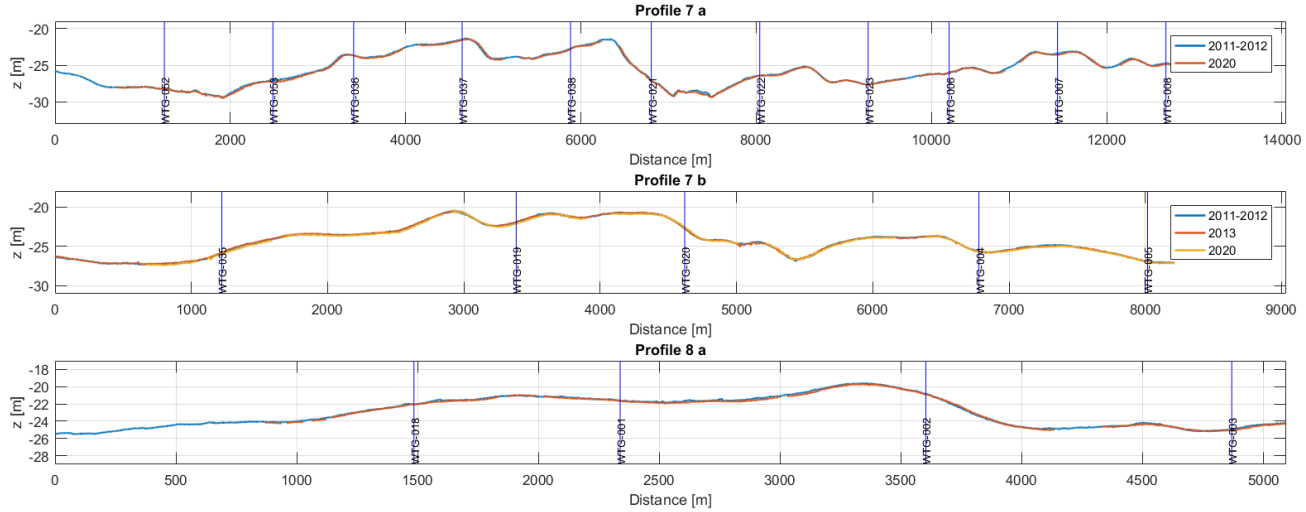

Figure 5-6 North west-south east profiles 7a to 8a across the lease area.

5.2 Sand Ridges

Tidal sand ridges are large-scale sandy bed forms, which are typically several kilometres long, tens of meters tall and with migration rates (relative to their wavelength) in the order of centuries. The crestline of sand ridges is usually angled in the range 10° to 30° relative to the mean current axis, which is also the primary migration direction of the ridge.

Within the lease area, the main characteristics of the seabed can be summarized as follows:

- Ridges are composed of coarse sand (d50>0.5/0.6 mm), that is poorly sorted
- There are no mega ripples on the top and edges of the large ridges
- Finer sand is trapped in the trough areas of the ridges

- There is a slow migration of ridges located in the south west of the lease area in shallower waters
- There is an extremely slow dynamics of the ridges in the north east of the Lease area in deeper waters – that is not detectable within the 10 years' time span between the bathymetry data of different sources.
- There is little movement of the finer sands in the deeper flat areas except at a few locations where the bathymetry is channelized.

A few characteristic examples are presented below to illustrate the findings. All other transects are presented in the Annexes. Migration rates were computed and are presented in Table 5-1 in the following.

In Figure 5-7 and Figure 5-8 two examples of seabed erosion that are representative of the area are presented. It shows that erosion mostly occurs in relatively locally deeper areas and engender an erosion of the bottom in the order 5 cm per year - 0.5 m for the 10-year observation period. All locations where such erosion spots are observed are reported in Figure 5 11. A few wind turbines are affected, especially wtg-146 or wtg-98.

In Figure 5-9 and Figure 5-10 two examples of sand ridge migration that are representative of the area are presented. It shows that migration mostly occurs towards the south east with migration rates of the order of 0.5 to 3 meters per year. The expected erosion in the vicinity of sand ridges is in the order of 0.5 m for the next 30 years.

Figure 5-11 summarizes all locations where erosion and sand ridge migration occur in the lease area. It clearly shows that mobile features are located in the shallow retreat massif south and southwest of the study domain. Also indicated are the sediment mean diameters (Schnabel, 2020).

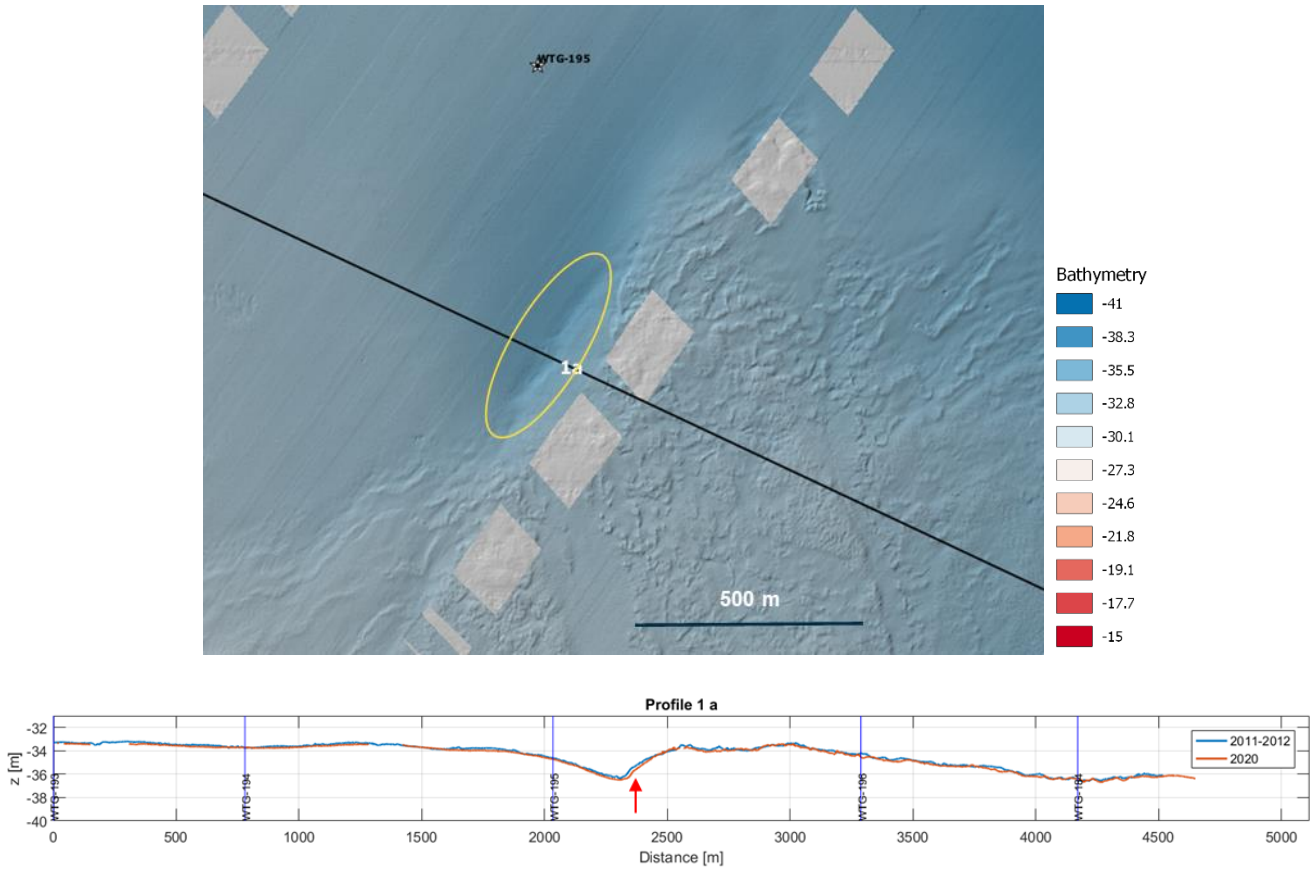

Figure 5-7 Example of a steady local erosion pattern in profile 1a.
All Profiles (inc. below) are extracted according to a North west-south east direction.

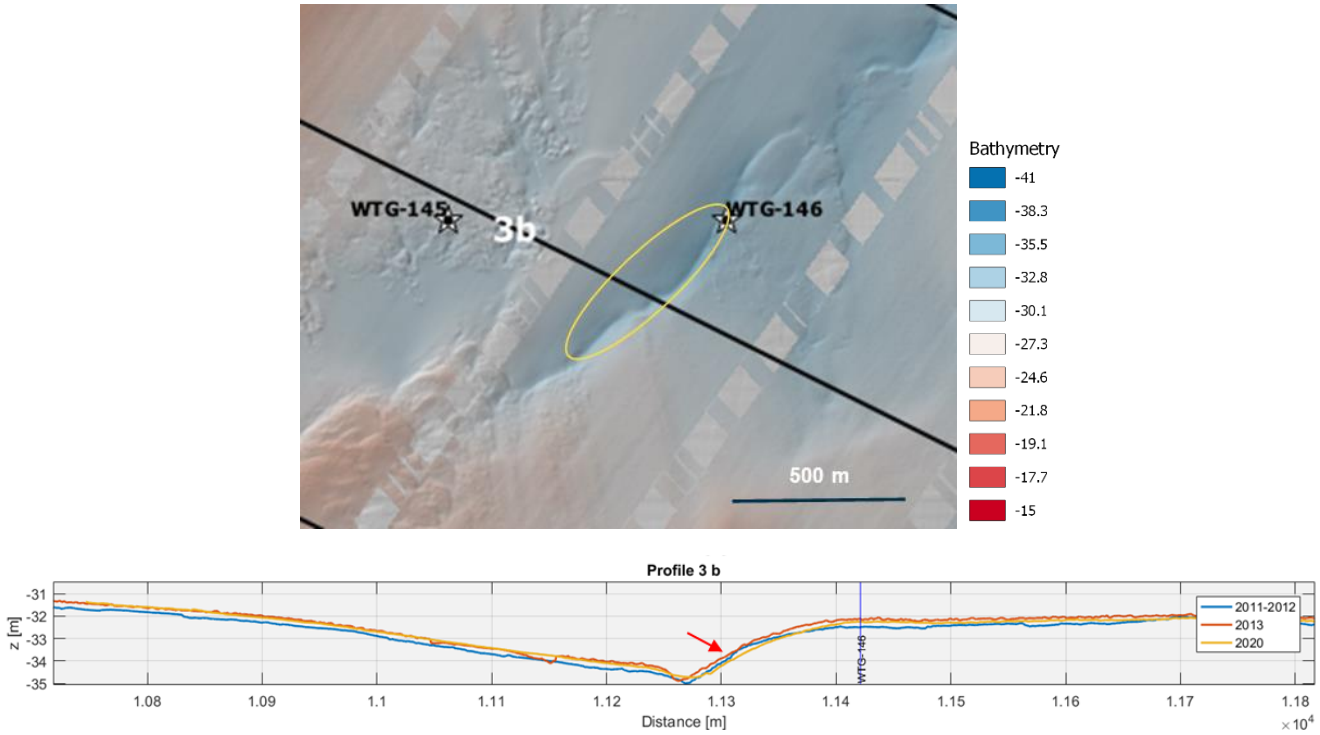

Figure 5-8 Example of a steady local erosion pattern in profile 3b.

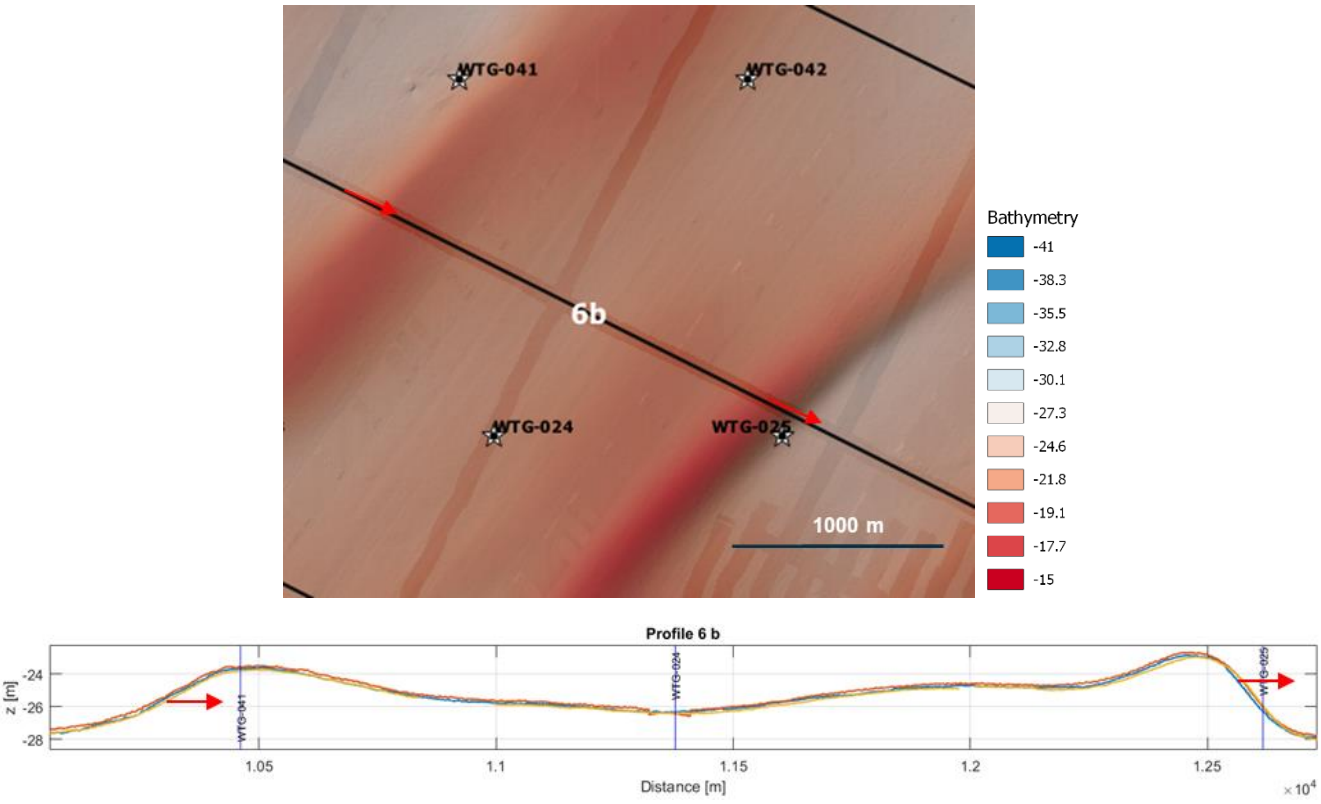

Figure 5-9 Example of a migrating sand ridge (SR1) in profile 6b.

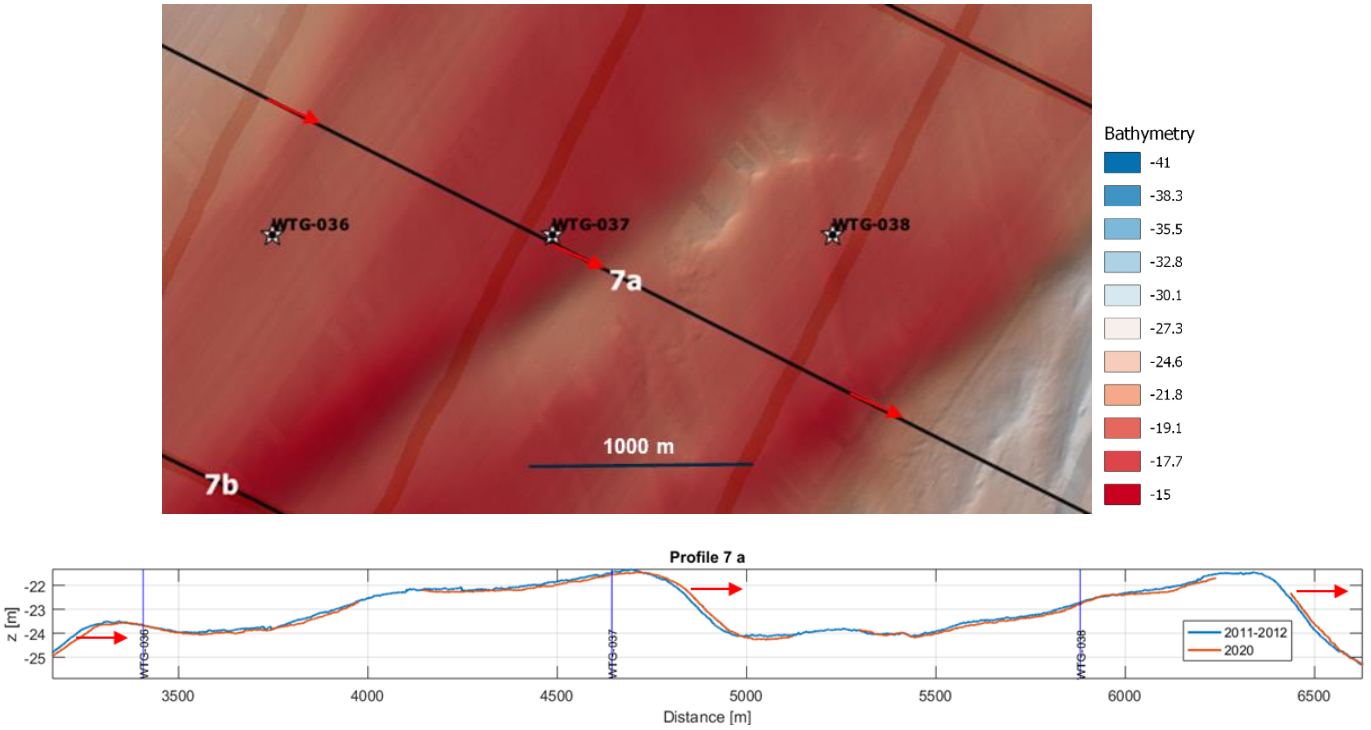

Figure 5-10 Example of a migrating sand ridge (SR1) in profile 7a.

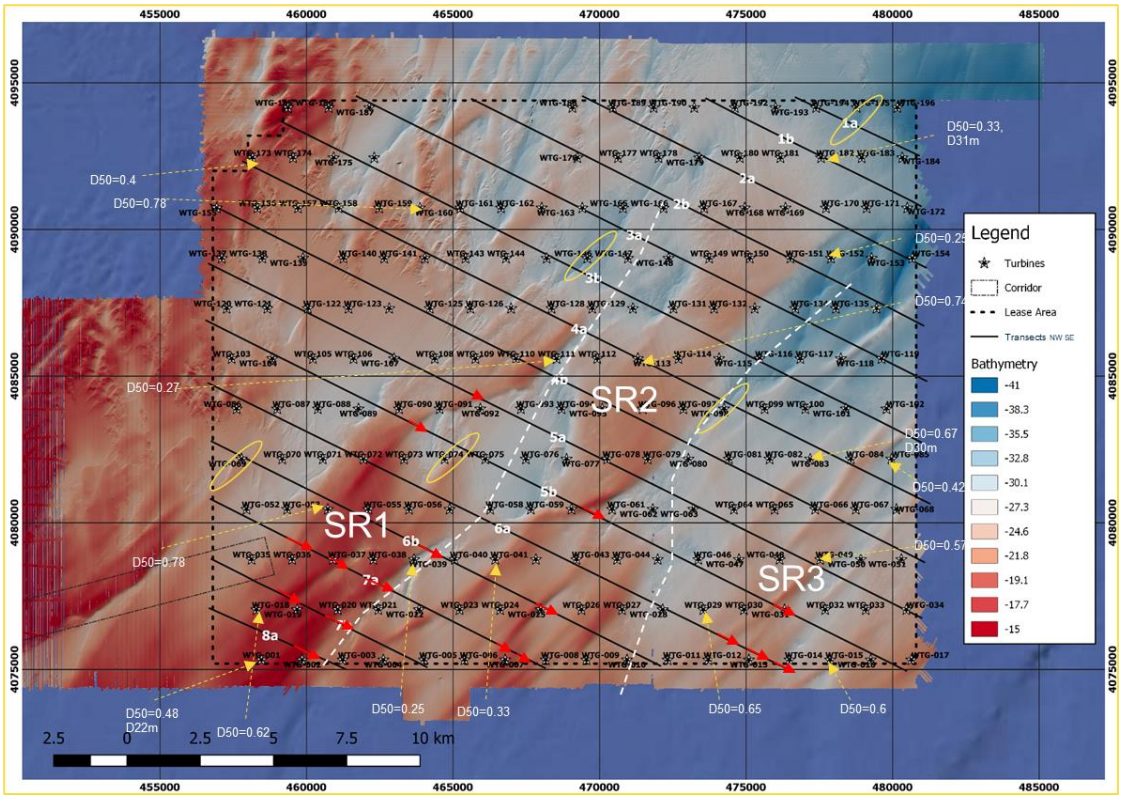

Figure 5-11 Overview of the sea bottom dynamics.
The red arrows represent the locations where a migration of the sand ridge is detected. Values of the computed migration rates are presented in Table 5-1. Yellow circles indicate erosion. Sediment mean diameters are shown at several locations.

5.3 Sand Ridge Migration Rates

Predicting the future migration of a sand ridge based on surveys is associated with uncertainty, since it is a large-scale bedform of wavelength of several kilometres with a migration period estimated in century long timescales Furthermore, there is an uncertainty related to the vertical datum of the surveys, which will have an effect on the migration estimation due to the gentle sand ridge slope. In particular, the NOAA survey is prone to badly assembled swaths leading to offsets in the range 0.2 - 0.4 m. The NOAA data was corrected by a value of +0.2 m to align with the Fugro and TERRASOND data in flat immobile areas.

With the uncertainties outlined above in mind, the approach adopted for estimation of the sand ridge migration in the future is as follows:

- It is assumed that the hydrographic climate remains similar to the present.
- Each survey was filtered using a low-pass FFT[1] filter to establish a mean bed level,
- For each profile, a depth range was assigned in which the horizontal shift (migration) was calculated, based on visual inspection on where the profiles express the sand ridge migration the most.
- The annual migration rate was then estimated within 0.5 m intervals in the above-mentioned depth range, from the following scenario:
- The horizontal difference between surveys is averaged within 2-year combinations (2011-2020, 2013-2020) as well as the depth range. The results can be seen in Table 5-1.
- The sand ridge mean migration rates were extrapolated 30 years into the future taking into account the standard deviation of the computes migration rates.

Table 5-1 Estimated sand ridge mean and standard deviation (SD) migration rates.

Profile	Depth	1 y		30 y		
	range	Mean	SD	Mean	Mean-SD	Mean+SD
	[m MLLW]	[m/year]	[m/year]	[m/30year]	[m/30year]	[m/30year]
P5bSR1	[-29.5 -25.5]	1.47	0.72	44.3	22.5	66.1
P5bSR2	[-26.5 -23.5]	2.7	0.48	80.6	66.2	95.4
P5bSR3	[-27.5 -24.5]	1.37	0.67	41.2	20.9	61.5
P6bSR1	[-31 -26]	1.36	0.59	41	23.1	58.3
P6bSR2	[-28 -23.5]	1.18	0.41	35.7	23.11	48.2
P7bSR1	[-24.2 -21]	3.36	0.48	101	86.5	115.6
P5aSR1	[-28.5 -25.5]	1.15	1.3	34.4	0	73.4
P6aSR3	[-28.5 -26]	3	0.95	92.5	63.8	121.2
P7aSR1	[-24 -21.5]	2	0.1	63	59.9	66.1
P7aSR2	[-25.5 -23.5]	0.6	1	18.8	0	51.3
P8aSR1	[-24 -20]	0.54	1.1	16.2	0	49

[1] Fast Fourier Transform

5.4 Sand Wave Area

Sand waves are essentially present in the north west corner of the lease area (Figure 5-12.) Sand waves are attached to ridges and are composed of the same poorly sorted coarse sediment. The areas laying between the sand waves are mostly flat, composed of silty sands and remain immobile between the bathymetric surveys.

After careful examination of all sand waves in the area, it was found that migration rates are fairly low with values around 2 m/y for the mobile sand waves. Other sand waves are stable or entrain only centimetric variations of the bed level mainly due to the development of superimposed ripples.

Consequently, only a few wind turbines lie in the axis of moving bedforms and may be concerned by erosion or accumulation of sediment along migration paths.

The overall expected variations of the seabed are of the order of ~0.5 m in the next 30 years at the utmost in the vicinity of mobile sand waves.

Figure 5-13 and Figure 5-14 show two examples of bathymetric profile comparison in the vicinity of the wind turbines. Both figures give a clear idea of the slow migration of sand waves and the low variation of the bed elevation that can be expected along the migration paths for the next 30 years, up to 0.5 m.

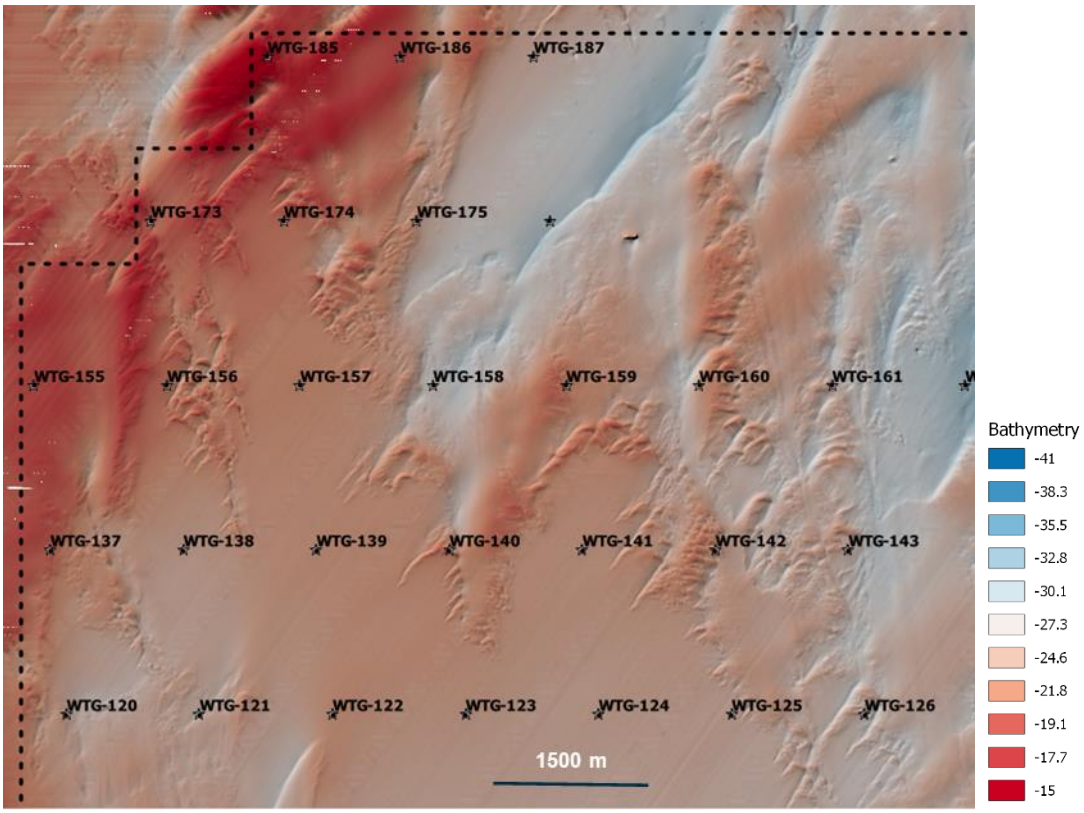

Figure 5-12 Sand waves in the north-west corner of the lease area.

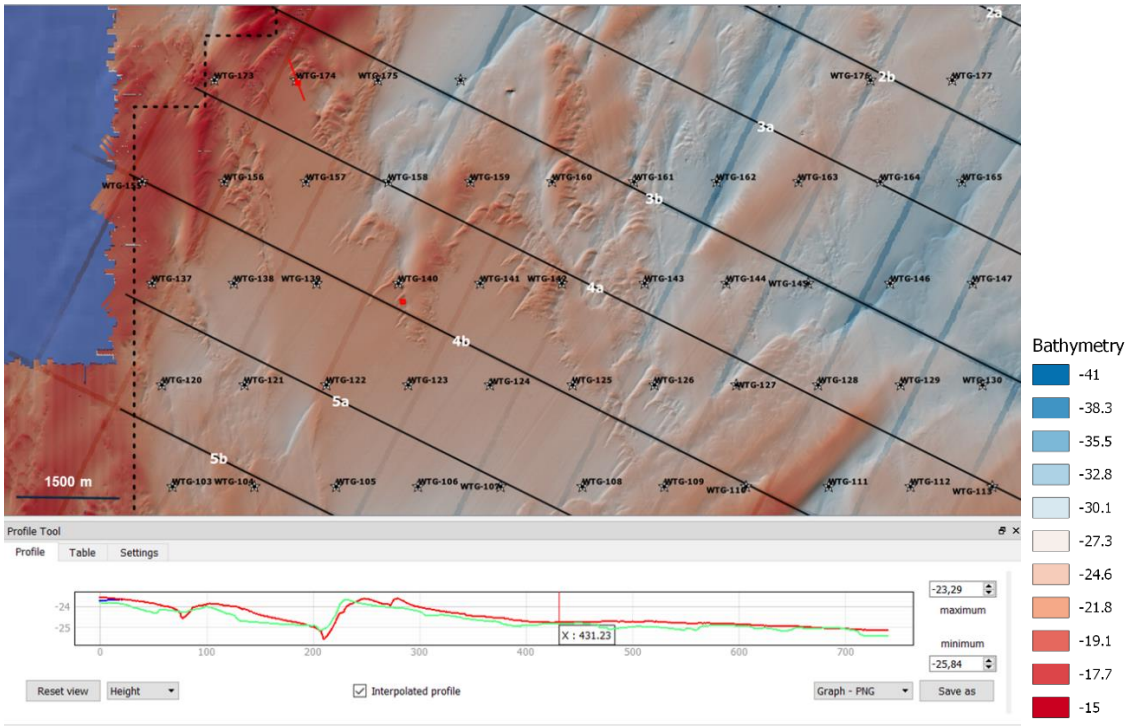

Figure 5-13 Sand wave profile (bottom) in the vicinity of wtg-174. NOAA survey from 2011 (green) and TERRASOND survey from 2020 (red).
The vertical red line along the profile mark the position of the wind turbine.

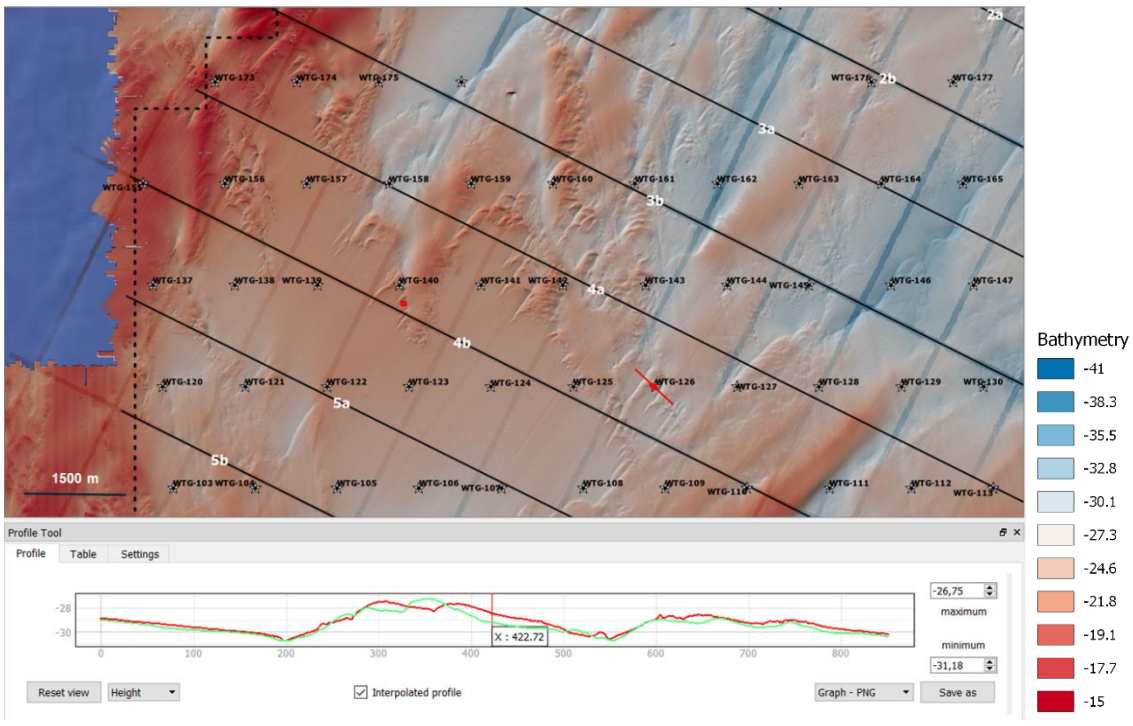

Figure 5-14 Sand wave profile (bottom) in the vicinity of wtg-126. NOAA survey from 2011 (green) and TERRASOND survey from 2020 (red).
The vertical red line along the profile mark the position of the wind turbine.

5.5 Synthesis: Lease Area

In Figure 5-15 we present the synthesis of the seabed dynamics in the lease area. Each red arrow represents a moving bedform (sand wave or sand ridge) with migration rates that could be estimated.

The area can be divided into a stable seabed part (north east of the lease area) and a dynamic seabed area (south west and north west of the area).

Estimations of bedform migration rates and expected variation of the seabed elevation are indicated on the left of the figure.

Along sand ridges and sand wave paths, the variation of the seabed elevation should not exceed 1 meter during the next 30 years (average 0.5 m in the next 30 years). Around localized erosion spots the variation of the seabed level is up to 5 cm per year.

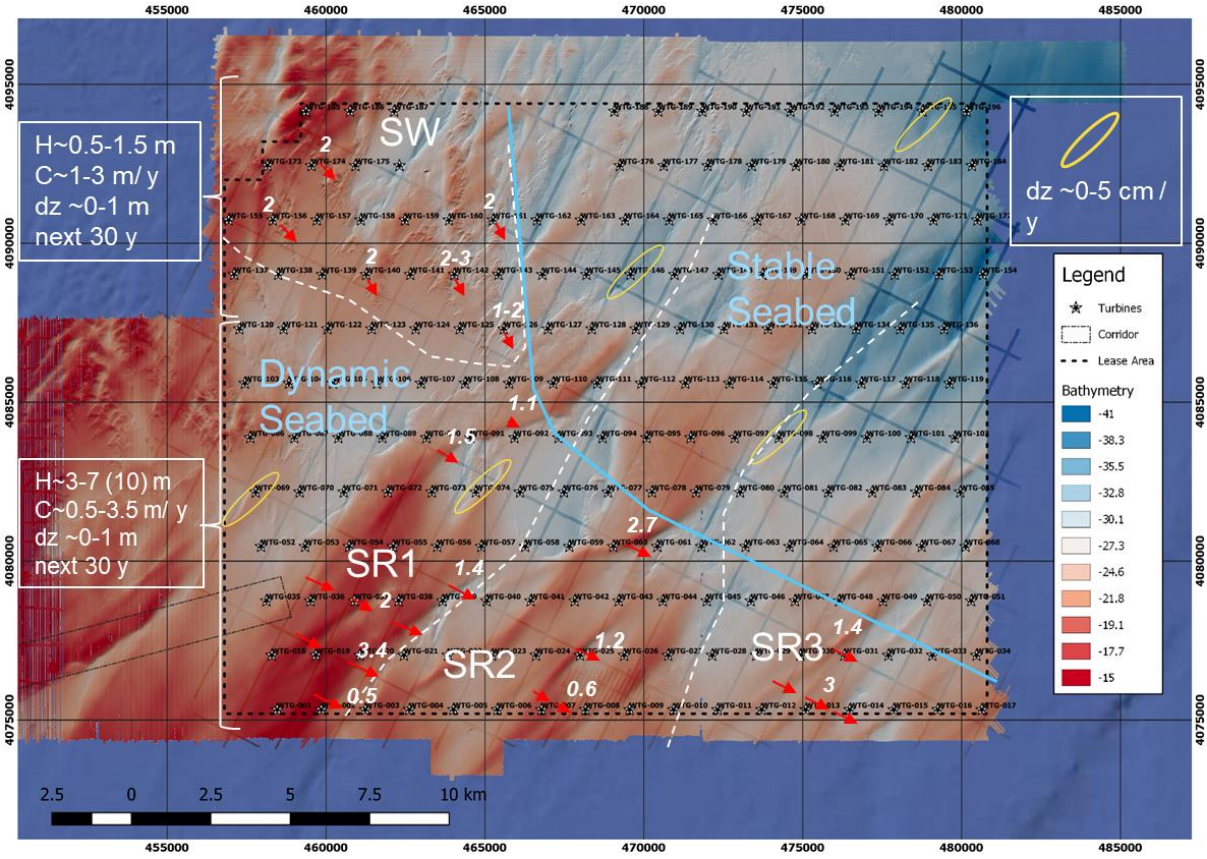

Figure 5-15 Synthesis of the seabed dynamics in the lease area.
'C' are the migration rates. Values of migration rates are indicated on the figure (unit is m/year). 'H' stands for the bedform height. 'dz' is the local bed elevation variation. 'SW' and 'SR' are the sand wave and sand ridge fields, respectively.

This page is intentionally left blank.

6 Export Cable Route Corridor Seabed Dynamics

6.1 Description

The export cable route corridor runs from the shore to the lease area and has a length of 44 km by an average width of 1.4 km (up to 2.3 km in the cable crossing part of the route). Depths are in the range -26 m to -9 m and decreasing from offshore, to the east, to the nearshore, to the west. Rambøll established a preliminary Kilometre Posting (KP intervals) list for the export cable route corridor (Figure 6-2 and Figure 6-3). Various bedforms of different sizes are present on the seabed, mostly sand waves of 1 to 2 m high and 100 to 300 m wavelength, distributed here and there, and a sand ridge in the eastern part of the export cable route corridor with a height of 6 meters. The sand ridge in the corridor does not appear to be connected/forming a continuous ridge that extends further into the lease area.

The bed features are mostly composed of coarse and poorly sorted sand, likewise the lease area, while the sediment in flat areas are a mix of sand and silt.

Eleven profiles were extracted along the export cable route corridor to investigate each sediment feature present on the seabed and assess their mobility and eventual migration rates. These profiles were complemented by two additional profiles C10a and C10b (aligned with the NOAA survey lines) to expand the analysis around a sand wave field. Each profile is extracted from the (north-)west to the (south-)east.

The analysis revealed that bedforms have higher migration rates in shallower waters, gradually from east to west, also generally higher than within the lease area. Migration rates were assessed according to the same methodology as for the ridges in the lease area (5.3). Table 6-1 synthesize the migration rates of the mobile bedforms in the export cable route corridor.

The expected migration rates vary between 1.5 and 18 meters per year, for the most mobile bedforms, at profile C10c. Sand wave migration will potentially induce changes in the bathymetry up to 2-2.5 m for the next 30 years along their migration paths near C10b and C10c. In the rest of the area changes in bathymetry are expected to remain in the range 0.5 to 1 meter.

It is noted that the bathymetry does not cover the area where the export cable crosses the shoreline and that the assessment of the seabed mobility on and near the shoreline is not included in the present study.

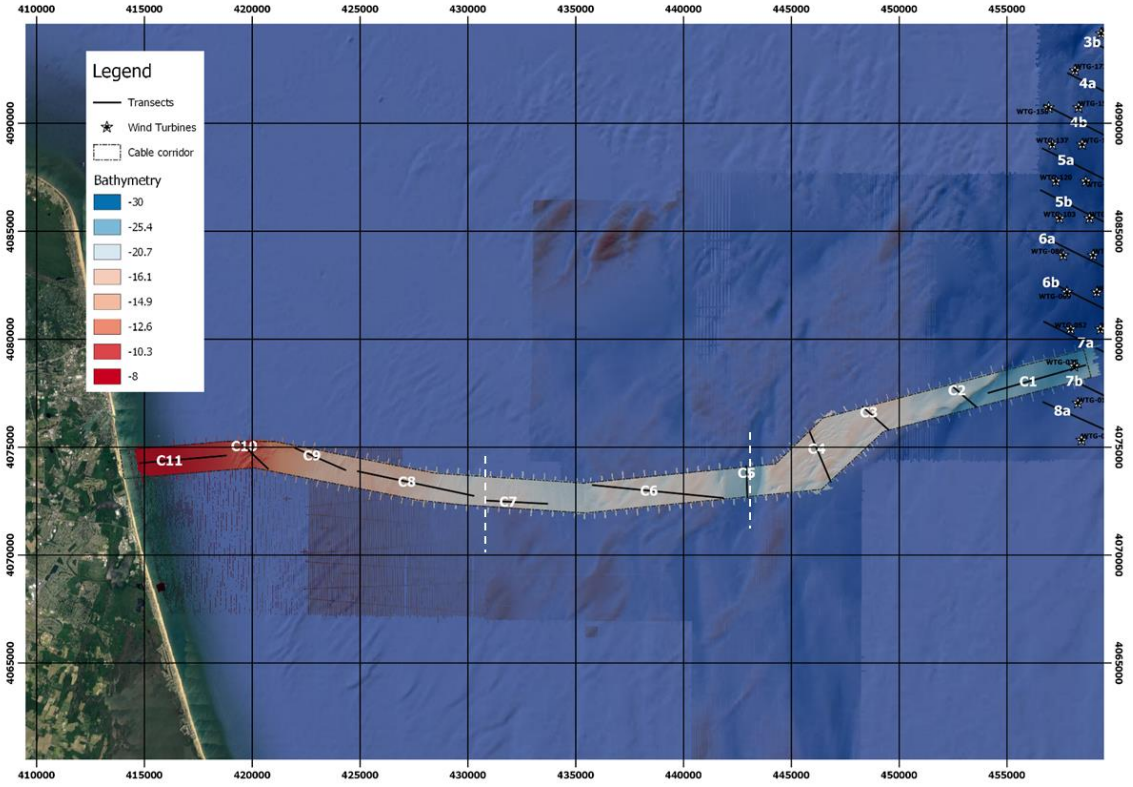

Figure 6-1 Overview of the export cable corridor.
Extracted profiles are represented by a black line.

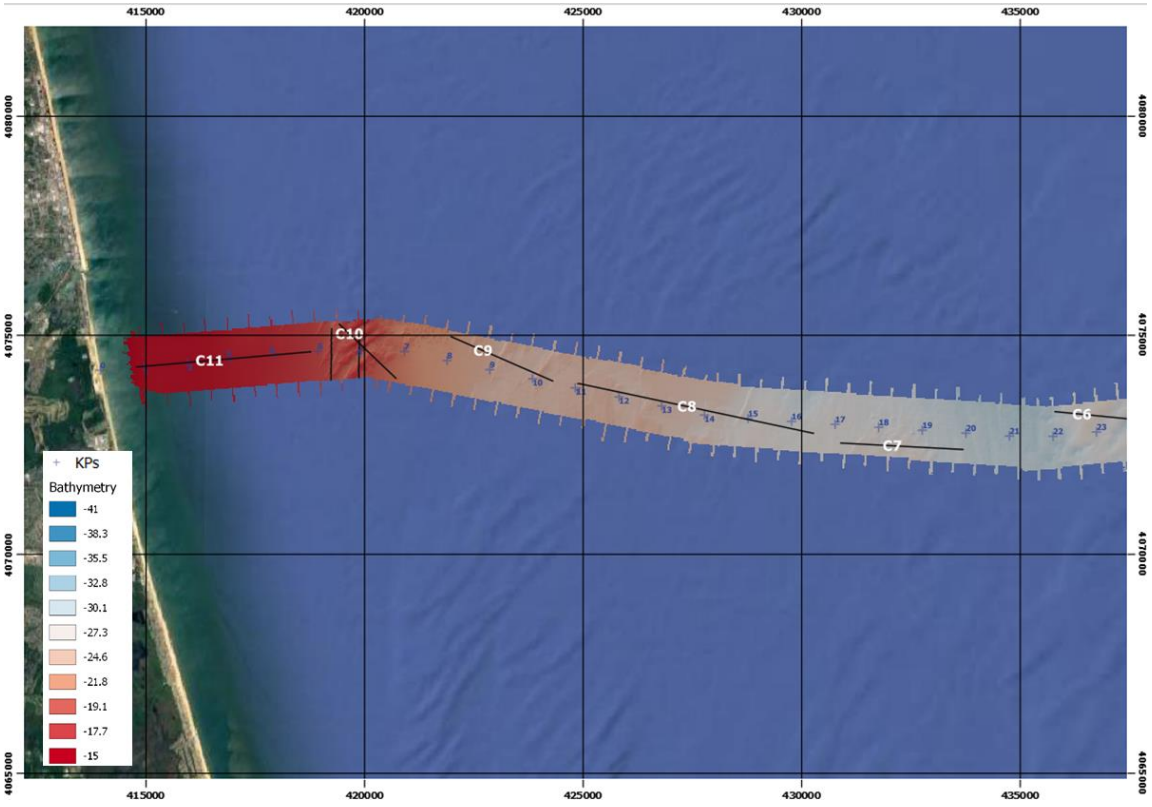

Figure 6-2 Position of the KP points along the western part of the export cable route.

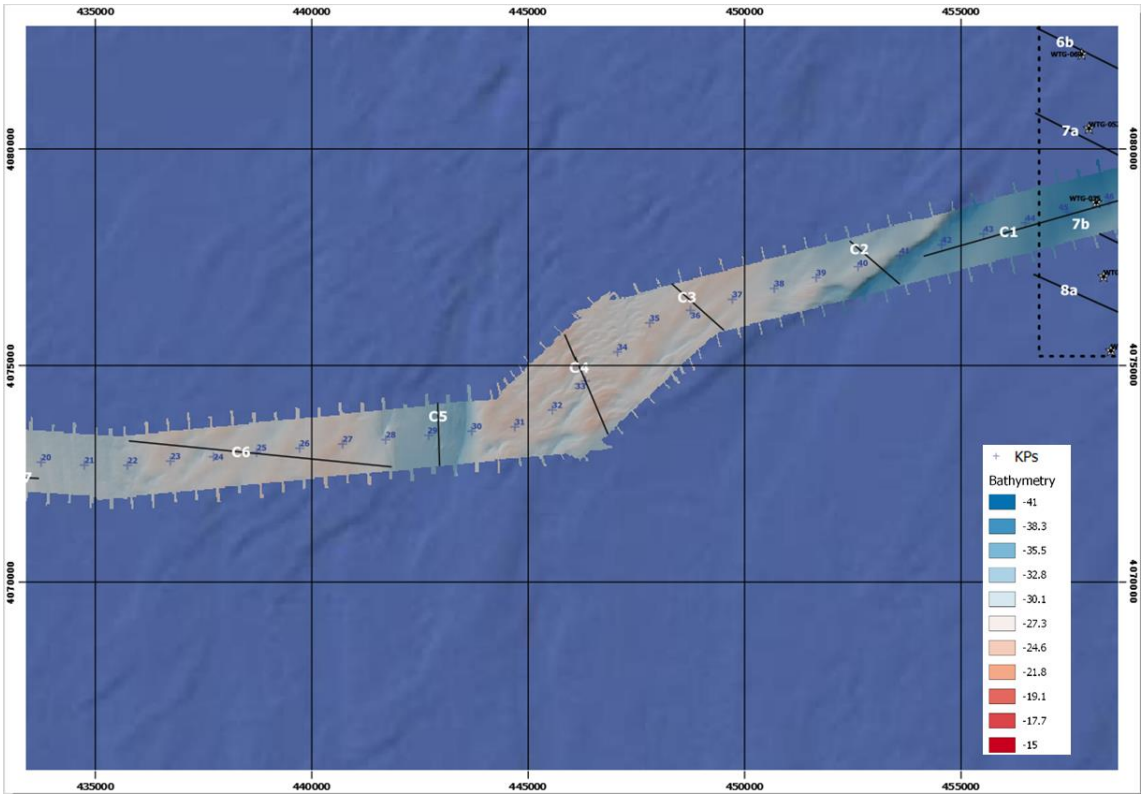

Figure 6-3 Position of the KP points along the eastern part of the export cable route.

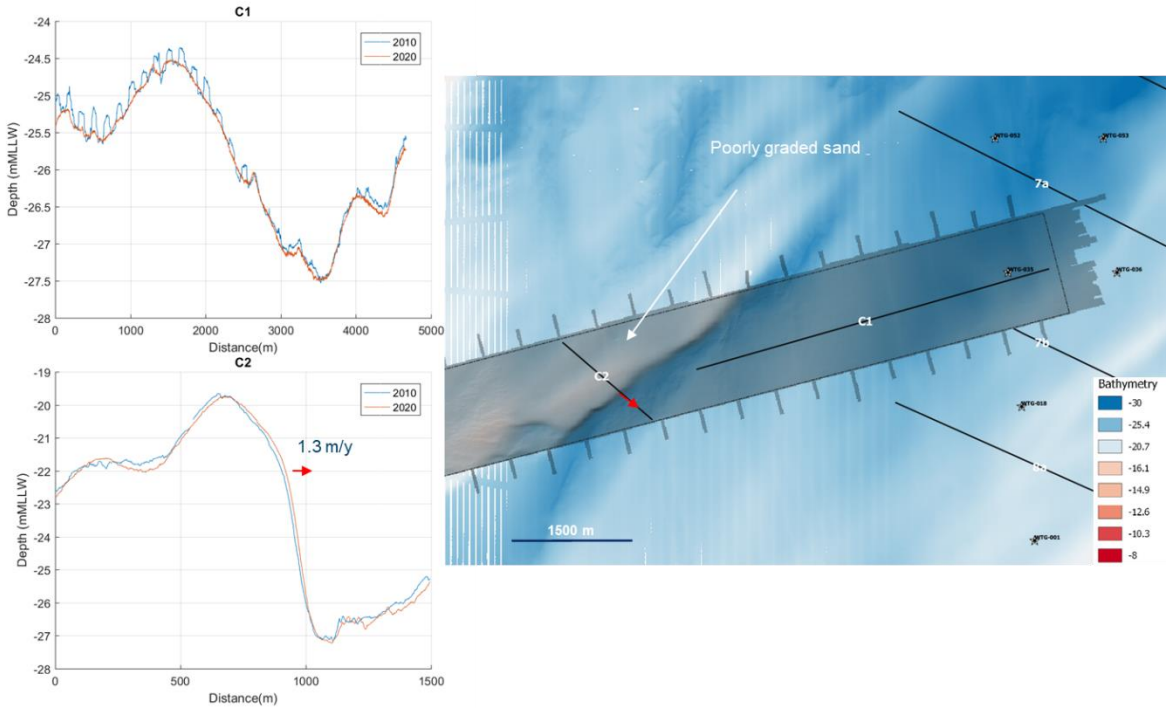

Figure 6-4 Bathymetric profiles C1 and C2 (left) and bathymetry (right).

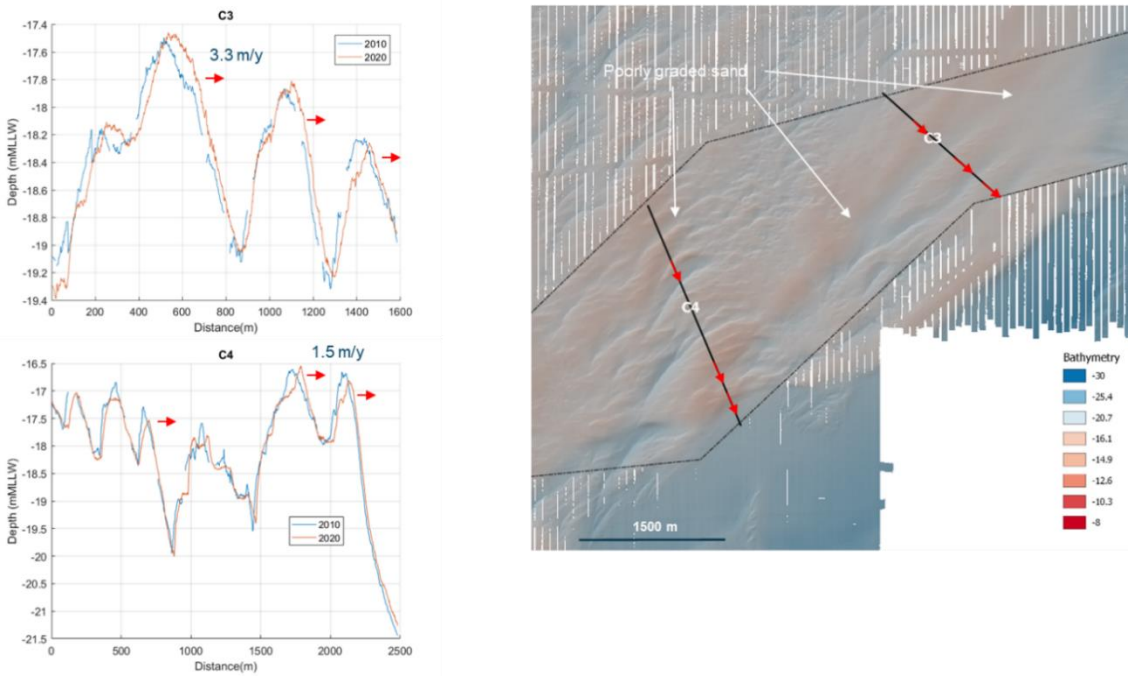

Figure 6-5 Bathymetric profiles C3 and C4 (left) and bathymetry (right).

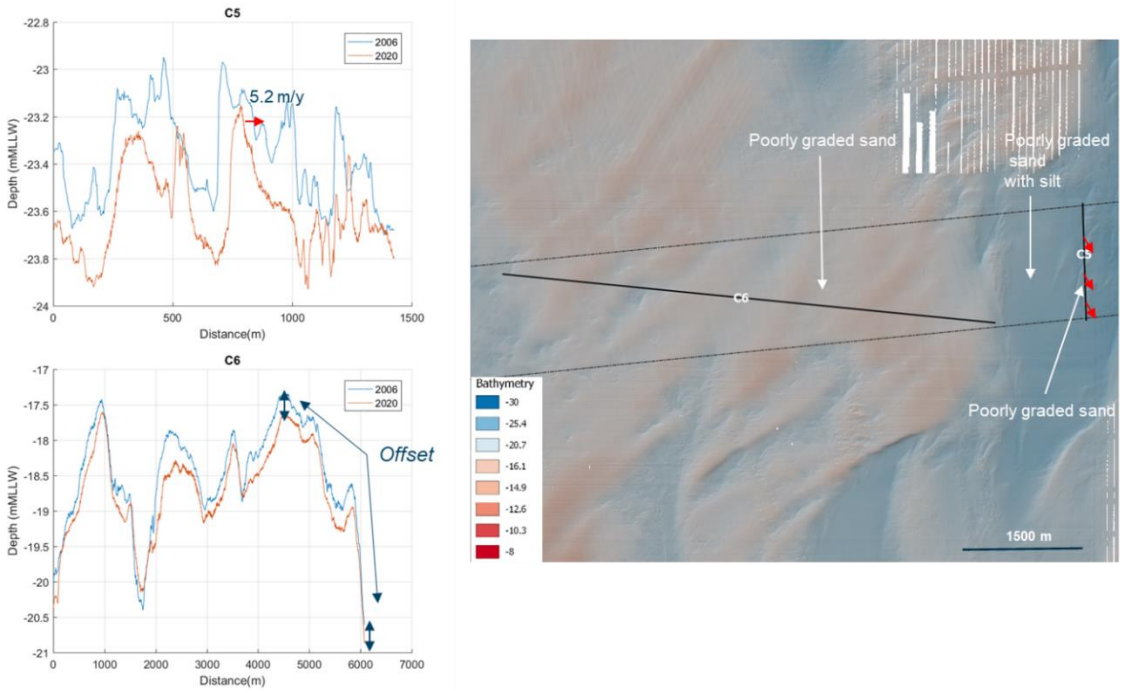

Figure 6-6 Bathymetric profiles C5 and C6 (left) and bathymetry (right).

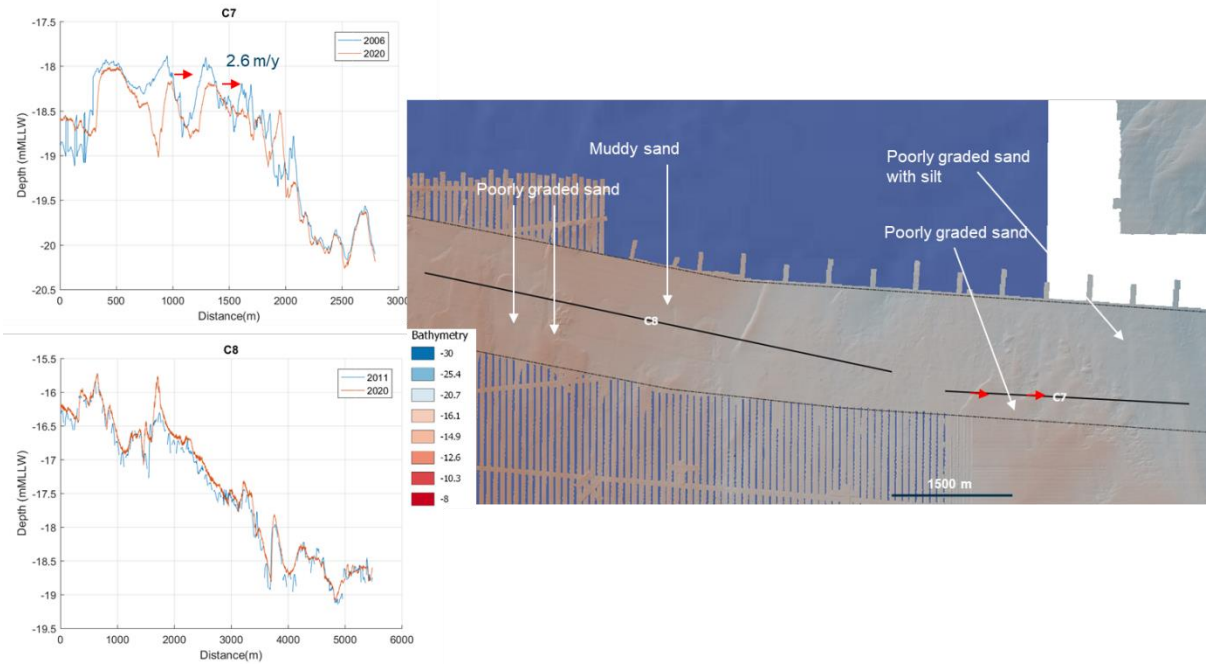

Figure 6-7 Bathymetric profiles C7 and C8 (left) and bathymetry (right).

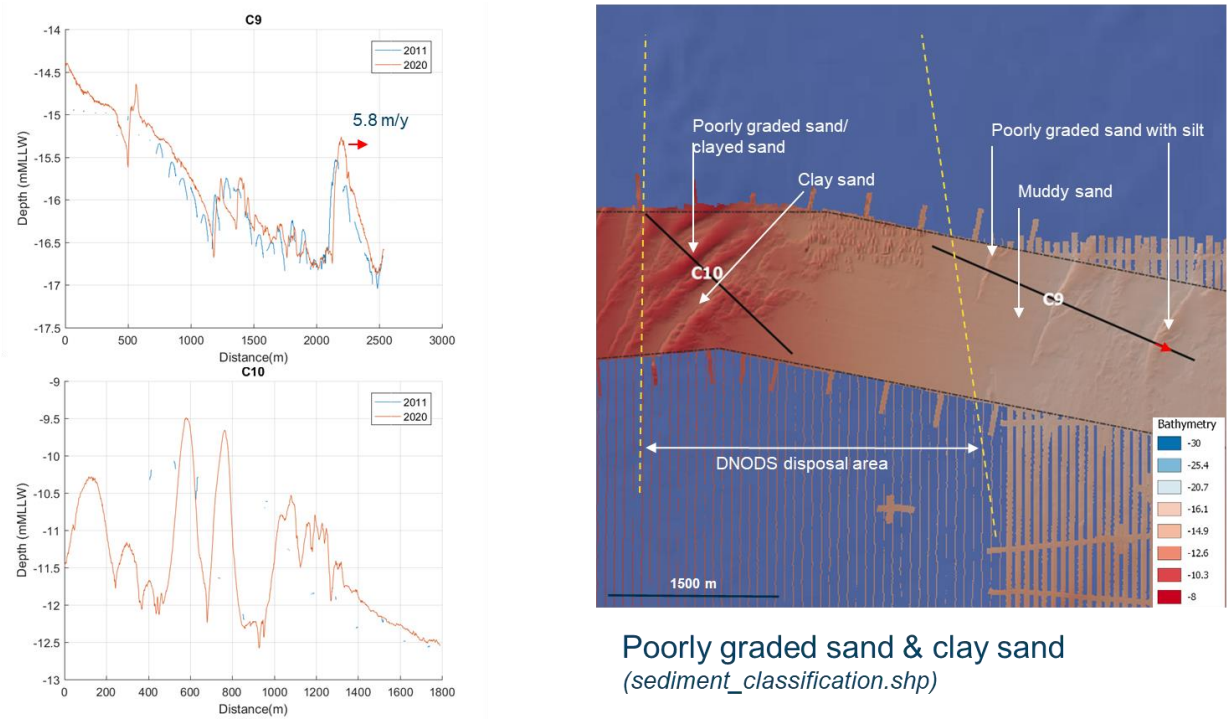

Figure 6-8 Bathymetric profiles C9 and C10 (left) and bathymetry (right).

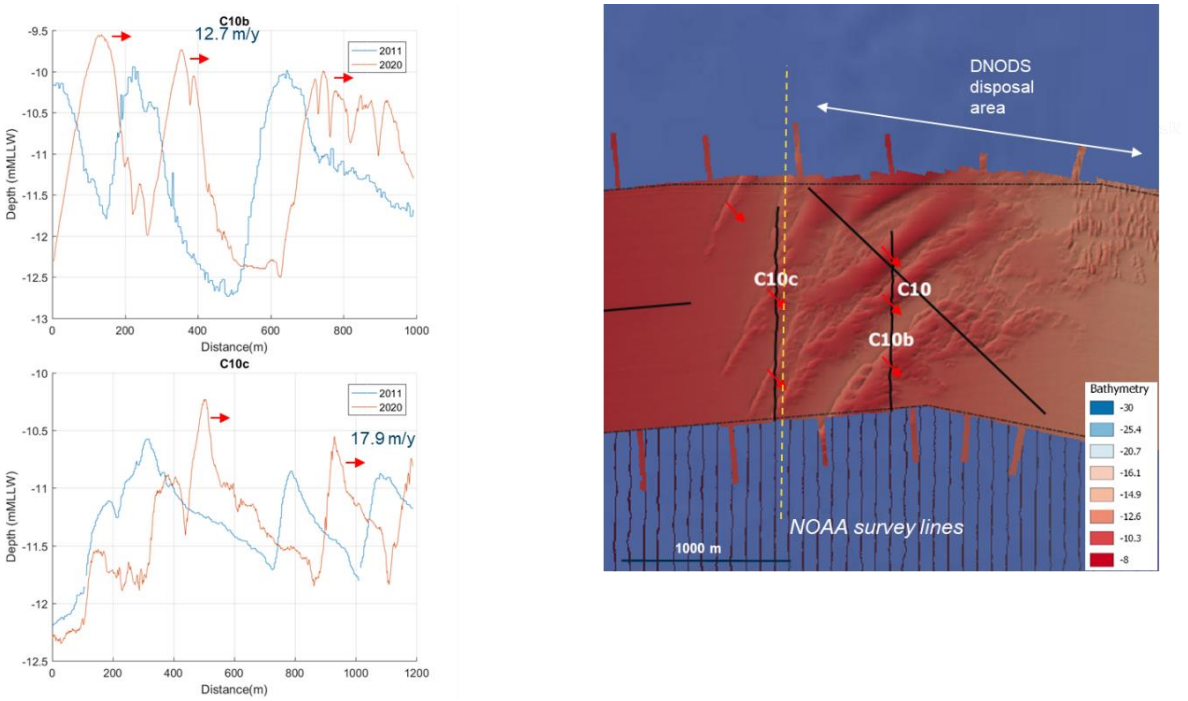

Figure 6-9 Bathymetric profiles C10b and C10c (left) and bathymetry (right).

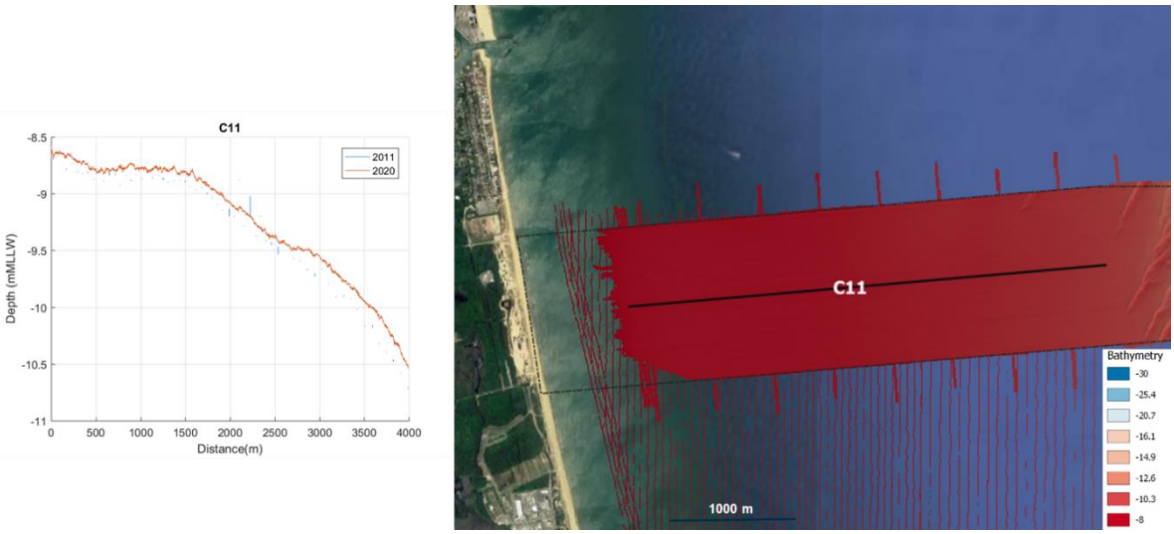

Figure 6-10 Bathymetric profile C11 (left) and bathymetry (right).

6.2 Migration Rates

Migration rates were assessed according to the same methodology as for the ridges in the lease area (5.3). Table 6-1 synthesize the migration rates of the mobile bedforms in the export cable route corridor.

It is seen that the highest migration rates correspond to a group of sand waves, at profiles C10b and C10c, with migration rates in the range 13 to 18 meters per year. C10b is lying within the DNODS disposal area.

Table 6-1 Estimated bedform mean and standard deviation (SD) migration rates.

Profile	Depth	Mid		30 y		
	range	Mean	SD	Mean	Mean-SD	Mean+SD
	[m MLLW]	[m/year]	[m/year]	[m/year]	[m/year]	[m/year]
C2	[-26 -20]	1.3	0.37	38.5	27.4	49.6
C3	[-18.8 -17.6]	3.3	2	98.7	37.8	159
C4	[-21 -17]	1.5	0.5	44.3	29.7	58.8
C5	[-23.8 -23.2]	5.2	1.48	155	111	200
C7	[-18.5 -18]	2.6	0.6	78	62	96
C9	[-16.8 -16]	5.8	1.9	173	114	231
C10b	[-12.5 -10]	12.7	2.14	381	317	445
C10c	[-11.7 -10.9]	17.9	0.5	538	523	553

6.3 Synthesis: Export Cable Route Corridor

Figure 6-11 present the synthesis map of the seabed mobility along the export cable route corridor. Light blue patches represent groups of mobile bedforms in the area. Other areas did not reveal any significant movement between the available surveys. The most mobile sand waves are localized within the DNODS disposal area (C10).

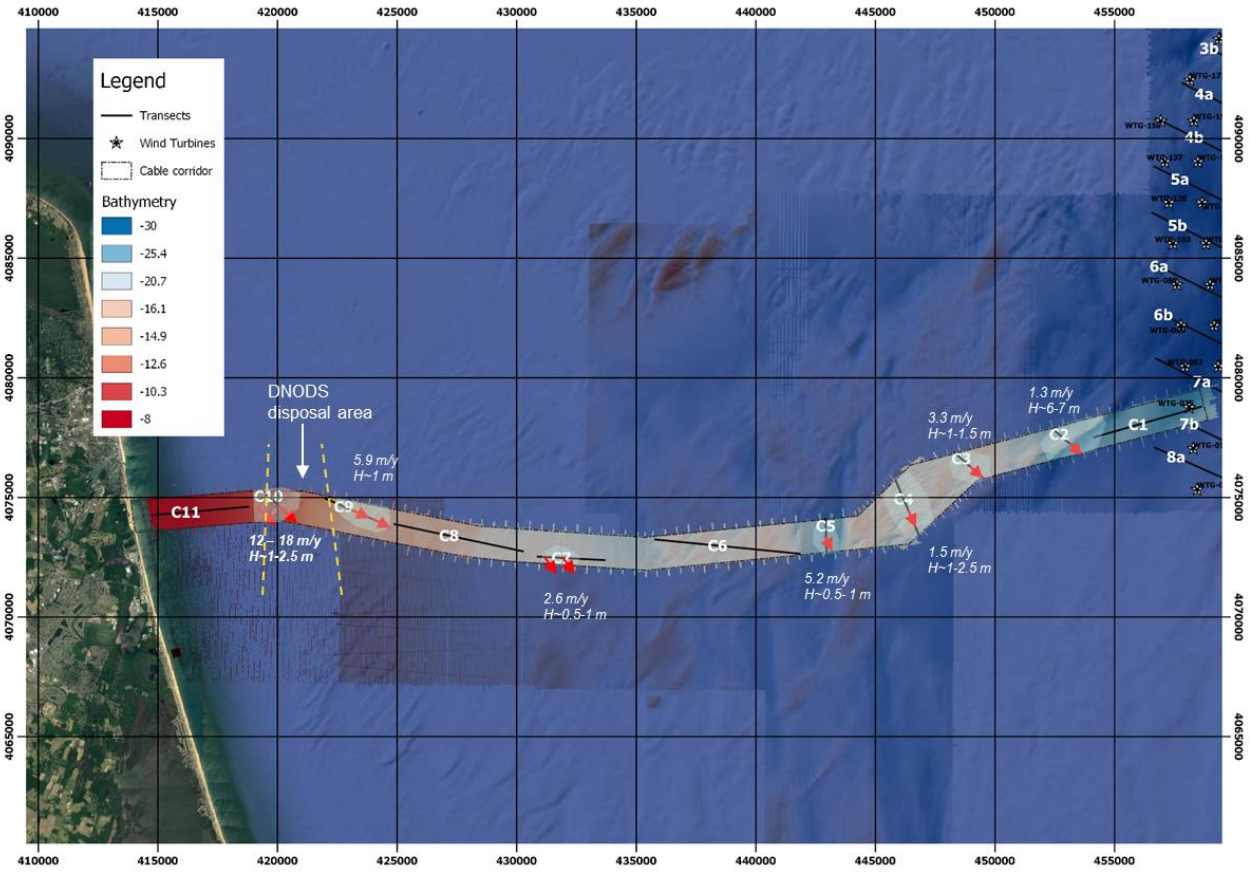

Figure 6-11 Synthesis of the seabed dynamics in the export cable route corridor.
Light blue patches represent the extension of the areas with migrating bedforms.

7 Prediction of Future Seabed Levels

Bedform migration rates were estimated in the previous sections. Values obtained allow the estimation of profiles migration and the related changes in the bathymetry in the vicinity of the wind turbines. In this section, we describe the methodology employed and the consecutive predicted changes of the bathymetry for the lease and export cable route corridor areas.

7.1 Methodology

The methodology implemented ensure a precise determination of the migration of the main bed features (sand waves and sand ridges) in the study area. It also accounts for the potential variability in migration directions by considering several profiles at each location. Noise generated by smaller disturbances is removed by using a low pass filter. The methodology follows a certain number of steps described as follows:

- The bathymetry from 2020 (Terrasond – Lease area & Alpine ECRC – corridor area) is filtered to remove smaller superimposed ripples using a low pass filter (Figure 7-1 and Figure 7-2).
- For each of the wind turbines located in mobile seabed areas, and each of the points in the export cable route corridor, three profiles with different orientations are extracted to account for the variability in the migration directions (Figure 7-3).
- At each location, a searching radius is computed based on the migration rates assessed in step 2. The standard deviation in the migration rates is taken into account leading to three different searching radius (mean migration, (mean migration) + (standard deviation), (mean migration-standard deviation)).
- Values of the average, maximum and minimum depths are computed along transects within the searching radii.
- A weighted average is performed for the three transects at each location to account for the most probable migration direction (bedform migration direction perpendicular to the crest).

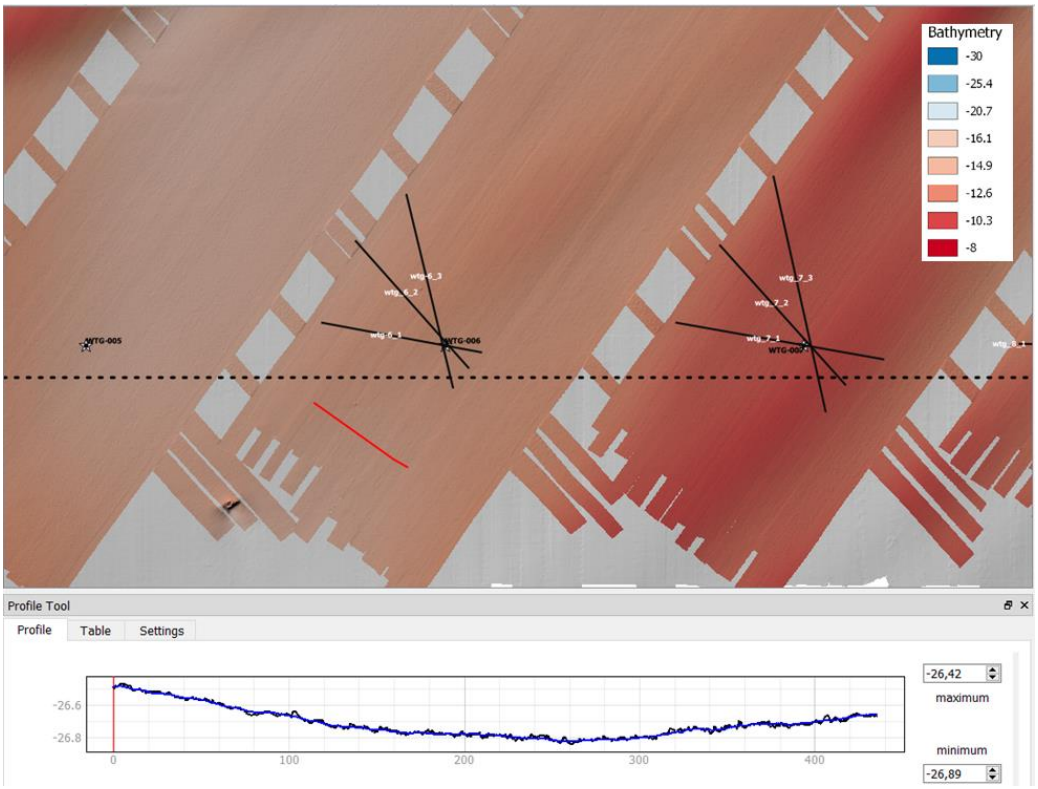

Figure 7-1 Example of bathymetry 'noise' filtering in the lease area.
Bathymetry (up) and extracted transects (bottom) along the red line in the upper figure. The black (blue) line stands for the original (filtered) depth. Extracted profiles for the depth variation analysis are represented by three black segments at each location (upper figure).

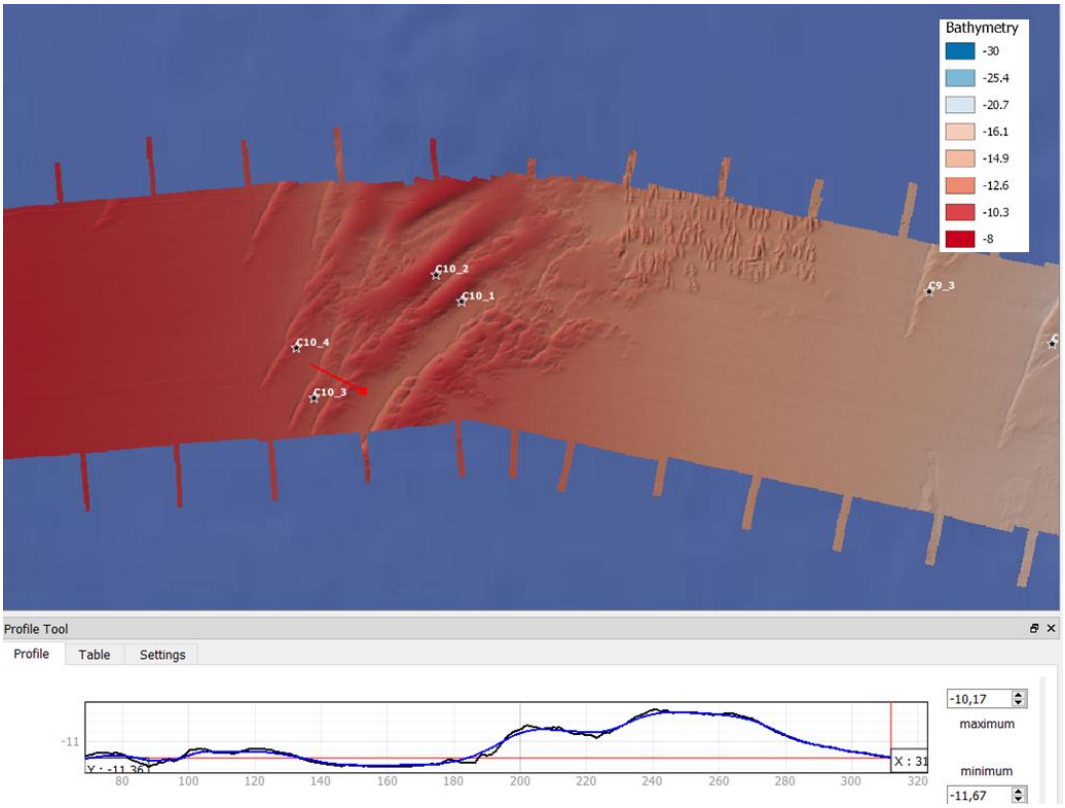

Figure 7-2 Example of bathymetry 'noise' filtering in the export cable corridor path.

7.2 Lease Area

As stated above, three profiles are extracted at each wind turbine location where bed mobility was detected between the surveys (see previous sections). At all locations, the middle transect is drawn perpendicular to the considered bedform's crest, meaning that the migration direction is most likely to occur in that direction. A total of ninety profiles at thirty locations were considered in the analysis (see Figure 7-3). Figure 7-4 and Figure 7-5 show four examples of how the searching radius is applied to anticipate future variations in the bathymetry depending on the migration rates.

Table 7-1 contains the projected values of the bed elevation at the wind turbine locations within the next 30 years from the analysis (see annex for the full table at all locations including where no significant movement was detected between the surveys). All values of bed elevation differences lie within the 0 to 1 meter interval with the majority of values around 0.5 meters difference or less. The maximum elevation difference is 1.5 meters at the two main erosional spots (wtg 146 and wtg 98) where a steady erosion rate of 5 cm per year was applied. Also, at wind turbines wtg 25, the bed will rise by 1 meter and at wtg 60 the bed will lower down by -1 m within the next 30 years due to the migration of the sand ridges.

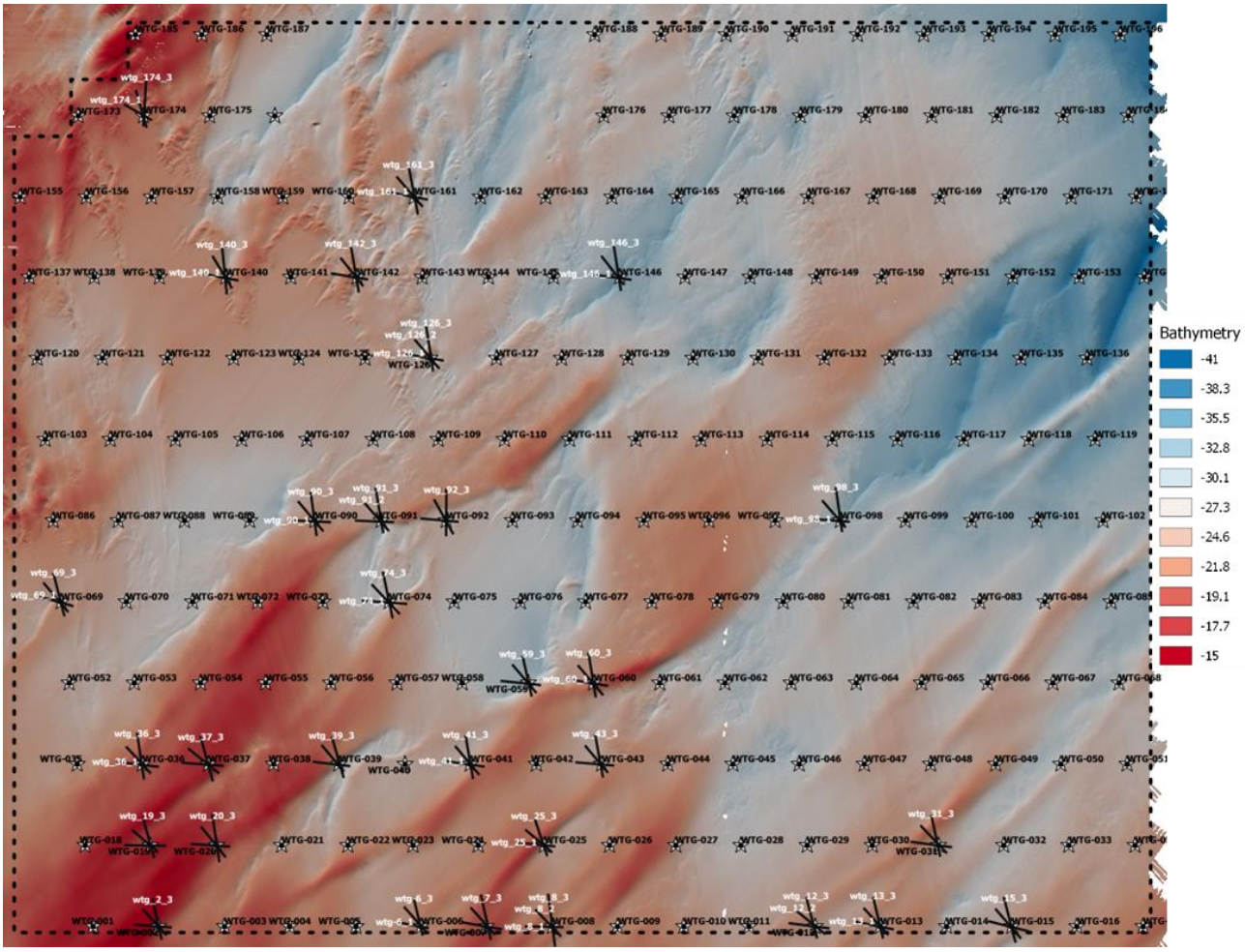

Figure 7-3 Location of the extracted transects for the analysis of the seabed variability.

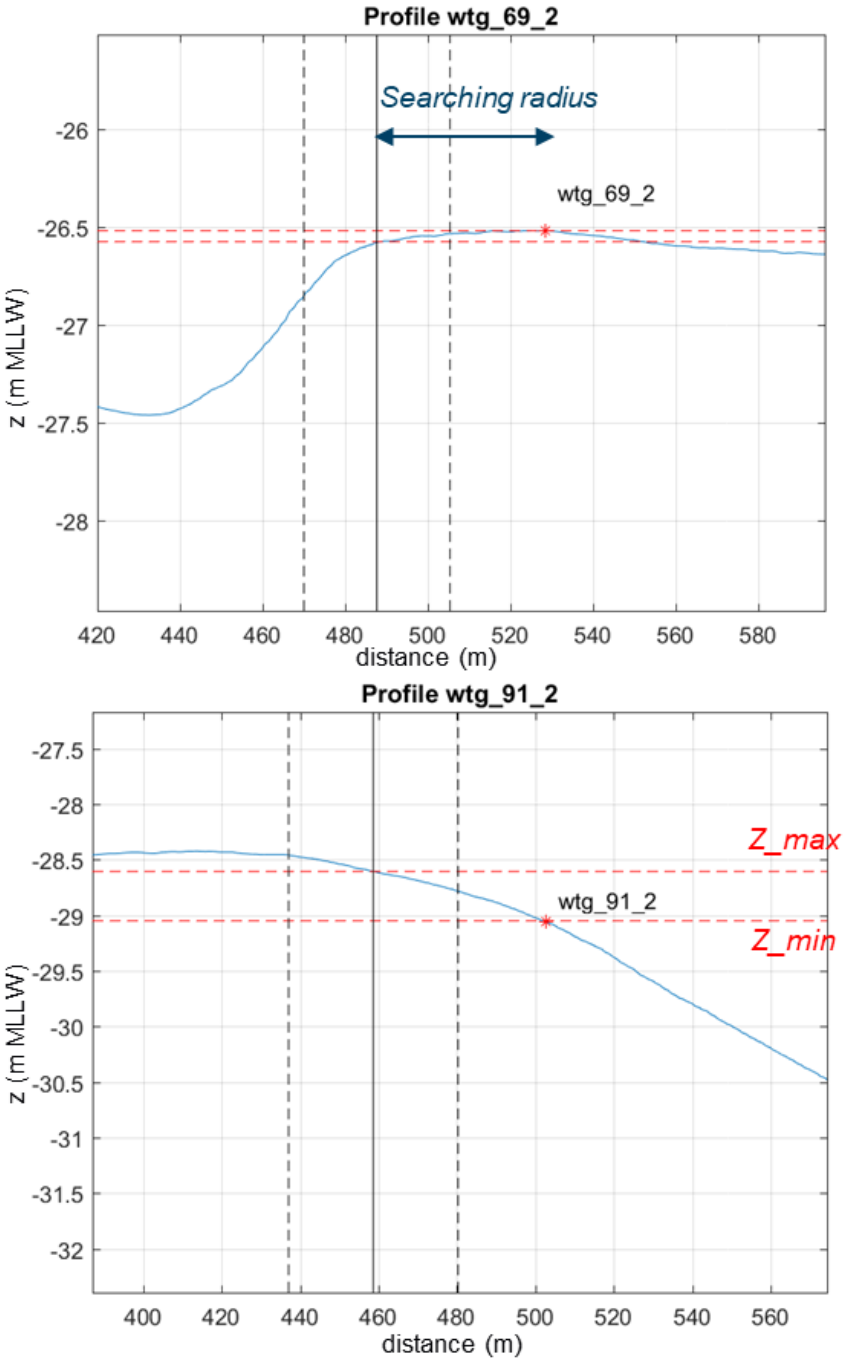

Figure 7-4 Extracted profiles at wind turbine number 69 (top) and 91 (bottom).
The searching radius for the computed migration rates (black line) and accounting for the standard deviation of the migration rate (dotted black lines) are shown on the figures. The red dotted lines show the maximum and minimum levels of the bathymetry within the searching radius. The red star corresponds to the present position of the wind turbine.

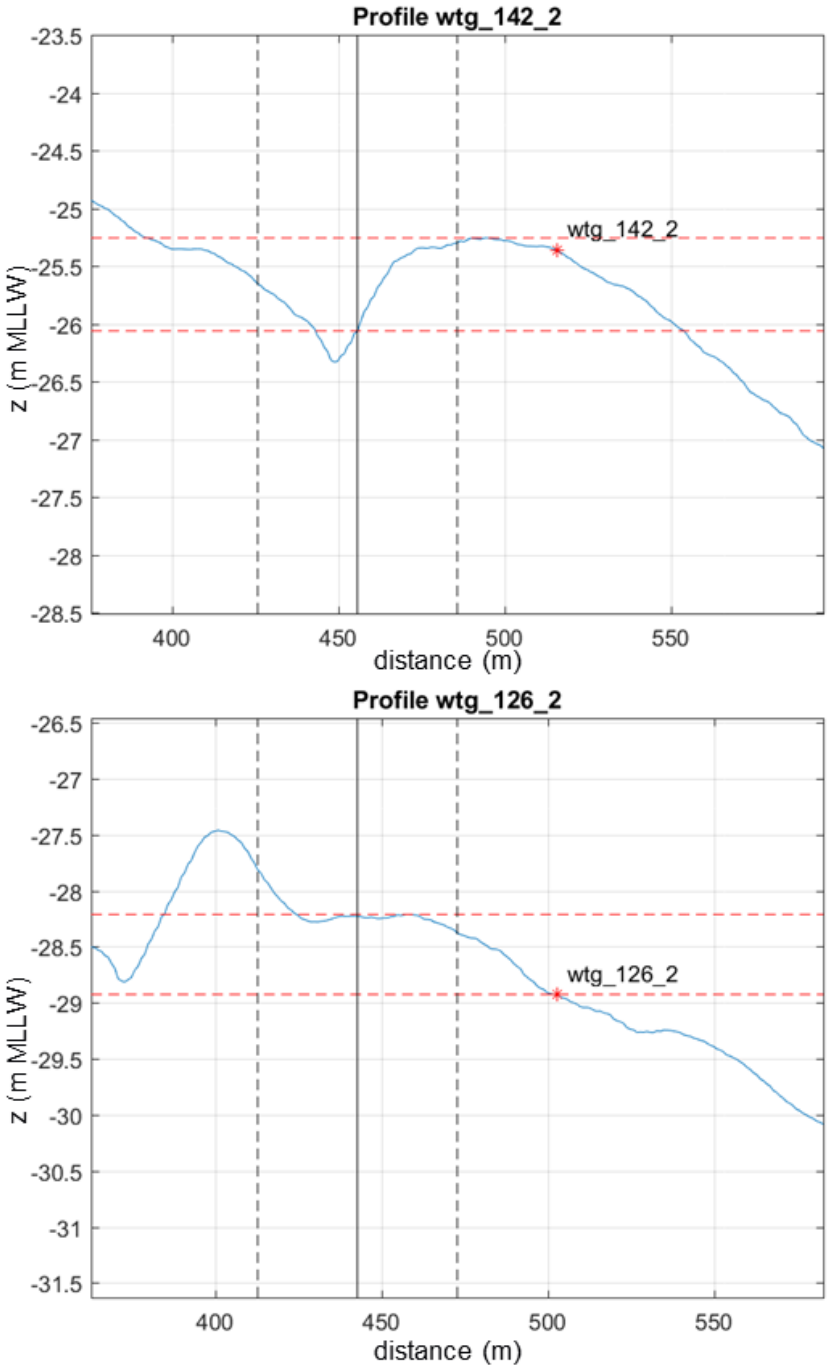

Figure 7-5 Extracted profiles at wind turbine number 142 (top) and 126 (bottom). The searching radius for the computed migration rates (black line) and accounting for the standard deviation of the migration rate (dotted black lines) are shown on the figures.

Table 7-1 Computed mean bed elevation at the present time (Z_pres), maximum bed elevation (Z_max), minimum bed elevation (Z_min), and mean bed elevation for the next 30 years (Z_mean).
Other fields present the same parameters considering the positive and negative standard deviation of the computed migration rate. Note that wtg 98 and wtg 146 are subjected to an average steady erosion of 5 centimetres per year and no standard deviation is considered.

Turbine #	Z_pres	Z_max	Z_min	Z_mean	Z_max+std	Z_min+std	Z_mean+std	Z_max-std	Z_min-std	Z_mean-std
wtg_126	-29.0	-28.2	-28.9	-28.5	-27.9	-28.9	-28.3	-28.4	-28.9	-28.7
wtg_12	-27.4	-27.0	-27.4	-27.3	-26.9	-27.4	-27.2	-27.2	-27.4	-27.3
wtg_13	-27.4	-27.2	-27.4	-27.3	-27.1	-27.4	-27.3	-27.3	-27.4	-27.3
wtg_140	-24.5	-24.1	-25.1	-24.4	-24.1	-25.2	-24.6	-24.1	-24.5	-24.2
wtg_142	-25.4	-25.3	-26.0	-25.5	-25.2	-26.2	-25.6	-25.3	-25.4	-25.3
wtg_146	-34.5	-36.0	-34.5	-	-	-	-	-	-	-
wtg_15	-27.2	-27.2	-27.7	-27.5	-27.2	-27.9	-27.6	-27.2	-27.6	-27.4
wtg_161	-28.2	-28.0	-28.4	-28.2	-27.9	-28.7	-28.2	-28.1	-28.4	-28.3
wtg_174	-24.6	-24.3	-24.6	-24.5	-24.1	-24.6	-24.4	-24.5	-24.6	-24.6
wtg_19	-21.2	-21.2	-21.9	-21.6	-21.2	-22.0	-21.6	-21.2	-21.8	-21.5
wtg_20	-21.9	-21.9	-22.1	-22.0	-21.9	-22.1	-22.0	-21.9	-22.1	-22.0
wtg_25	-26.7	-25.7	-26.7	-26.2	-25.3	-26.7	-26.0	-26.1	-26.7	-26.4
wtg_2	-21.8	-21.6	-21.8	-21.7	-21.1	-21.8	-21.5	-21.8	-21.8	-21.8
wtg_31	-27.5	-27.3	-27.5	-27.4	-27.2	-27.5	-27.4	-27.4	-27.5	-27.5
wtg_36	-23.5	-23.5	-23.5	-23.5	-23.5	-23.5	-23.5	-23.5	-23.5	-23.5
wtg_37	-21.6	-21.6	-21.8	-21.7	-21.6	-21.8	-21.7	-21.6	-21.8	-21.7
wtg_39	-29.7	-28.8	-29.6	-29.3	-28.2	-29.6	-29.0	-29.2	-29.6	-29.5
wtg_41	-27.3	-27.3	-27.8	-27.6	-27.3	-27.9	-27.7	-27.3	-27.6	-27.5
wtg_43	-27.2	-27.2	-27.3	-27.3	-27.2	-27.4	-27.3	-27.2	-27.3	-27.2
wtg_59	-31.7	-31.8	-32.2	-32.1	-31.8	-32.2	-32.1	-31.8	-32.2	-32.1
wtg_60	-24.4	-24.4	-25.4	-24.9	-24.4	-25.5	-25.0	-24.4	-25.2	-24.8
wtg_69	-26.5	-26.5	-26.6	-26.6	-26.5	-26.9	-26.6	-26.5	-26.6	-26.5
wtg_6	-26.1	-26.1	-26.1	-26.1	-26.0	-26.1	-26.1	-26.1	-26.1	-26.1
wtg_74	-30.1	-30.0	-30.2	-30.1	-30.0	-30.2	-30.1	-30.0	-30.1	-30.0
wtg_7	-23.2	-23.2	-23.3	-23.2	-23.2	-23.4	-23.3	-23.2	-23.2	-23.2
wtg_8	-25.4	-25.4	-25.4	-25.4	-25.4	-25.5	-25.4	-25.4	-25.4	-25.4
wtg_90	-26.6	-26.6	-26.6	-26.6	-26.6	-26.6	-26.6	-26.6	-26.6	-26.6
wtg_91	-29.1	-28.7	-29.1	-28.9	-28.6	-29.1	-28.8	-28.8	-29.1	-29.0
wtg_92	-28.8	-28.8	-28.9	-28.8	-28.8	-28.9	-28.9	-28.8	-28.8	-28.8
wtg_98	-32.0	-33.5	-32.0	-	-	-	-	-	-	-

7.3 Export Cable Route Corridor

For the export cable route corridor, a series of points were carefully selected to perform the analysis of the seabed mobility. The points are located at strategic locations where the seabed is the most dynamic in agreement with the findings in section 6. Consequently, each point is representative of the migration rates of the group of bedforms present in the area considered (blue patches in Figure 6-11).

As stated above, three profiles are extracted at each point location where bed mobility was detected between the surveys. At all locations, the middle transects is drawn perpendicular to the considered bedform's crest, meaning that the migration direction is most likely to occur in that direction. Fifty-four profiles at eighteen locations were considered in the analysis (see Figure 7-6).

Table 7-2 contains the projected values of the bed elevation at the point locations within the next 30 years assessed during the analysis. Sand waves in the export cable route corridor are much more mobile than the bedforms in the lease area. As a consequence, bed elevation changes are more important with values up to 2 meters. This is particularly the case in the c10 area (Figure 6-11), where a group of highly mobile sand dunes is present (migration rates up to 18 m/y, see section 6.2). Immediately downstream of the sand ridge in the C2 area, towards the south east, a bed elevation of + 1.8 meters is to be expected within the next 30 years due to the migration of the ridge 40 to 50 meters downstream. The group of sand waves in the C3 and C9 areas will engender changes of the order of 1 meter along their migration path, over a distance that

depends on their migration rates. For C4 to C7, changes of the order of 0.5 meters in the next 30 years are expected.

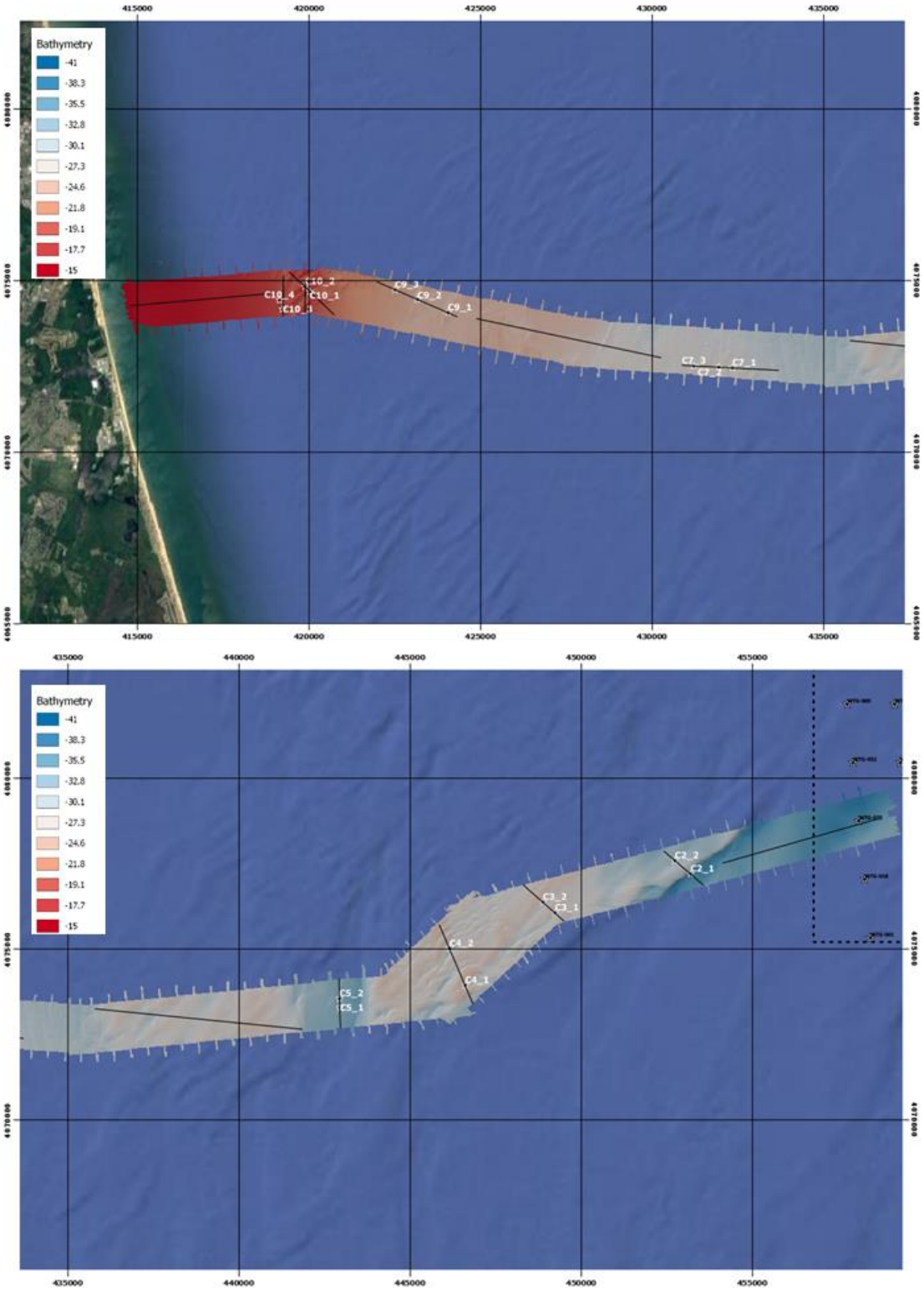

Figure 7-6 Location of the points selected for the analysis of the seabed elevation in the export cable route corridor.

Table 7-2 Computed mean bed elevation at the present time (Z_pres), maximum bed elevation (Z_max), minimum bed elevation (Z_min), and mean bed elevation for the next 30 years (Z_mean).
Other fields present the same parameters considering the positive and negative standard deviation of the computed migration rate.

prof	Z_pres	Z_max	Z_min	Z_mean	Z_max+std	Z_min+std	Z_mean+std	Z_max-std	Z_min-std	Z_mean-std
C10_1	-11.7	-9.6	-12.2	-10.8	-9.6	-12.2	-11.0	-9.6	-12.0	-10.6
C10_2	-10.3	-9.5	-12.1	-11.1	-9.5	-12.1	-11.1	-9.5	-12.1	-11.2
C10_3	-11.0	-10.4	-11.5	-10.9	-10.4	-11.5	-10.9	-10.4	-11.5	-10.9
C10_4	-10.6	-10.3	-11.3	-10.8	-10.3	-11.3	-10.8	-10.3	-11.3	-10.8
C2_1	-26.1	-24.3	-26.1	-25.3	-23.8	-26.1	-25.0	-24.9	-26.1	-25.5
C2_2	-21.9	-21.9	-22.0	-21.9	-21.9	-22.0	-21.9	-21.9	-21.9	-21.9
C3_1	-18.8	-17.9	-18.8	-18.3	-17.9	-18.7	-18.2	-18.4	-18.7	-18.6
C3_2	-18.4	-17.8	-18.4	-18.1	-17.5	-18.4	-17.9	-18.1	-18.4	-18.3
C4_1	-17.8	-17.4	-17.8	-17.6	-17.3	-17.8	-17.5	-17.5	-17.8	-17.7
C4_2	-18.1	-17.6	-18.1	-17.8	-17.6	-18.1	-17.7	-17.7	-18.1	-17.9
C5_1	-23.4	-23.2	-23.9	-23.6	-23.2	-23.9	-23.6	-23.2	-23.9	-23.5
C5_2	-23.5	-23.3	-23.9	-23.7	-23.3	-23.9	-23.6	-23.4	-23.9	-23.7
C7_1	-18.4	-18.2	-18.4	-18.3	-18.2	-18.4	-18.2	-18.2	-18.4	-18.3
C7_2	-18.5	-18.3	-18.5	-18.4	-18.3	-18.6	-18.4	-18.3	-18.5	-18.4
C7_3	-18.3	-18.3	-18.8	-18.7	-18.3	-18.8	-18.7	-18.3	-18.8	-18.7
C9_1	-15.6	-15.3	-16.6	-15.8	-15.3	-16.8	-16.0	-15.3	-16.3	-15.5
C9_2	-16.1	-15.8	-16.5	-16.1	-15.8	-16.5	-16.1	-15.8	-16.5	-16.1
C9_3	-14.7	-14.7	-15.4	-15.1	-14.7	-15.4	-15.1	-14.7	-15.4	-15.1

7.4 Disposal Sites

The Atlantic Ocean Channel is part of the Port of Virginia and Baltimore system of channels, and is the segment providing access for all ships calling on port facilities, naval bases, and shipyards in the Hampton Roads, York River and Baltimore areas. All commercial tonnage entering and leaving the Ports of Virginia and Baltimore pass through this channel. The channel is currently maintained to a full width and a required depth of 52 feet to enable loaded colliers, container ships and military vessels to transit the channel with ship drafts as great as 50 feet. Material is typically dredged via hopper dredge from this channel. Dredged material is placed at Dam Neck Ocean Disposal Site (DNODS). The sediment composition in this channel segment is largely fine sand (85%) with some silt (15%).

The DNODS disposal site is overlapping the export cable corridor route around profiles C10 (Figure 7-9). Figure 7-10 and Figure 7-11 show two examples of bathymetric differentials around the DNODS area (2011 and 2020 surveys). The figures show differentials of up to 1.5 m due to the regular disposal of sediment linked to the dredging of the access channel in Chesapeake Bay. Note that the NOAA data is far from covering the whole area. There are potentially higher bathymetric differentials between the surveys in the disposal area.

No study on the monitoring of the fate of the disposed sediment was found. Nevertheless, the sediment is repositing in an area where active sand waves are present. The fine sediment lying on an otherwise silty bottom has therefore the potential to generate sand waves that will potentially migrate towards the south east. The available bathymetric surveys did not allow for a careful analysis of the fate of the deposited sediment. It is highly recommended to engage a monitoring campaign of the disposal area or to enter in contact with local authorities to investigate if monitoring campaigns are planned.

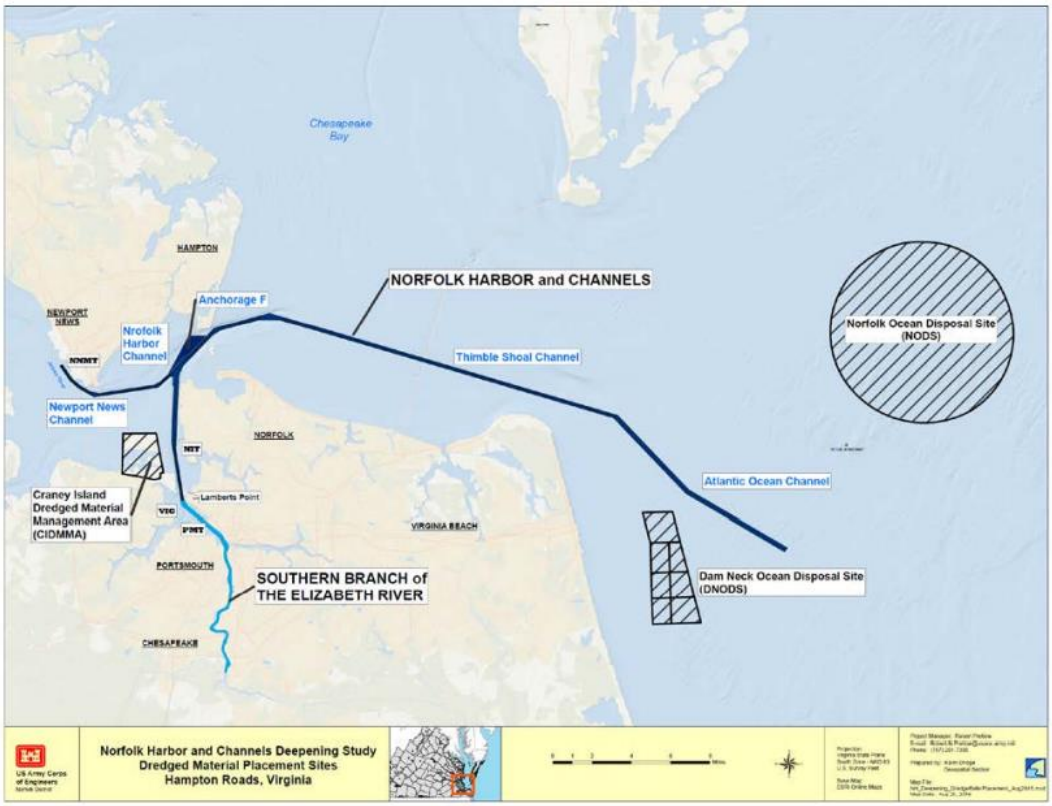

Figure 7-7 The Norfolk Harbor and Channels from the Atlantic Ocean Channel to the Lamberts Bend. Dredged material placement/disposal sites are shown within the hatched areas (US Army corps of Engineers).

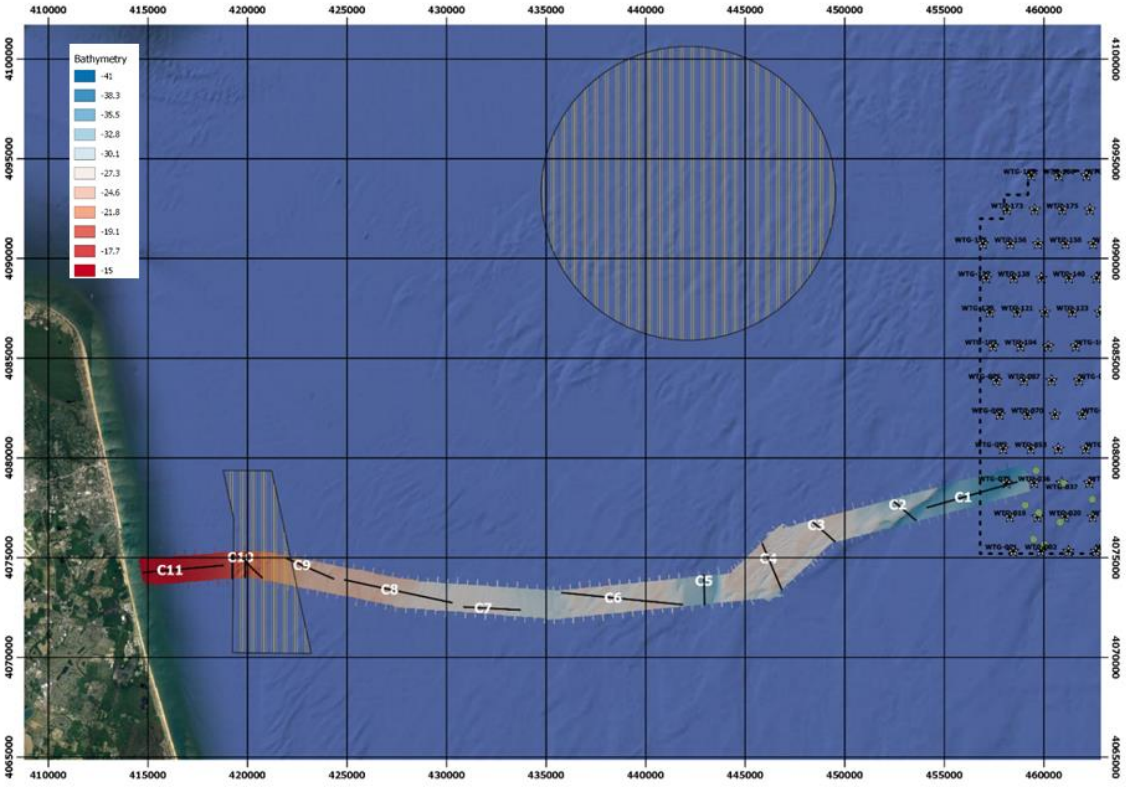

Figure 7-8 Location of the disposal sites around the study area (yellow hatched areas).

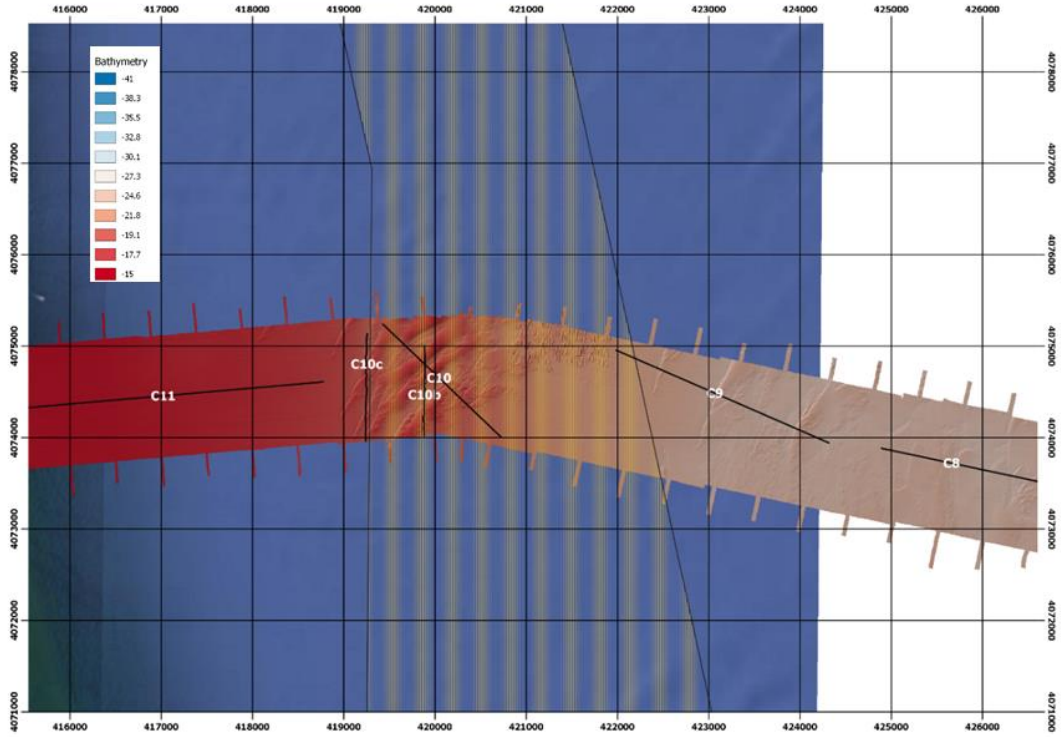

Figure 7-9 Close up view of the disposal sites around C10 profiles (yellow hatched area).

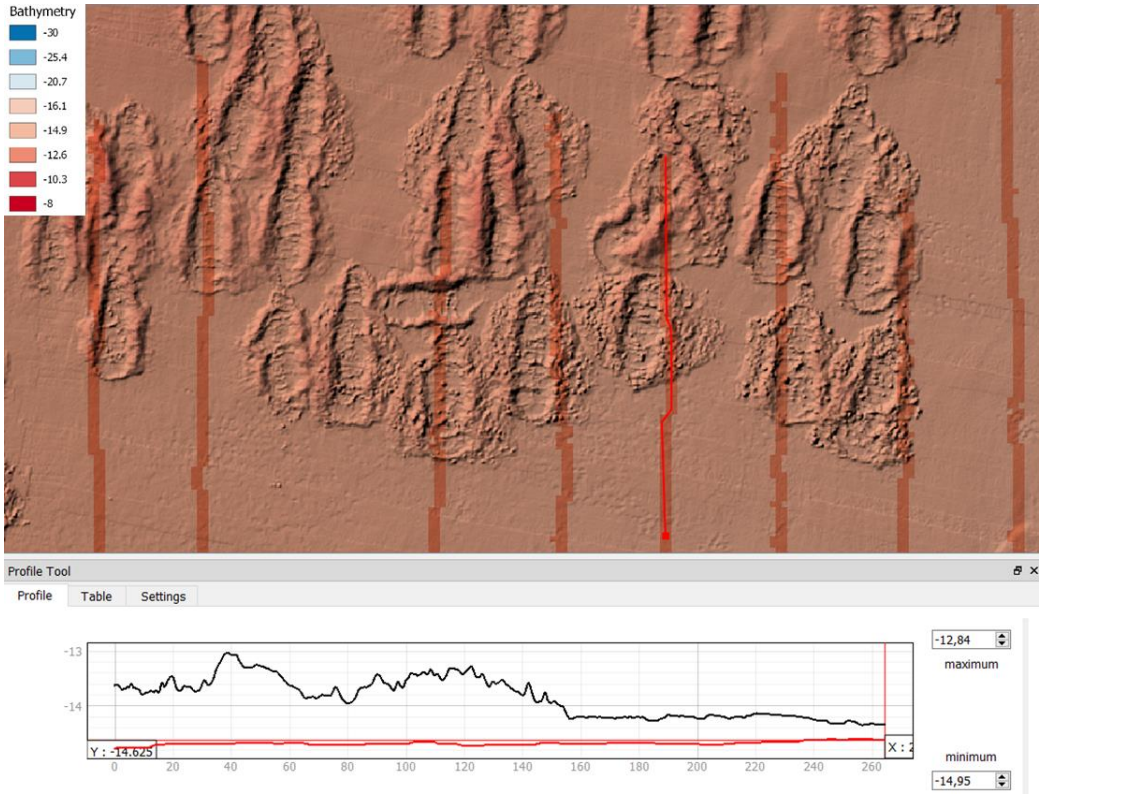

Figure 7-10 Close up view of the bathymetry (top) and example of vertical profile (bottom) within the disposal area. Bathymetry from 2020 (black line, Alpine ECRC) and 2011 (red line, NOAA).

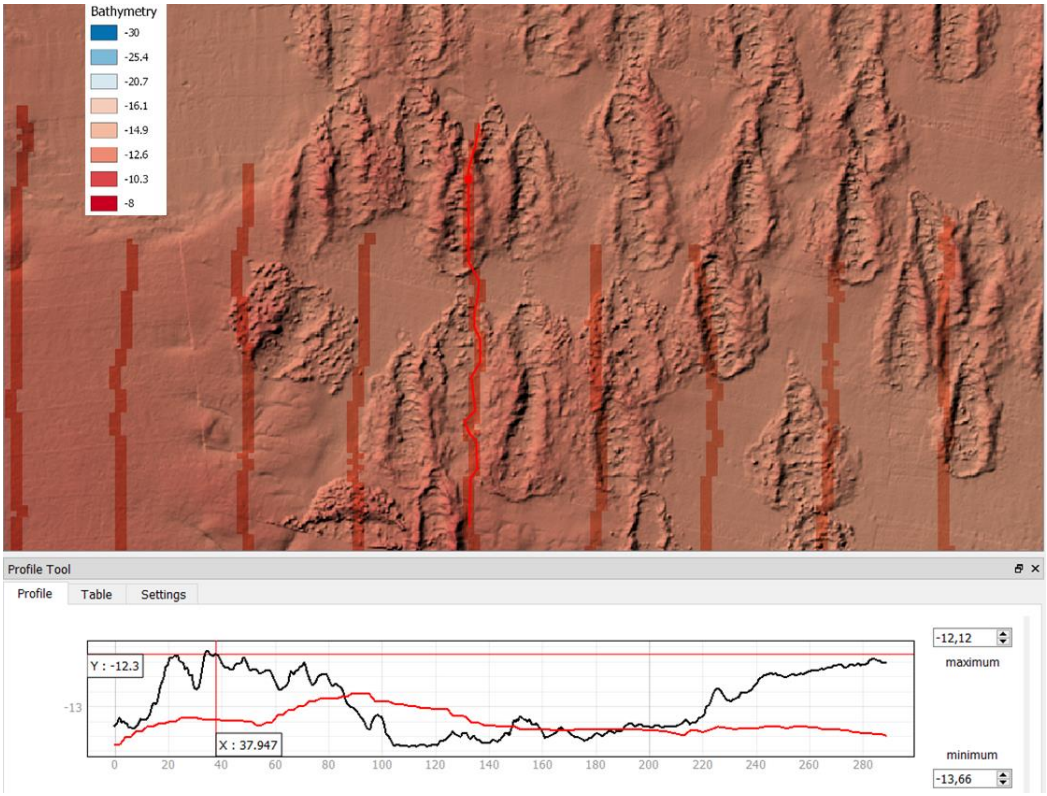

Figure 7-11 Close up view of the bathymetry (top) and example of vertical profile (bottom) within the disposal area. Bathymetry from 2020 (black line, Alpine ECRC) and 2011 (red line, NOAA).

This page is intentionally left blank.

8 Conclusions

A seabed mobility study was carried out for the Coastal Virginia Offshore Wind Farm. The study focused first on the lease area, where wind turbines will be deployed, and secondly the export cable route corridor, which extends from the shore to the wind turbine lease area.

The study revealed the presence of different sediment features on the seabed, mainly sand ridges and sand waves. The observed sand ridges have dimensions of several kilometres in length and few kilometres in width, and heights of several meters. The observed sand waves have heights in the range 0.5 to 2 meters and wavelengths in the range 100 to 300 meters.

The mobility of seabed features was evaluated, and it appeared that sand ridges and sand waves are slowly moving towards the south-east with migrations rate generally in the range 1 to 3 meters per year in the lease area. The changes in bathymetry along their paths will most likely remain limited in the order of 0.5 meters in the next 30 years (0 to 1 meter). Within deeper flat areas the sea-bottom is stable with erosion spots here and there in locally channelized areas that will engender local erosion up to 5 cm per year, however it is unlikely that this erosion will continue for 30 years.

Within the export cable route corridor, seabed features migrate faster in shallower waters (meters) towards the south east. Locally, a group of sand waves with heights from 1 to 2.5 meters have migration rates up to 12 to 18 meters per year, potentially generating changes in the seabed up to 2 meters in the next 30 years. Apart from this group of sand waves, changes of bathymetry should remain moderate in the range of 0.5 to 1 meter in the export cable route corridor. The migration of the sand ridge (height of 6.5 m) in the eastern part of the corridor will potentially generate bathymetric changes up to +2 meters downstream of the south east flank.

A disposal area exists west of the export cable corridor path (DNODS). Fine sands are deposited on a regular basis due to the dredging of the access channels to the Chesapeake Bay. The deposited sediment has the potential to generate sand waves that will migrate towards the south east in the future that may require a monitoring campaign of the area.

It is noted that the crossing of the export cable of the shoreline is not covered by the present study and it is likely that large seabed level changes are occurring near the shoreline due to the much more dynamic conditions caused by wave breaking in this area.

It is further noted that the interaction between the wind turbine foundations or cables and the seabed has not been considered in the present work. The presence of the foundations are likely to cause local amplification of the bed shear stresses near the foundation resulting in local scour which has not been considered in the present study.

This page is intentionally left blank.

9 References

[1] Ashley, G.M., (1990). Classification of large-scale subaqueous bedforms: a new look at an old problem. Journal of Sedimentary Research 01/1990; Vol. 60.

[2] AWS 2015. METEO ASSESMENT FOR THE PROPOSED VIRGINIA OFFSHORE WIND TECHNOLOGY ADVANCEMENT PROJECT (VOWTAP), 170 pp, April 2015.

[3] Belderson, R. H., Johnson, M. A. & Kenyon, N. H. (1982). Offshore Tidal Sands: Processes and Deposits, London, Chapman and Hall Ltd.

[4] Fugro 2013: 'McNeilan, T.W., K.R. Smith, and J.E. Fisher. 2013. Regional Geophysical Survey and Interpretive Report: Virginia Wind Energy Area Offshore Southeastern Virginia. US Dept. of the Interior, Bureau of Ocean Energy Management, Office of Renewable Energy Programs, Herndon. OCS Study BOEM 2013-220, 240 pp.

[5] Fugro 2013: METOCEAN CRITERIA FOR VIRGINIA OFFSHORE WIND TECHNOLOGY ADVANCEMENT PROJECT VOWTAP, Report Number C5646 2 7907 /R7, 125 pp, 06 December 2013.

[6] Fugro 2014: Geophysical survey report HDD cable route VOWTAP demonstration project Virgina outer continental shelf. Prepared for Dominion Resources, Fugro job 0481140004, September 2014.

[7] NOAA 2006-2010-2011-2012. Publicly available high resolution multibeam bathymetry data. (https://maps.ngdc.noaa.gov/viewers/bathymetry/).

[8] Rambøll 2021: DOMINION ENERGY - CVOW-C – OWNERS ENGINEER METOCEAN ASSESSMENT, project 1690016328, 152 pp, January 2021.

[9] Schnabel Engineering 2020: Surficial sediment sample collection and analysis - Coastal Virginia Offshore Wind (CVOW) Lease Area, Schnabel Reference 20C13110, 116 pp, December 2020.

[10] TetraTech 2013: Marine Site Characterization survey report Virginia Offshore Wind Technology Advancement Project (VOWTAP), 77 pp.

[11] TerraSond 2020: Geophysical Survey Report Dominion Commercial Virginia Offshore Wind (CVOW) BOEM Renewable Energy Lease Number OCS-A 0483, Project No. 2020-004, 177 pp.

[12] Alpine 2021: Coastal Virginia Offshore Wind – Commercial Export Cable Route Corridor Geophysical Survey, Project number 1889, Interpretation report, doc. Num. AOSS-R-SUR-01-02, 2021.01.29.

This page is intentionally left blank.

APPENDICES

APPENDIX A – Additional Plots and Tables

A Additional Plots and Tables

A.1 Additional Plots

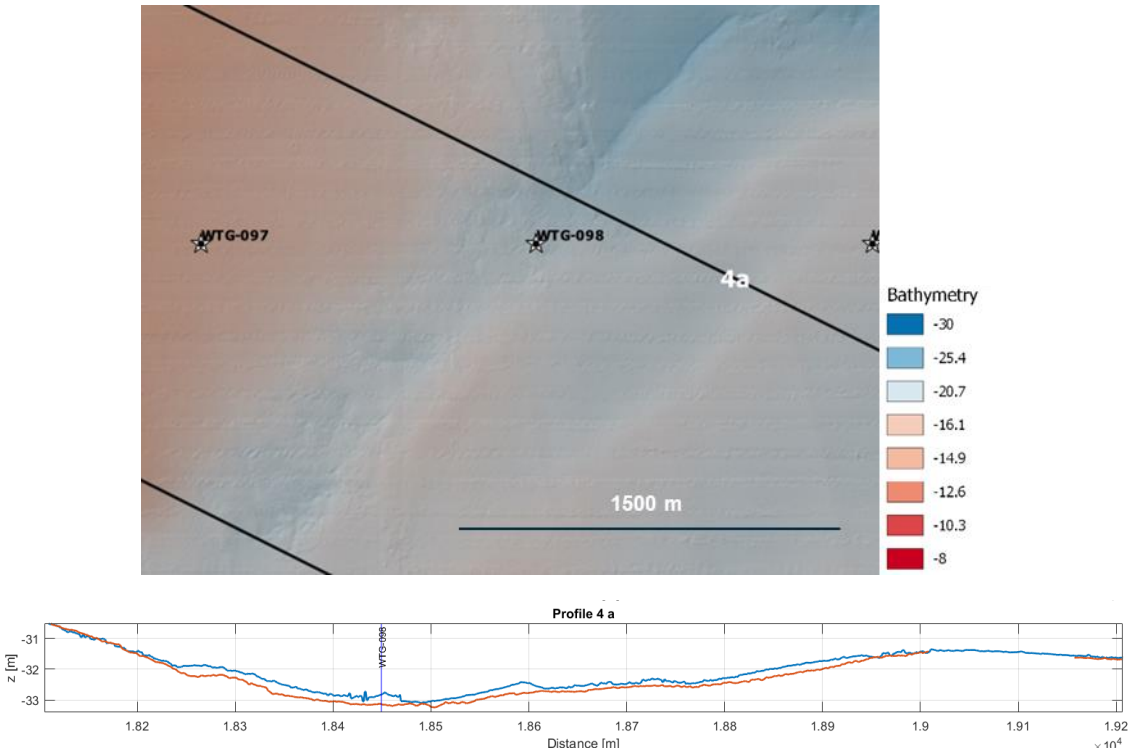

Figure A-1 Example of a steady local erosion pattern in profile 4a.

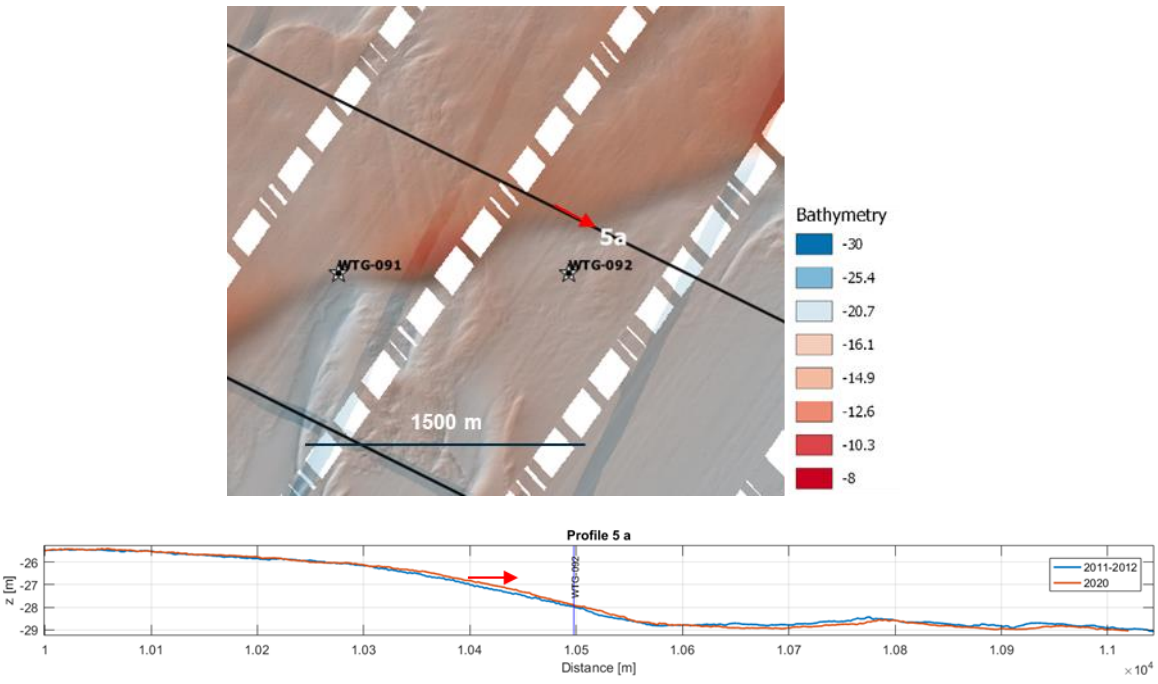

Figure A-2 Example of ridge migration (SR1) at profile 5a.

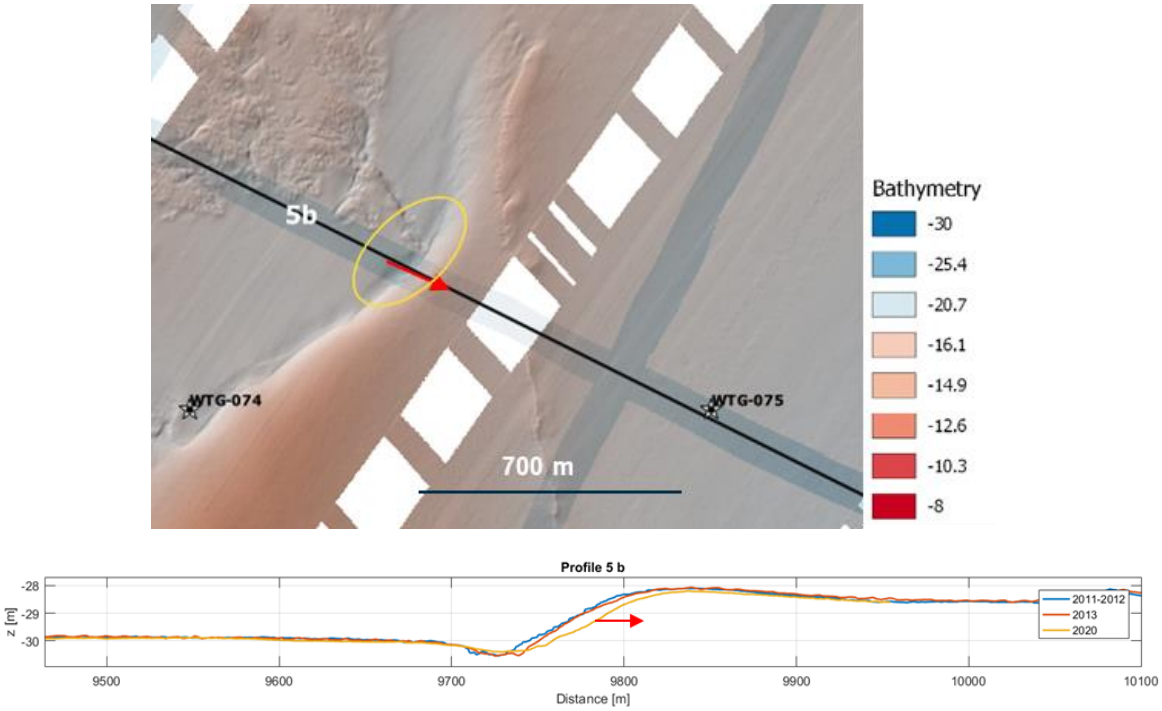

Figure A-3 Example of a steady local erosion pattern in profile 5b.

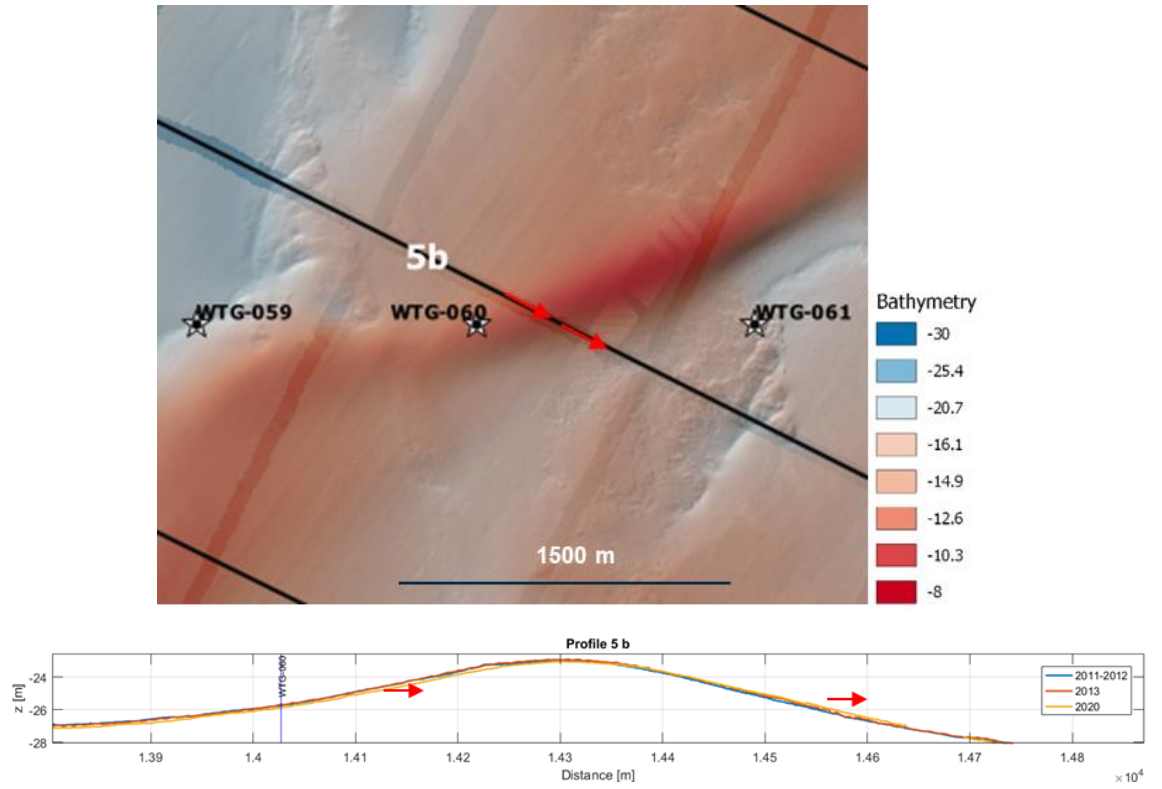

Figure A-4 Example of ridge migration (SR2) at profile 5b.

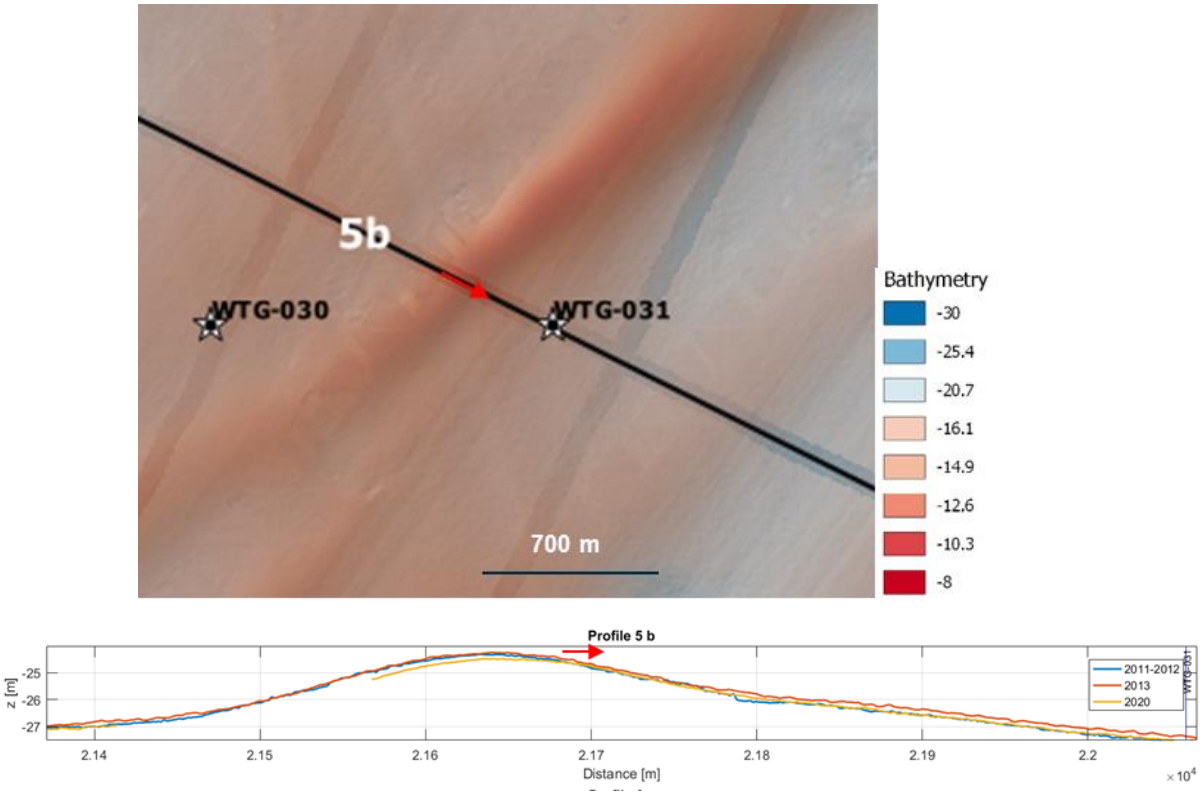

Figure A-5 Example of ridge migration (SR3) at profile 5b.

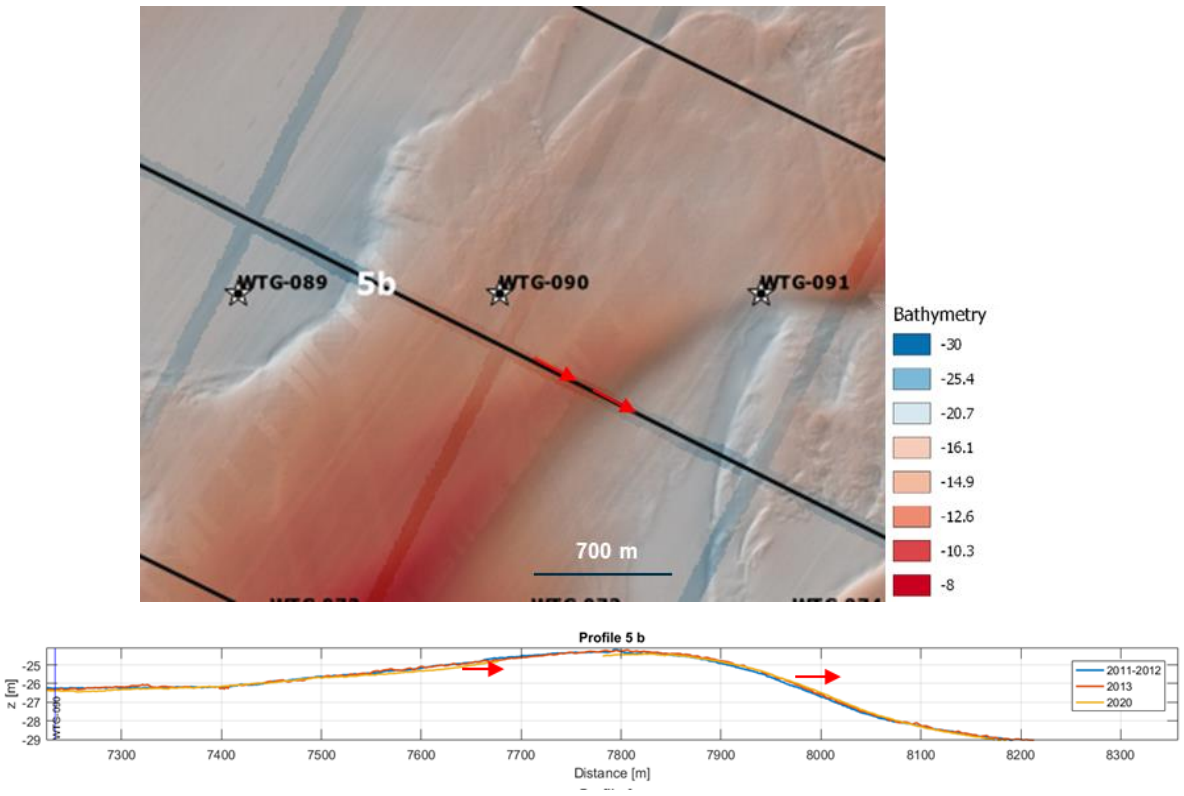

Figure A-6 Example of ridge migration (SR1) at profile 5b.

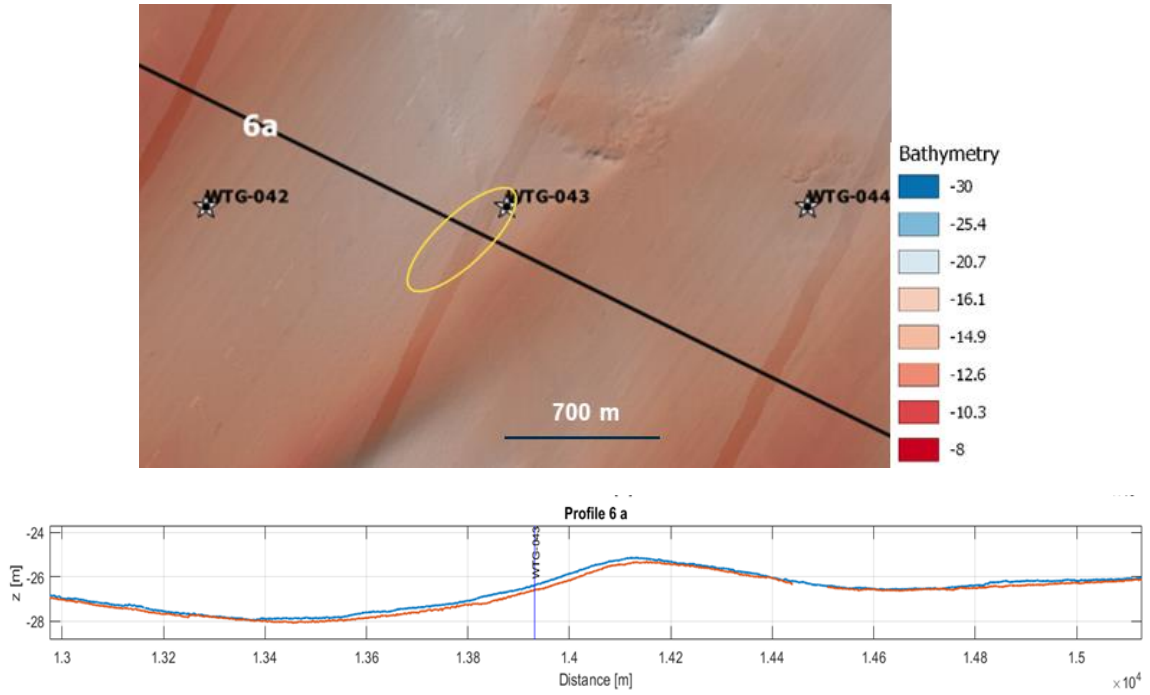

Figure A-7 Example of a steady local erosion pattern at the rear of a sand ridge (SR2) in profile 6a.

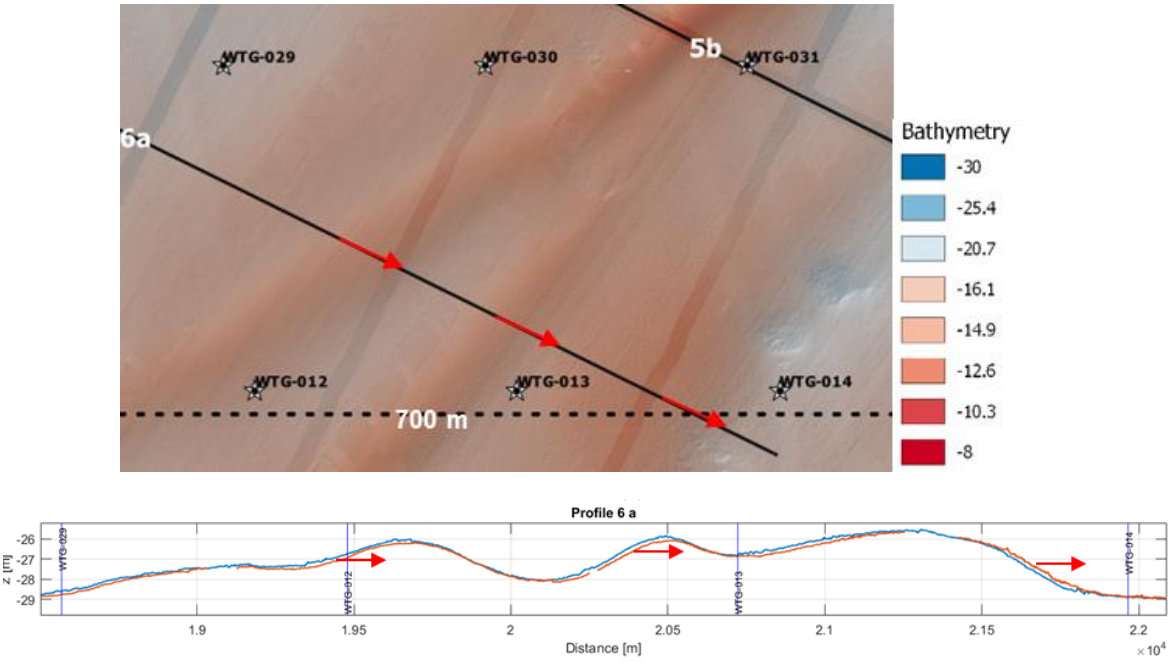

Figure A-8 Example of ridge migration (SR3) at profile 6a.

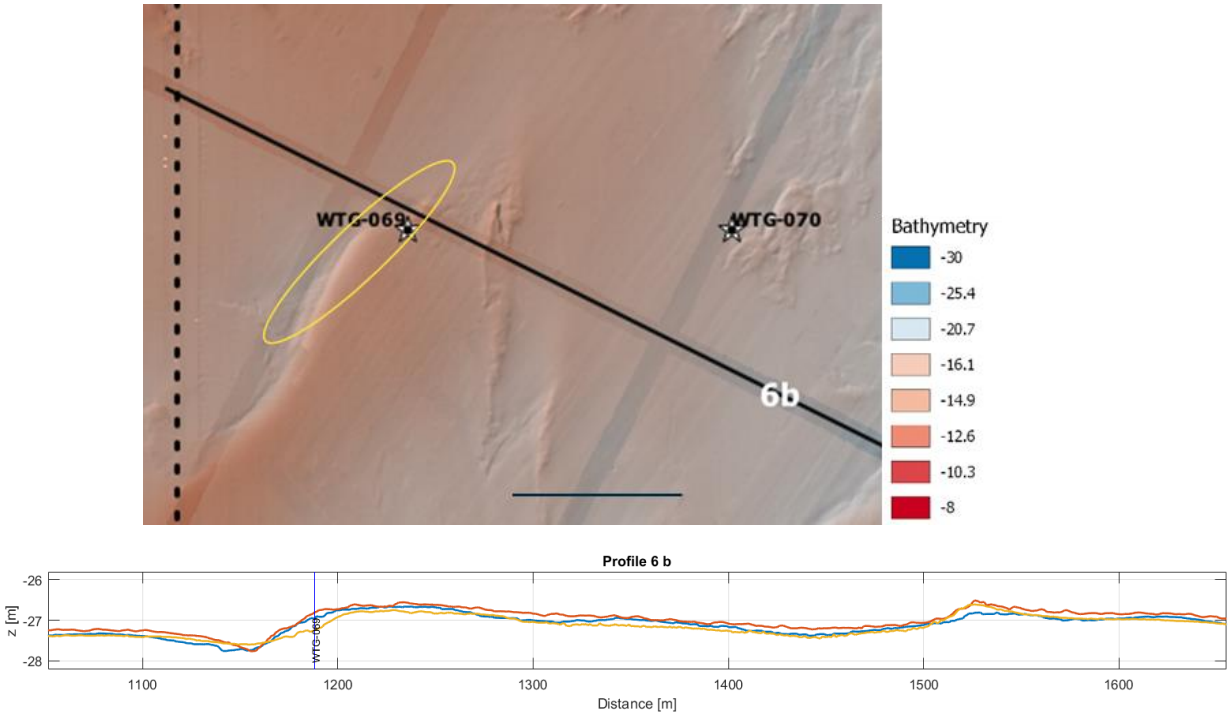

Figure A-9 Example of a steady local erosion pattern in profile 6b.

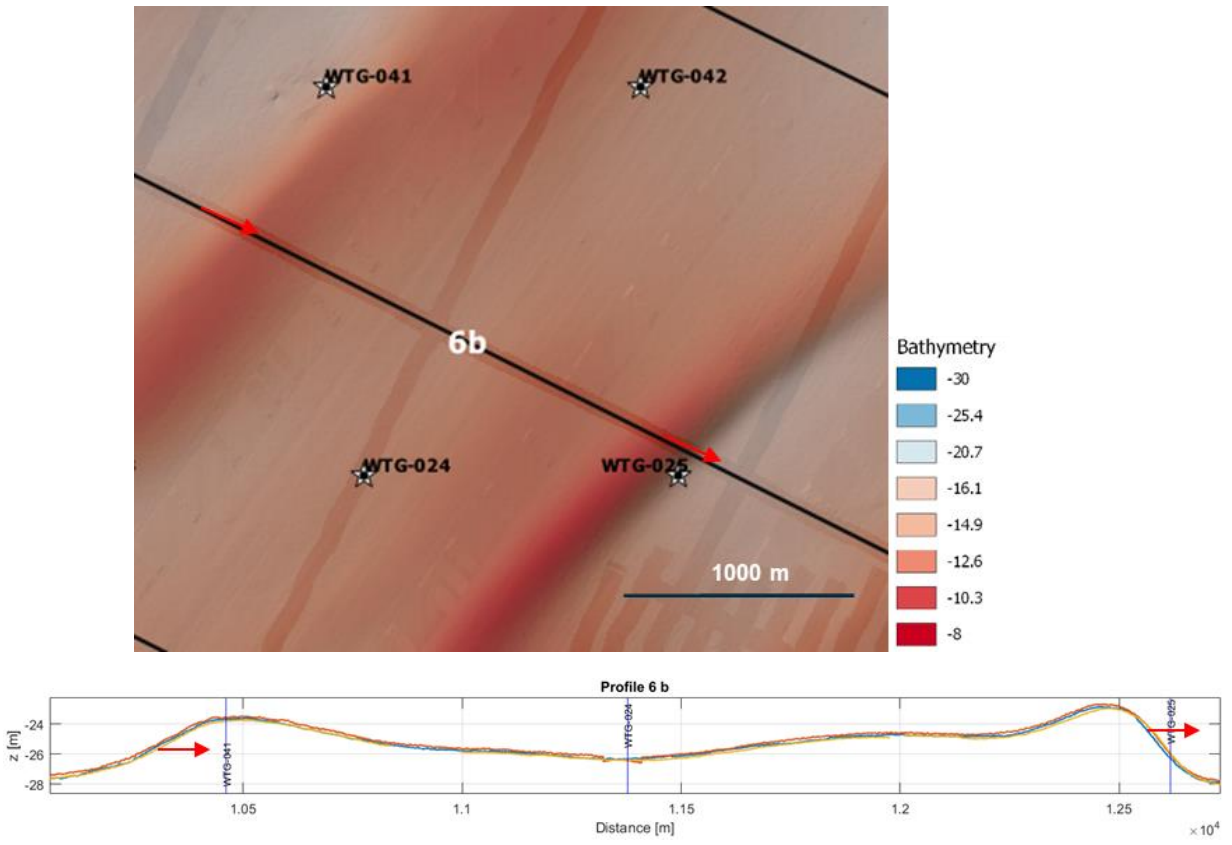

Figure A-10 Example of ridge migration (SR2) at profile 6b.

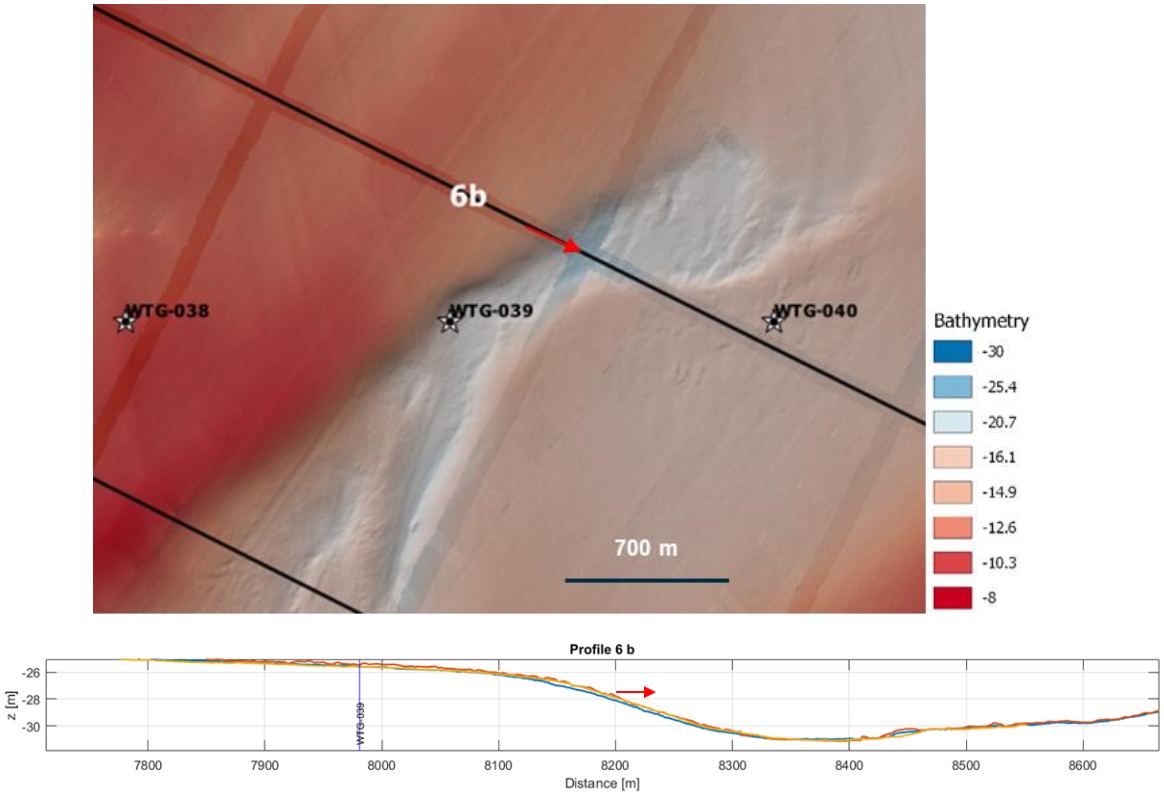

Figure A 11 Example of ridge migration (SR1) at profile 6b.

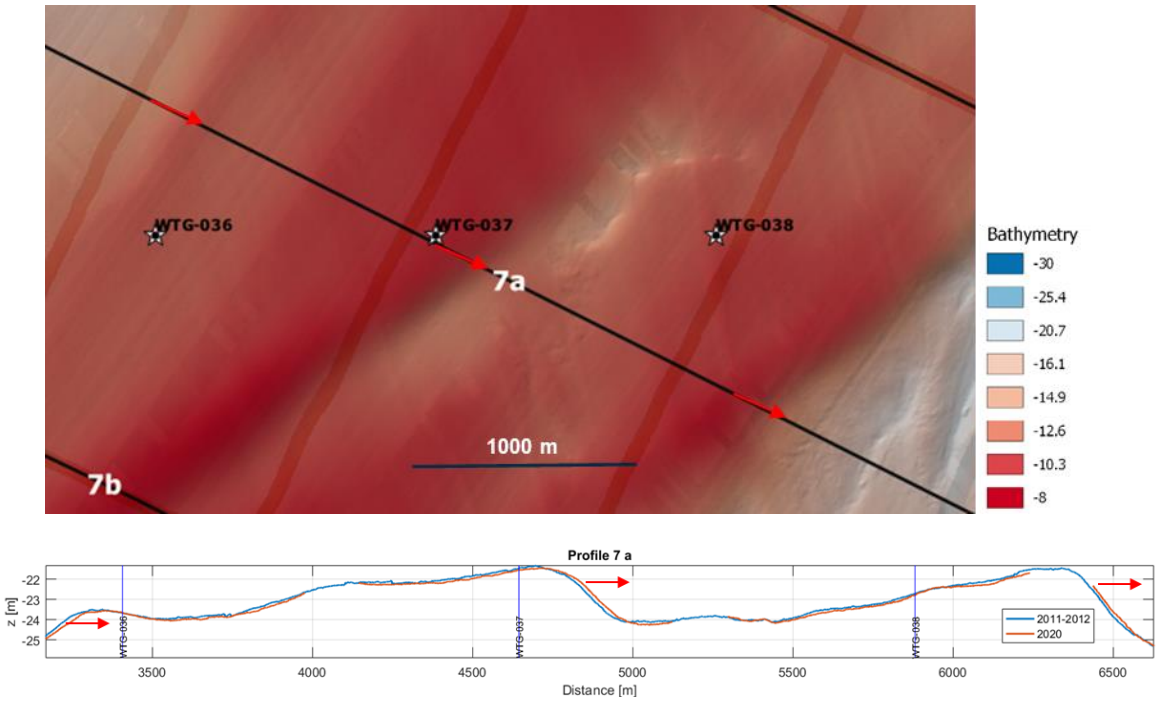

Figure A-12 Example of ridge migration (SR1) at profile 7a.

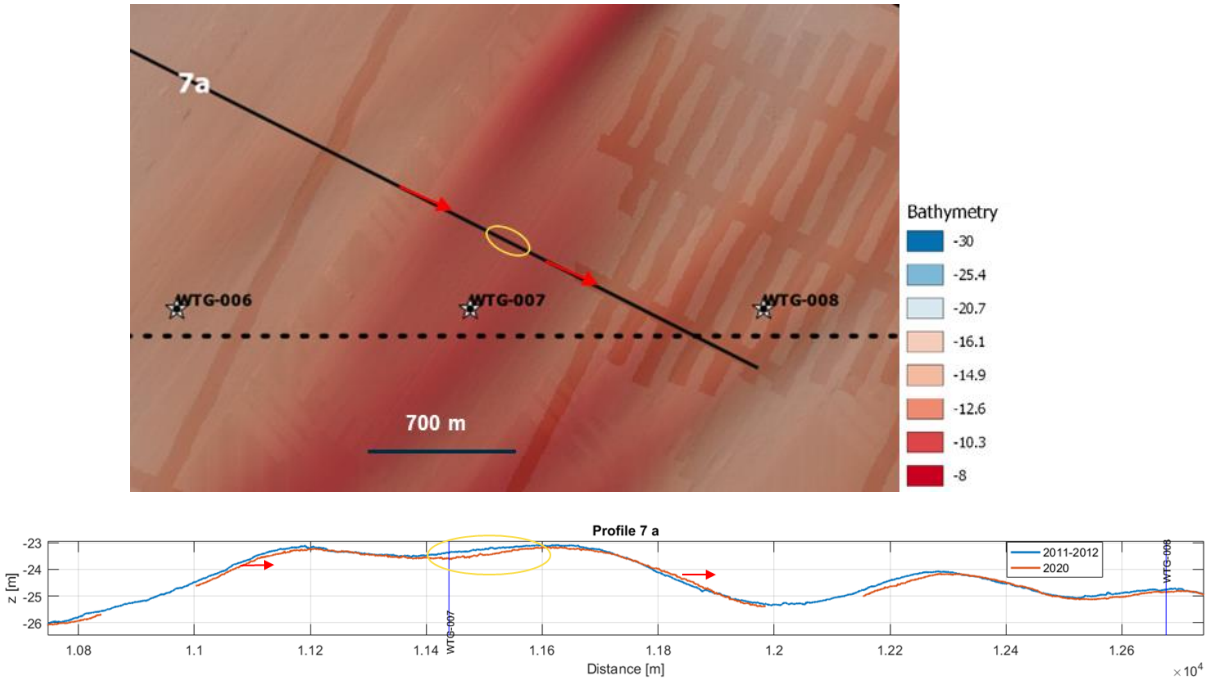

Figure A-13 Example of ridge migration (SR2) at profile 7a.

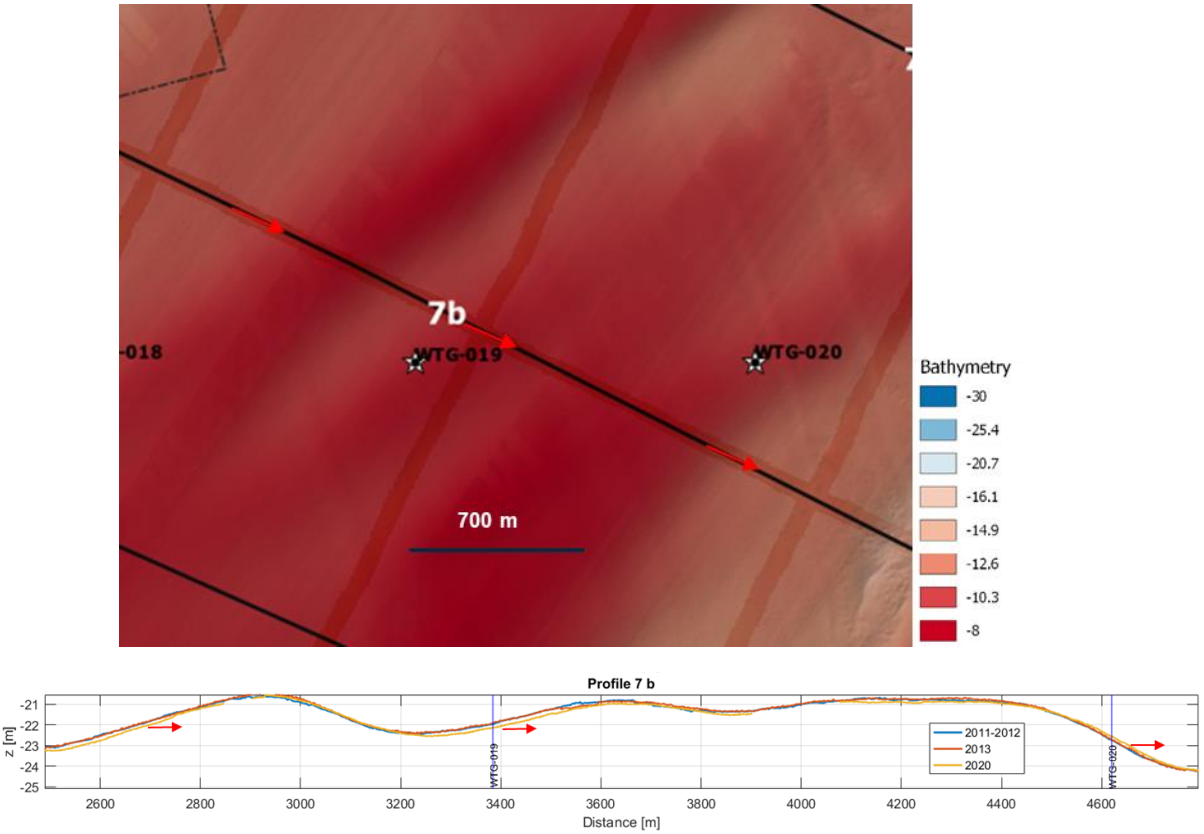

Figure A-14 Example of ridge migration (SR1) at profile 7b.

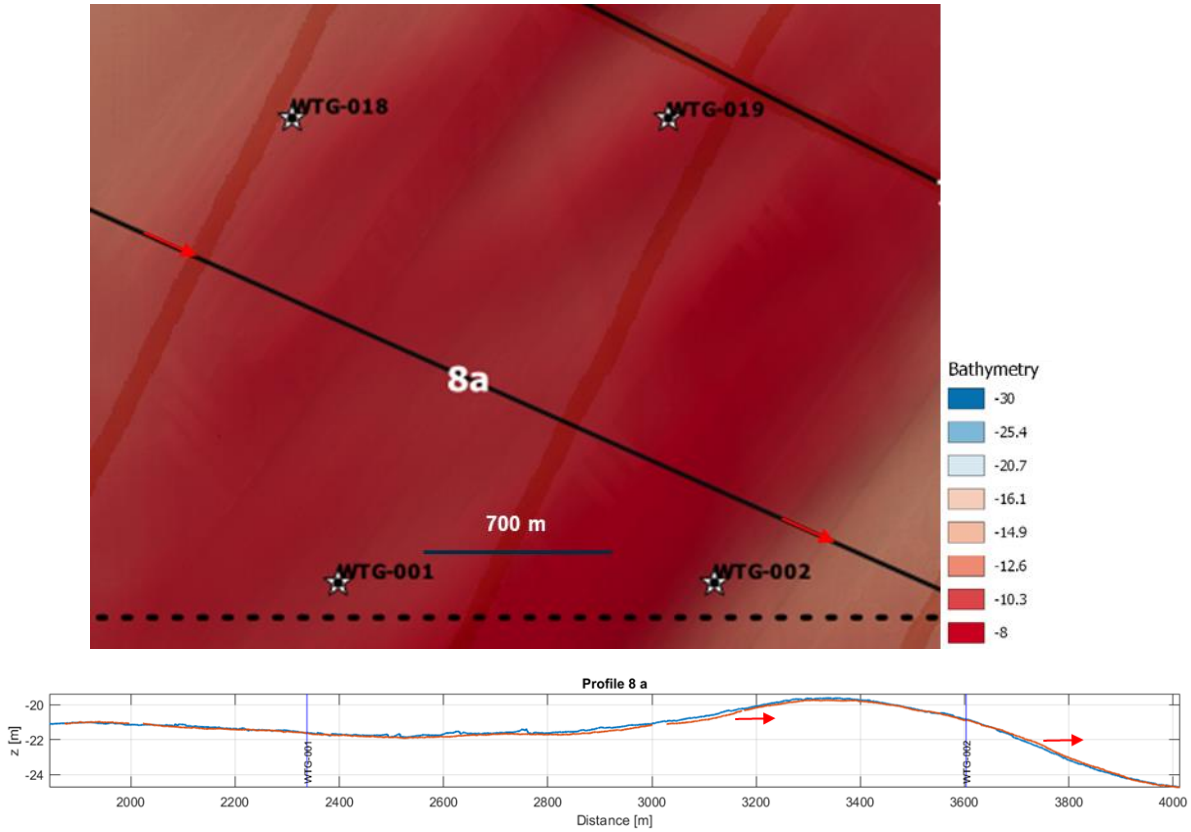

Figure A-15 Example of ridge migration (SR1) at profile 8a.

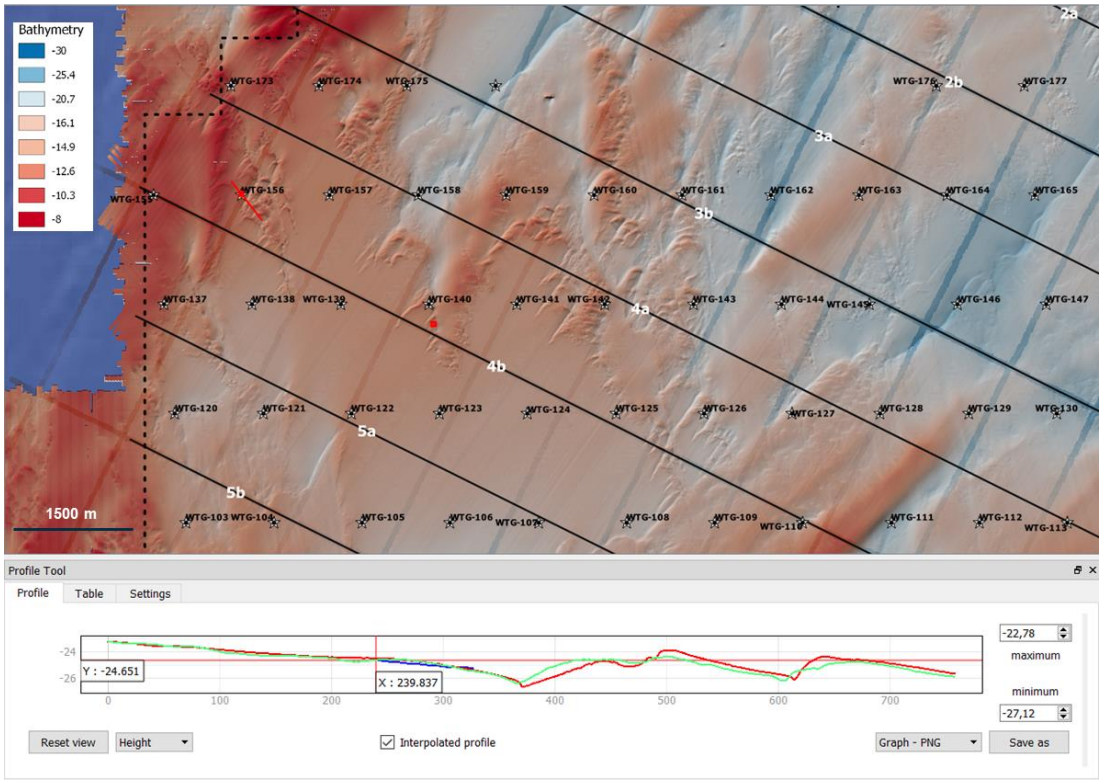

Figure A-16 Sand wave profile (bottom) in the vicinity of wtg-156. NOAA survey from 2011 (green) and TERRASOND survey from 2020 (red). The vertical red line along the profile mark the position of the wind turbine.

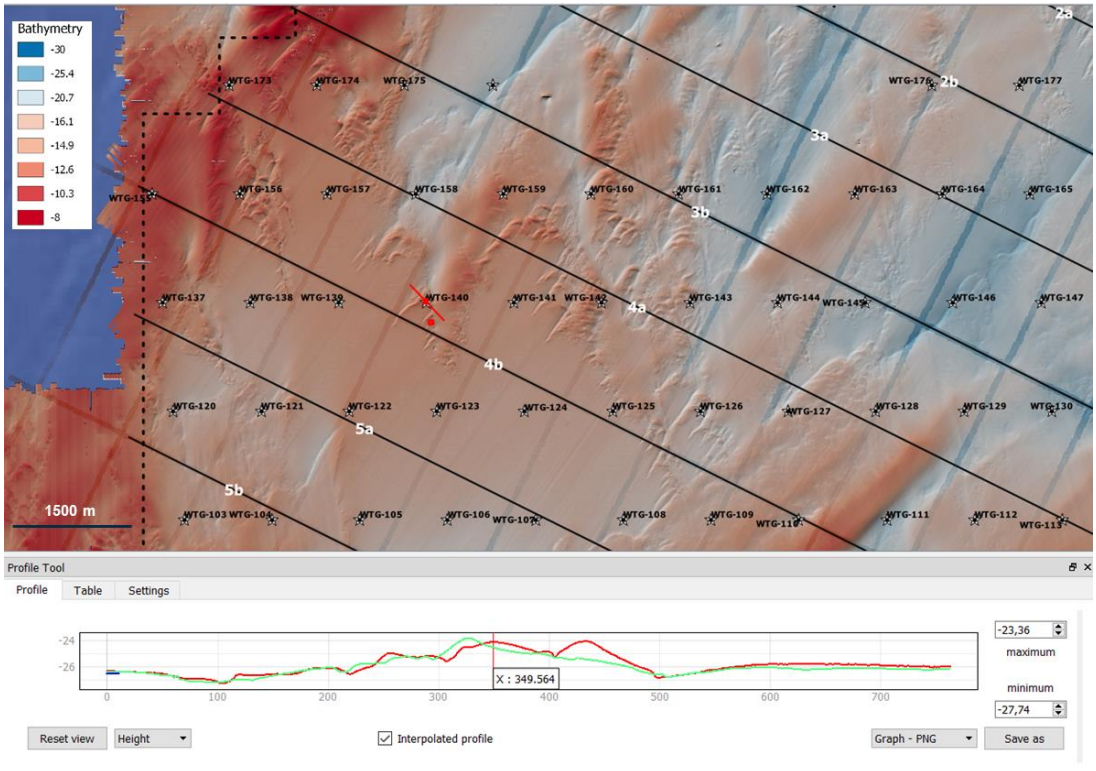

Figure A-17 Sand wave profile (bottom) in the vicinity of wtg-140. NOAA survey from 2011 (green) and TERRASOND survey from 2020 (red). The vertical red line along the profile mark the position of the wind turbine.

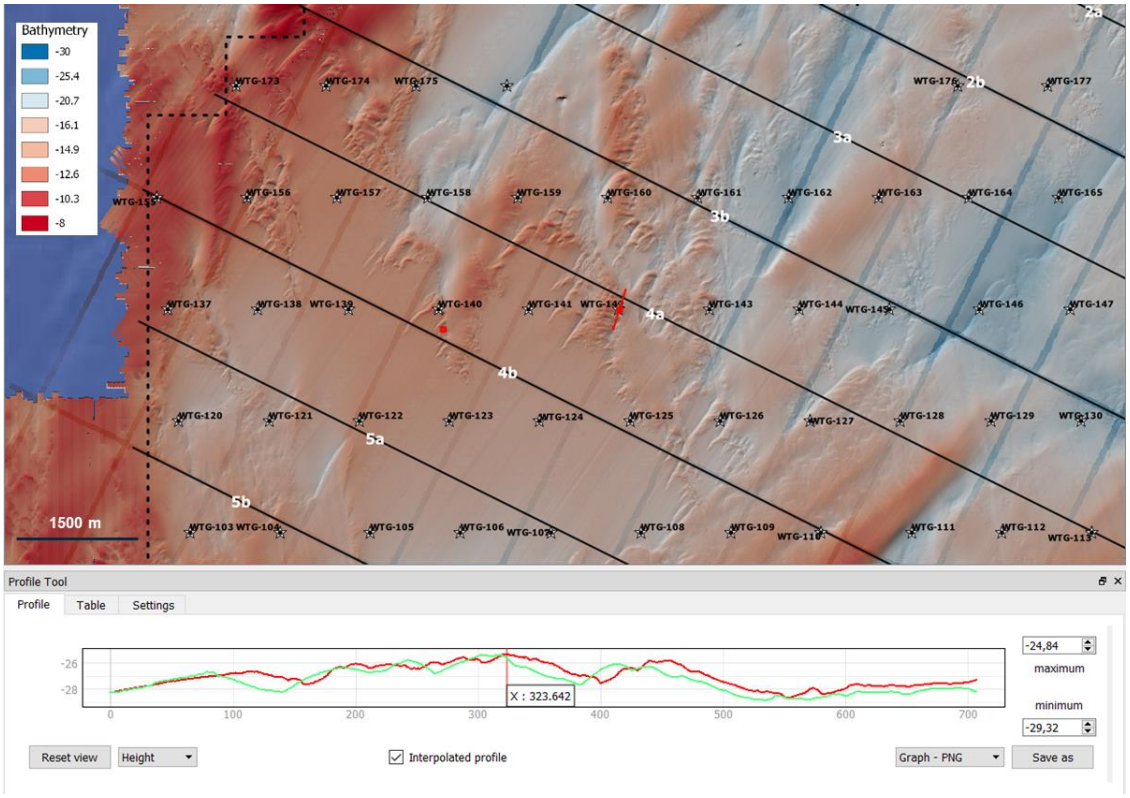

Figure A-18 Sand wave profile (bottom) in the vicinity of wtg-142. NOAA survey from 2011 (green) and TERRASOND survey from 2020 (red). The vertical red line along the profile mark the position of the wind turbine.

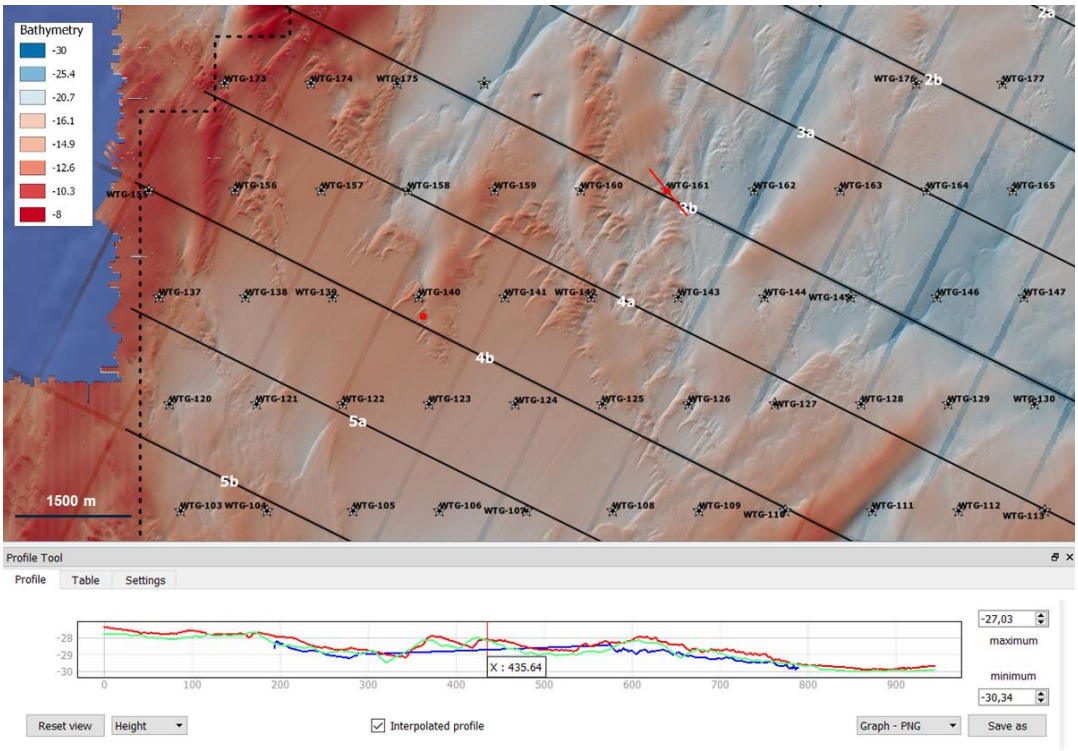

Figure A-19 Sand wave profile (bottom) in the vicinity of wtg-161. NOAA survey from 2011 (green) and TERRASOND survey from 2020 (red). The vertical red line along the profile mark the position of the wind turbine.

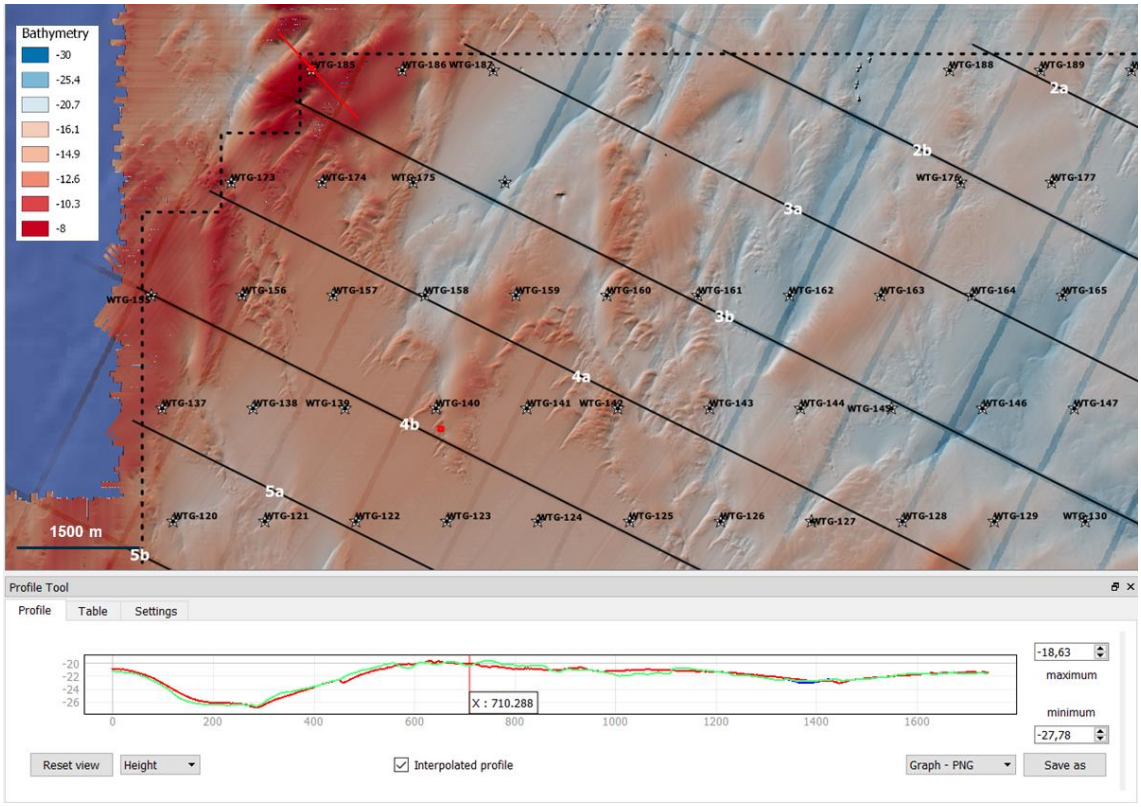

Figure A-20 Sand wave profile (bottom) in the vicinity of wtg-185. NOAA survey from 2011 (green) and TERRASOND survey from 2020 (red). The vertical red line along the profile mark the position of the wind turbine.

A.2 Additional Tables

Table A-1 Computed mean bed elevation at the present time (Z_pres), maximum bed elevation (Z_max), minimum bed elevation (Z_min), and mean bed elevation for the next 30 years (Z_mean). Other fields present the same parameters considering the positive and negative standard deviation of the computed migration rate. Lines with a '-' sign indicate that no significant movement of the bed was detected between the surveys.

Turbine #	Z_pres	Z_max	Z_min	Z_mean	Z_max+std	Z_min+std	Z_mean+std	Z_max-std	Z_min-std	Z_mean-std
wtg-1	-	-	-	-	-	-	-	-	-	-
wtg_2	-21.8	-21.6	-21.8	-21.7	-21.1	-21.8	-21.5	-21.8	-21.8	-21.8
wtg_3	-	-	-	-	-	-	-	-	-	-
wtg_4	-	-	-	-	-	-	-	-	-	-
wtg_5	-	-	-	-	-	-	-	-	-	-
wtg_6	-26.1	-26.1	-26.1	-26.1	-26.0	-26.1	-26.1	-26.1	-26.1	-26.1
wtg_7	-23.2	-23.2	-23.3	-23.2	-23.2	-23.4	-23.3	-23.2	-23.2	-23.2
wtg_8	-25.4	-25.4	-25.4	-25.4	-25.4	-25.5	-25.4	-25.4	-25.4	-25.4
wtg_9	-	-	-	-	-	-	-	-	-	-
wtg_10	-	-	-	-	-	-	-	-	-	-
wtg_11	-	-	-	-	-	-	-	-	-	-
wtg_12	-27.4	-27.0	-27.4	-27.3	-26.9	-27.4	-27.2	-27.2	-27.4	-27.3
wtg_13	-27.4	-27.2	-27.4	-27.3	-27.1	-27.4	-27.3	-27.3	-27.4	-27.3
wtg_14	-	-	-	-	-	-	-	-	-	-
wtg_15	-27.2	-27.2	-27.7	-27.5	-27.2	-27.9	-27.6	-27.2	-27.6	-27.4
wtg_16	-	-	-	-	-	-	-	-	-	-
wtg_17	-	-	-	-	-	-	-	-	-	-
wtg_18	-	-	-	-	-	-	-	-	-	-
wtg_19	-21.2	-21.2	-21.9	-21.6	-21.2	-22.0	-21.6	-21.2	-21.8	-21.5
wtg_20	-21.9	-21.9	-22.1	-22.0	-21.9	-22.1	-22.0	-21.9	-22.1	-22.0
wtg_21	-	-	-	-	-	-	-	-	-	-
wtg_22	-	-	-	-	-	-	-	-	-	-
wtg_23	-	-	-	-	-	-	-	-	-	-
wtg_24	-	-	-	-	-	-	-	-	-	-
wtg_25	-26.7	-25.7	-26.7	-26.2	-25.3	-26.7	-26.0	-26.1	-26.7	-26.4
wtg_26	-	-	-	-	-	-	-	-	-	-
wtg_27	-	-	-	-	-	-	-	-	-	-
wtg_28	-	-	-	-	-	-	-	-	-	-
wtg_29	-	-	-	-	-	-	-	-	-	-
wtg_30	-	-	-	-	-	-	-	-	-	-
wtg_31	-27.5	-27.3	-27.5	-27.4	-27.2	-27.5	-27.4	-27.4	-27.5	-27.5
wtg_32	-	-	-	-	-	-	-	-	-	-
wtg_33	-	-	-	-	-	-	-	-	-	-
wtg_34	-	-	-	-	-	-	-	-	-	-
wtg_35	-	-	-	-	-	-	-	-	-	-
wtg_36	-23.5	-23.5	-23.5	-23.5	-23.5	-23.5	-23.5	-23.5	-23.5	-23.5
wtg_37	-21.6	-21.6	-21.8	-21.7	-21.6	-21.8	-21.7	-21.6	-21.8	-21.7
wtg_38										
wtg_39	-29.7	-28.8	-29.6	-29.3	-28.2	-29.6	-29.0	-29.2	-29.6	-29.5
wtg_40										
wtg_41	-27.3	-27.3	-27.8	-27.6	-27.3	-27.9	-27.7	-27.3	-27.6	-27.5
wtg_42										
wtg_43	-27.2	-27.2	-27.3	-27.3	-27.2	-27.4	-27.3	-27.2	-27.3	-27.2
wtg_44	-	-	-	-	-	-	-	-	-	-
wtg_45	-	-	-	-	-	-	-	-	-	-
wtg_46	-	-	-	-	-	-	-	-	-	-
wtg_47	-	-	-	-	-	-	-	-	-	-
wtg_48	-	-	-	-	-	-	-	-	-	-
wtg_49	-	-	-	-	-	-	-	-	-	-
wtg_50	-	-	-	-	-	-	-	-	-	-

Table A-2 Computed mean bed elevation at the present time (Z_pres), maximum bed elevation (Z_max), minimum bed elevation (Z_min), and mean bed elevation for the next 30 years (Z_mean). Other fields present the same parameters considering the positive and negative standard deviation of the computed migration rate. Lines with a '-' sign indicate that no significant movement of the bed was detected between the surveys.

Turbine #	Z_pres	Z_max	Z_min	Z_mean	Z_max+std	Z_min+std	Z_mean+std	Z_max-std	Z_min-std	Z_mean-std
wtg_51	-	-	-	-	-	-	-	-	-	-
wtg_52	-	-	-	-	-	-	-	-	-	-
wtg_53	-	-	-	-	-	-	-	-	-	-
wtg_54	-	-	-	-	-	-	-	-	-	-
wtg_55	-	-	-	-	-	-	-	-	-	-
wtg_56	-	-	-	-	-	-	-	-	-	-
wtg_57	-	-	-	-	-	-	-	-	-	-
wtg_58	-	-	-	-	-	-	-	-	-	-
wtg_59	-31.7	-31.8	-32.2	-32.1	-31.8	-32.2	-32.1	-31.8	-32.2	-32.1
wtg_60	-24.4	-24.4	-25.4	-24.9	-24.4	-25.5	-25.0	-24.4	-25.2	-24.8
wtg_61	-	-	-	-	-	-	-	-	-	-
wtg_62	-	-	-	-	-	-	-	-	-	-
wtg_63	-	-	-	-	-	-	-	-	-	-
wtg_64	-	-	-	-	-	-	-	-	-	-
wtg_65	-	-	-	-	-	-	-	-	-	-
wtg_66	-	-	-	-	-	-	-	-	-	-
wtg_67	-	-	-	-	-	-	-	-	-	-
wtg_68	-	-	-	-	-	-	-	-	-	-
wtg_69	-26.5	-26.5	-26.6	-26.6	-26.5	-26.9	-26.6	-26.5	-26.6	-26.5
wtg_70	-	-	-	-	-	-	-	-	-	-
wtg_71	-	-	-	-	-	-	-	-	-	-
wtg_72	-	-	-	-	-	-	-	-	-	-
wtg_73	-	-	-	-	-	-	-	-	-	-
wtg_74	-30.1	-30.0	-30.2	-30.1	-30.0	-30.2	-30.1	-30.0	-30.1	-30.0
wtg_75	-	-	-	-	-	-	-	-	-	-
wtg_76	-	-	-	-	-	-	-	-	-	-
wtg_77	-	-	-	-	-	-	-	-	-	-
wtg_78	-	-	-	-	-	-	-	-	-	-
wtg_79	-	-	-	-	-	-	-	-	-	-
wtg_80	-	-	-	-	-	-	-	-	-	-
wtg_81	-	-	-	-	-	-	-	-	-	-
wtg_82	-	-	-	-	-	-	-	-	-	-
wtg_83	-	-	-	-	-	-	-	-	-	-
wtg_84	-	-	-	-	-	-	-	-	-	-
wtg_85	-	-	-	-	-	-	-	-	-	-
wtg_86	-	-	-	-	-	-	-	-	-	-
wtg_87	-	-	-	-	-	-	-	-	-	-
wtg_88	-	-	-	-	-	-	-	-	-	-
wtg_89	-	-	-	-	-	-	-	-	-	-
wtg_90	-26.6	-26.6	-26.6	-26.6	-26.6	-26.6	-26.6	-26.6	-26.6	-26.6
wtg_91	-29.1	-28.7	-29.1	-28.9	-28.6	-29.1	-28.8	-28.8	-29.1	-29.0
wtg_92	-28.8	-28.8	-28.9	-28.8	-28.8	-28.9	-28.9	-28.8	-28.8	-28.8
wtg_93	-	-	-	-	-	-	-	-	-	-
wtg_94	-	-	-	-	-	-	-	-	-	-
wtg_95	-	-	-	-	-	-	-	-	-	-
wtg_96	-	-	-	-	-	-	-	-	-	-
wtg_97	-	-	-	-	-	-	-	-	-	-
wtg_98	-32.0	-33.5	-32.0	0.0	0.0	0.0	0.0	0.0	0.0	0.0
wtg_99	-	-	-	-	-	-	-	-	-	-
wtg_100	-	-	-	-	-	-	-	-	-	-

Table A-3 Computed mean bed elevation at the present time (Z_pres), maximum bed elevation (Z_max), minimum bed elevation (Z_min), and mean bed elevation for the next 30 years (Z_mean). Other fields present the same parameters considering the positive and negative standard deviation of the computed migration rate. Lines with a '-' sign indicate that no significant movement of the bed was detected between the surveys.

Turbine #	Z_pres	Z_max	Z_min	Z_mean	Z_max+std	Z_min+std	Z_mean+std	Z_max-std	Z_min-std	Z_mean-std
wtg_101	-	-	-	-	-	-	-	-	-	-
wtg_102	-	-	-	-	-	-	-	-	-	-
wtg_103	-	-	-	-	-	-	-	-	-	-
wtg_104	-	-	-	-	-	-	-	-	-	-
wtg_105	-	-	-	-	-	-	-	-	-	-
wtg_106	-	-	-	-	-	-	-	-	-	-
wtg_107	-	-	-	-	-	-	-	-	-	-
wtg_108	-	-	-	-	-	-	-	-	-	-
wtg_109	-	-	-	-	-	-	-	-	-	-
wtg_110	-	-	-	-	-	-	-	-	-	-
wtg_111	-	-	-	-	-	-	-	-	-	-
wtg_112	-	-	-	-	-	-	-	-	-	-
wtg_113	-	-	-	-	-	-	-	-	-	-
wtg_114	-	-	-	-	-	-	-	-	-	-
wtg_115	-	-	-	-	-	-	-	-	-	-
wtg_116	-	-	-	-	-	-	-	-	-	-
wtg_117	-	-	-	-	-	-	-	-	-	-
wtg_118	-	-	-	-	-	-	-	-	-	-
wtg_119	-	-	-	-	-	-	-	-	-	-
wtg_120	-	-	-	-	-	-	-	-	-	-
wtg_121	-	-	-	-	-	-	-	-	-	-
wtg_122	-	-	-	-	-	-	-	-	-	-
wtg_123	-	-	-	-	-	-	-	-	-	-
wtg_124	-	-	-	-	-	-	-	-	-	-
wtg_125	-	-	-	-	-	-	-	-	-	-
wtg_126	-29.0	-28.2	-28.9	-28.5	-27.9	-28.9	-28.3	-28.4	-28.9	-28.7
wtg_127	-	-	-	-	-	-	-	-	-	-
wtg_128	-	-	-	-	-	-	-	-	-	-
wtg_129	-	-	-	-	-	-	-	-	-	-
wtg_130	-	-	-	-	-	-	-	-	-	-
wtg_131	-	-	-	-	-	-	-	-	-	-
wtg_132	-	-	-	-	-	-	-	-	-	-
wtg_133	-	-	-	-	-	-	-	-	-	-
wtg_134	-	-	-	-	-	-	-	-	-	-
wtg_135	-	-	-	-	-	-	-	-	-	-
wtg_136	-	-	-	-	-	-	-	-	-	-
wtg_137	-	-	-	-	-	-	-	-	-	-
wtg_138	-	-	-	-	-	-	-	-	-	-
wtg_139	-	-	-	-	-	-	-	-	-	-
wtg_140	-24.5	-24.1	-25.1	-24.4	-24.1	-25.2	-24.6	-24.1	-24.5	-24.2
wtg_141	-	-	-	-	-	-	-	-	-	-
wtg_142	-25.4	-25.3	-26.0	-25.5	-25.2	-26.2	-25.6	-25.3	-25.4	-25.3
wtg_143	-	-	-	-	-	-	-	-	-	-
wtg_144	-	-	-	-	-	-	-	-	-	-
wtg_145	-	-	-	-	-	-	-	-	-	-
wtg_146	-34.5	-36.0	-34.5	0.0	0.0	0.0	0.0	0.0	0.0	0.0
wtg_147	-	-	-	-	-	-	-	-	-	-
wtg_148	-	-	-	-	-	-	-	-	-	-
wtg_149	-	-	-	-	-	-	-	-	-	-
wtg_150	-	-	-	-	-	-	-	-	-	-

Table A-4 Computed mean bed elevation at the present time (Z_pres), maximum bed elevation (Z_max), minimum bed elevation (Z_min), and mean bed elevation for the next 30 years (Z_mean). Other fields present the same parameters considering the positive and negative standard deviation of the computed migration rate. Lines with a '-' sign indicate that no significant movement of the bed was detected between the surveys.

Turbine #	Z_pres	Z_max	Z_min	Z_mean	Z_max+std	Z_min+std	Z_mean+std	Z_max-std	Z_min-std	Z_mean-std
wtg_151	-	-	-	-	-	-	-	-	-	-
wtg_152	-	-	-	-	-	-	-	-	-	-
wtg_153	-	-	-	-	-	-	-	-	-	-
wtg_154	-	-	-	-	-	-	-	-	-	-
wtg_155	-	-	-	-	-	-	-	-	-	-
wtg_156	-	-	-	-	-	-	-	-	-	-
wtg_157	-	-	-	-	-	-	-	-	-	-
wtg_158	-	-	-	-	-	-	-	-	-	-
wtg_159	-	-	-	-	-	-	-	-	-	-
wtg_160	-	-	-	-	-	-	-	-	-	-
wtg_161	-28.2	-28.0	-28.4	-28.2	-27.9	-28.7	-28.2	-28.1	-28.4	-28.3
wtg_162	-	-	-	-	-	-	-	-	-	-
wtg_163	-	-	-	-	-	-	-	-	-	-
wtg_164	-	-	-	-	-	-	-	-	-	-
wtg_165	-	-	-	-	-	-	-	-	-	-
wtg_166	-	-	-	-	-	-	-	-	-	-
wtg_167	-	-	-	-	-	-	-	-	-	-
wtg_168	-	-	-	-	-	-	-	-	-	-
wtg_169	-	-	-	-	-	-	-	-	-	-
wtg_170	-	-	-	-	-	-	-	-	-	-
wtg_171	-	-	-	-	-	-	-	-	-	-
wtg_172	-	-	-	-	-	-	-	-	-	-
wtg_173	-	-	-	-	-	-	-	-	-	-
wtg_174	-24.6	-24.3	-24.6	-24.5	-24.1	-24.6	-24.4	-24.5	-24.6	-24.6
wtg_175	-	-	-	-	-	-	-	-	-	-
wtg_176	-	-	-	-	-	-	-	-	-	-
wtg_177	-	-	-	-	-	-	-	-	-	-
wtg_178	-	-	-	-	-	-	-	-	-	-
wtg_179	-	-	-	-	-	-	-	-	-	-
wtg_180	-	-	-	-	-	-	-	-	-	-
wtg_181	-	-	-	-	-	-	-	-	-	-
wtg_182	-	-	-	-	-	-	-	-	-	-
wtg_183	-	-	-	-	-	-	-	-	-	-
wtg_184	-	-	-	-	-	-	-	-	-	-
wtg_185	-	-	-	-	-	-	-	-	-	-
wtg_186	-	-	-	-	-	-	-	-	-	-
wtg_187	-	-	-	-	-	-	-	-	-	-
wtg_188	-	-	-	-	-	-	-	-	-	-
wtg_189	-	-	-	-	-	-	-	-	-	-
wtg_190	-	-	-	-	-	-	-	-	-	-
wtg_191	-	-	-	-	-	-	-	-	-	-
wtg_192	-	-	-	-	-	-	-	-	-	-
wtg_193	-	-	-	-	-	-	-	-	-	-
wtg_194	-	-	-	-	-	-	-	-	-	-
wtg_195	-	-	-	-	-	-	-	-	-	-
wtg_196	-	-	-	-	-	-	-	-	-	-
wtg_197	-	-	-	-	-	-	-	-	-	-